Application of genome editing to marine aquaculture as a new breeding technology

Kenta Kishimoto

2019

Contents

General introduction

Genome is a word which is a blend of the words “gene” and “ome” meaning chromosome. Thus, it includes all of the genes in an organism. An organism represents characteristics, features, and traits by using genome as genetic materials. Genome sequences and the genome sizes differ among species. According to Ensemble genome browser [**1**] and red sea bream genome database, the genome sizes of human (*Homo sapiens*), red sea bream (*Pagrus major*), and fugu (*Takifugu rubripes*) are 3,609,003,417 [**1**]; 752,042,544 [unpublished]; and 391,484,725 [**1**] base pairs, respectively. Therefore, the variation of genome contributes the variation of species. Of course, the cording sequences (CDS), which are the region translated into protein, are different among species. For example, the CDS sequence identities of myostatin gene (*mstn*) are 63.2% in human vs red sea bream, 61.7% in human vs fugu, and 87.0% in red sea bream vs fugu by analysis with ClustalW [**2**] [unpublished data]. In addition, an individual differs from each other in the same species since a few variations of genome exist in the same species. By investigating the variations among six red sea bream in breeding population by whole genome sequence, it was revealed that there is variation in the genome sequence in one of 113.2 bp [unpublished data]. Thus, an individual with a valuable trait for aquaculture occurs by genetic variations and/or spontaneous mutations. A classical “selective breeding” is the process by which a new breed is developed with a heritance by selecting individuals with particular phenotypic traits from natural or breeding populations.

In crop and livestock, there are various breeds with valuable traits since selective breeding has been performed over a long period. For example, *Brassica oleracea* comprises many important vegetable crop breeds including cauliflower, broccoli, cabbage, brussels sprouts, and kale. Cattle, pig, and chicken consist of various valuable traits for human. They are completely distinguished from original animals in nature. On the other hand, in marine aquaculture fish, selective breeding had not developed because fish production had mainly relied on exploitation of wild stocks until late 1900s. Recently, an importance of aquaculture is highlighted due to the increasing demand for fishery protein and awareness about conservation of natural resources. Thus, highly productive aquaculture breeds are desirable for both producers and consumers [**3**].

The classical selective breeding techniques have the following issues in marine

aquaculture fish species; (1) it is impossible to intentionally obtain a desired phenotype because natural mutations occur at random, (2) a long-time period is required to establish new breeds since most marine aquaculture fish have a long sex maturation (2 years in red sea bream, 3 years in fugu), and (3) administration and observation of aquatic animals need more efforts than of land animals. These characteristics constitute a considerable barrier to work for breed improvement. For overcoming these issues in aquaculture, the application of new breeding techniques (NBTs) in aquaculture have been conducted. One of them is the breeding method with random mutagenesis by physical energy (e.g. gamma radiation or high energy ion beam) and chemical mutagens (e.g. ethylmethane sulfonate or *N*-ethyl-*N*-nitrosourea), by which various plant breeds have been established until now [**4**]. The random mutagenesis breeding method has been tried also in aquaculture fish, fugu [**5**]. However, the method requires laborious efforts for screening mutants with a desirable phenotype. Transgenic technology had come under the spotlight as a new technology which can quickly produce new breeds harboring beneficial traits [**6-8**]. The well-known one is a transgenic Atlantic salmon *Salmo salar* breed which harbors an integration of growth hormone from chinook salmon *Oncorhynchus tshawytscha* with an antifreeze protein gene promotor derived from ocean pout *Zoarces americanus* [**6**]. The transgenic Atlantic salmon exhibits a drastic growth enhancement, and was the first genetically modified animal approved by the Food and Drug Administration (FDA) in 2015. These organisms made by transgenic technology are defined as genetically modified organisms (GMOs), which have exogenous genes and do not exist in nature. Therefore, GMOs including aquaculture products generally have not been positively accepted as food stuffs because of the concerns about food safety and about genetic contamination of wild stocks by escaped GMOs.

Recently, genome editing technology has developed as a latest NBT in agriculture, livestock industry, and also aquaculture. There are three tools for genome editing: zinc finger nucleases (ZFNs), transcriptional activator like effector nucleases (TALENs), and clustered regularly interspaced short palindromic repeats / CRISPR associated nuclease 9 (CRISPR/Cas9) RNA guided endonuclease (RGEN) system, which have been developed and used in a wide range of organisms [**9-11**]. In particular, TALENs and CRISPR/Cas9 have been wildly used because of its high efficiency. These artificial restriction enzymes and RGEN system are programmed to generate site specific double

strand DNA breaks (DSBs) that can be repaired by DNA repair process, non-homologous end joining (NHEJ) or homology directed repair (HDR). By using these process, the following genetically engineering can be performed: targeted gene disruptions with insertions and/or deletions by an error of DNA repair, or target genome modification caused by homologous recombination [**12**]. The genome editing via NHEJ can cause a specific endogenous gene disruption without adding exogenous gene. Genome editing breeding have several merits that it is gene-targetable, simple, low-cost, and rapid for researchers and aquaculture workers. As the previous genetic research which compared genetic variations among six red sea bream in aquaculture, the numbers of 1-10 and 11-20 bp deleted sites against reference genome database were 530,307 and 59,620, respectively [unpublished data]. Thus, genome edited breeds are hardly distinguishable from the wild ones since such in/del mutations occur also in nature. Therefore, genome edited breeds are expected as food staffs. Now, genome editing has been applied to several plants, animals, and fish which are used as commercial food stuffs [**13-15**].

In this study, the establishment of breeding method with genome editing was performed in marine aquaculture fish, red sea bream and fugu. In chapter 1, the microinjection method was established by which genome editing tools are introduced into fertilized eggs by resolving the problems derived from characteristics of marine aquaculture species. In chapter 2, a breed of red sea bream with increased skeletal muscle mass was produced by *mstn* knockout with genome editing CRISPR/Cas9. In chapter 3, a breed of fugu with increased skeletal muscle mass was also produced with CRISPR/Cas9.

References

1. Ensemble Genome Browser 94, http://www.ensembl.org
2. ClustalW ver. 2.1, http://clustalw.ddbj.nig.ac.jp
3. Gjedrem, Trygve, Nick Robinson, and Morten Rye. "The importance of selective breeding in aquaculture to meet future demands for animal protein: a review." Aquaculture 350 (2012): 117-129.
4. Jain, S. Mohan. "Mutagenesis in crop improvement under the climate change." Romanian biotechnological letters 15.2 (2010): 88-106.
5. Kuroyanagi, Miwa, et al. "New approach for fish breeding by chemical mutagenesis: establishment of TILLING method in fugu (Takifugu rubripes) with ENU mutagenesis." BMC genomics 14.1 (2013): 786.
6. Du, Shao Jun, et al. "Growth enhancement in transgenic Atlantic salmon by the use of an “all fish” chimeric growth hormone gene construct." Nature Biotechnology 10.2 (1992): 176.
7. Kato, Keitaro, et al. "Construction of an expression vector containing a β-actin promoter region for gene transfer by microinjection in red sea bream Pagrus major." Fisheries Science 73.2 (2007): 440-445.

8. Pinkert, Carl, A., 2014. Transgenic Animal Technology: A Laboratory Handbook. Newnes.
9. Carroll, Dana. "Genome engineering with zinc-finger nucleases." Genetics 188.4 (2011): 773-782.
10. Joung, J. Keith, and Jeffry D. Sander. "TALENs: a widely applicable technology for targeted genome editing." Nature reviews Molecular cell biology 14.1 (2013): 49.
11. Harrison, Melissa M., et al. "A CRISPR view of development." Genes & development 28.17 (2014): 1859-1872.
12. Urnov, Fyodor D., et al. "Genome editing with engineered zinc finger nucleases." Nature Reviews Genetics 11.9 (2010): 636.
13. Barman, Hirak Kumar, et al. "Gene editing tools: state-of-the-art and the road ahead for the model and non-model fishes." Transgenic research 26.5 (2017): 577-589.
14. Hilscher, Julia, Hermann Bürstmayr, and Eva Stoger. "Targeted modification of plant genomes for precision crop breeding." Biotechnology journal 12.1 (2017): 1600173.
15. Van Eenennaam, Alison Louise. "Genetic modification of food animals." Current opinion in biotechnology 44 (2017): 27-34.

Chapter 1
An effective microinjection method for genome editing of marine aquaculture fish: tiger pufferfish *Takifugu rubripes* and red sea bream *Pagrus major*

C1.1 Abstract

Genome editing technology is getting accepted as a way to improve traits in marine fish aquaculture. In fish, microinjection is a major method for introducing RNA or protein into eggs for genome editing; however, this method has not been established yet in aquaculture fish. I successfully established microinjection methods achieving high survival rates for tiger pufferfish *Takifugu rubripes* (fugu) and red sea bream *Pagrus major* by optimizing the following three parameters: (1) the soaking solution of fertilized eggs during microinjection, (2) the elapsed time from *in vitro* fertilization to microinjection, (3) the elapsed time from stripping to microinjection. In fugu, Iwamatsu solution or diluted sea water is effective as the soaking solution. *In vitro* fertilization can be performed at intervals of 15 minutes from fertilization until 2.5 hours after stripping. Similarly, in red sea bream, Leibovitz's L-15 medium or Iwamatsu solution is effective as the soaking solution and *in vitro* fertilization can be performed at intervals of 10 minutes from fertilization until 2.5 hours after stripping. I anticipate that the findings in the present study will contribute to effectively establish genome edited aquaculture breeds.

C1.2 Introduction

Gene specific knockout with genome editing is becoming increasingly accepted as a way to improve breeding efficiency in marine fish aquaculture because it allows modification of endogenous genes without the need to integrate exogenous genes [**1**]. For genome editing in fish, it is necessary to introduce nucleic acid or proteins as genome editing tools into fertilized eggs with a glass needle micropipette under a microscope, that is, the microinjection method [**1-5**]. Since the characteristics of fish eggs vary depending on each species [**6-7**], the microinjection method for genome editing needs to be optimized for each fish species.

There are several problems in breeding with genome editing using the microinjection method. First, the survival rate of eggs after microinjection decreases because of the physical damage to the chorion. Second, the number of eggs that can be microinjected in a day is limited because the microinjection of genome editing tools into fertilized eggs is performed on single eggs one at a time and this procedure is time-consuming. For breeding with genome editing, a microinjection method, in which eggs have a high survival rate and a large number of eggs can be treated, needs to be established to overcome these two problems.

In order to overcome the first problem, I investigated the effect of different soaking solutions for fertilized eggs during microinjection on the survival rate in experiment 1 (T1 for fugu and R1 for red sea bream). My experience that most fertilized eggs died after microinjection using sea water as the soaking solution led me to think that the effect of osmolality of the soaking solution on egg survival was critical. Therefore, I investigated several isotonic solutions with lower osmotic pressure; i.e., balanced salt solution, cell culture solution, and diluted sea water as a substitute for sea water.

In order to overcome the second problem, I investigated the effect of the elapsed time from *in vitro* fertilization to microinjection in experiment 2 (T2 for fugu and R2 for red sea bream). The chorion of fish eggs hardens several minutes after fertilization and prevents microinjection. Thus, to microinject into a lot of eggs, it is important to perform microinjection just after fertilization so that the chorion is still soft enough to allow penetration of the chorion with the glass needle. Therefore, I investigated the time point when the needle cannot easily penetrate the chorion because of the chorion hardening and the survival rate of the injected eggs until that time.

Then, I investigated the effect of the elapsed time from stripping to microinjection on the survival rate of eggs in experiment 3 (T3 for fugu and R3 for red sea bream). In a series of microinjections with marine fish eggs, *in vitro* fertilization can be carried out repeatedly so that newly fertilized eggs with the chorion still soft enough to be penetrated by the glass needle are available for microinjection. Fertility of sperm can be maintained throughout the day by storage in a refrigerator. In contrast, fertility of unfertilized eggs gradually decreases over several hours after stripping, and is completely lost several hours later. Thus, it is thought that the survival rate of the injected eggs also decreases gradually after stripping. Therefore, I investigated the elapsed time prior to microinjection in which a high survival rate of injected eggs was maintained.

In the present study, I optimized the microinjection method concerning the above three factors and established microinjection methods for fugu *Takifugu rubripes* and red sea bream *Pagrus major*, which are important marine aquaculture fish in Japan.

C1.3 Materials and methods

1.3.1 Experimental fish and gametes for in vitro fertilization

1.3.1.1 Fugu

Parent fish were purchased from a commercial supplier (Watanabe Suisan, Kagawa, Japan). Females were administered an LHRH analogue (des Gly10 [D-Ala6]-LHRH, 400 μg/kg body weight) to promote ovulation. Males were injected with human chorionic gonadotropin (hCG, 500 IU/kg body weight) intramuscularly to promote spermiation. Unfertilized eggs and sperm were squeezed from each parent fish by the stripping method and were preserved in covered plastic cups until *in vitro* fertilization at 17°C while preventing the eggs from drying. For microinjection, *in vitro* fertilization was carried out using the preserved eggs and sperm.

1.3.1.2 Red sea bream

Unfertilized eggs and sperm of red sea bream were squeezed from broodstocks at Kindai University by the stripping method [**8**]. The parent fish were at a natural point of ovulation and spermiation. The collected unfertilized eggs and sperm were preserved in covered plastic cups to prevent the eggs from drying until *in vitro* fertilization. The eggs were kept

at 17-20°C, and sperm were kept on ice. For microinjection, *in vitro* fertilization was carried out using the preserved eggs and sperm.

1.3.2 Microinjection set-up

The following tools were used for microinjection under a stereomicroscope: a pneumatic injector IM-12, an injection holder HI-7, a manipulator M-152, and a magnetic stand GJ-1 (Narishige, Tokyo, Japan). The glass needles for microinjection were made from a glass capillary (GD-1; Narishige) with a puller; PC-10 (Narishige). The set-up of instruments for microinjection is outlined in **Fig. 1.1a**. The mixture of Cas9 RNA (100 ng/μl) and sgRNA (50 ng/μl), targeted for the myostatin gene, was injected in the present experiments because it is known that myostatin deficiency does not affect the viability of fish [**1, 9-10**]. The target sites were 5'-CCGGGACACGGTGAAGCAGCTCC-3' in fugu (GenBank accession number LOC446041, reverse strand in exon 1) and 5'-CCGGGACATCGTGAAGCAGCTCC-3' in red sea bream (DDBJ accession number AY965686, reverse strand in exon 1). *In vitro* transcriptions of Cas9 RNA and each of the sgRNAs were performed according to the method of previous report [**3**]. These target sites were consistent with sgRNA#2 in **chapter 3** and sgRNA#1 in **chapter 2**.

1.3.3 In vitro fertilization and microinjection

First, about one thousand unfertilized eggs were fertilized with sperm in sea water *in vitro*. Second, handling of eggs was started at 1 minutes after *in vitro* fertilization to prevent the chorion from being broken by handling because the chorion is fragile just after fertilization. In the fugu experiment, 1 minutes after *in vitro* fertilization, eggs were arranged in sea water in a line along both sides of a G-1 glass capillary (Narishige) on a plastic dish (90 mm in diameter) utilizing the characteristic that fugu eggs adhere to glass materials [**11**] (**Fig. 1.1b**). Then, the sea water was replaced with the soaking solution. In the red sea bream experiment, fertilized eggs were washed with soaking solution using a net, and then arranged with the soaking solution in a line in a groove on an acryl plate as described in a previous report [**8**] (**Fig. 1.1c**). On one plate, 70-100 eggs and 30-100 eggs were arranged in the fugu experiment and the red sea bream experiment, respectively. Finally, microinjection was performed. The injected eggs were incubated in sea water at 17°C and 20°C in fugu eggs and in red sea bream eggs, respectively.

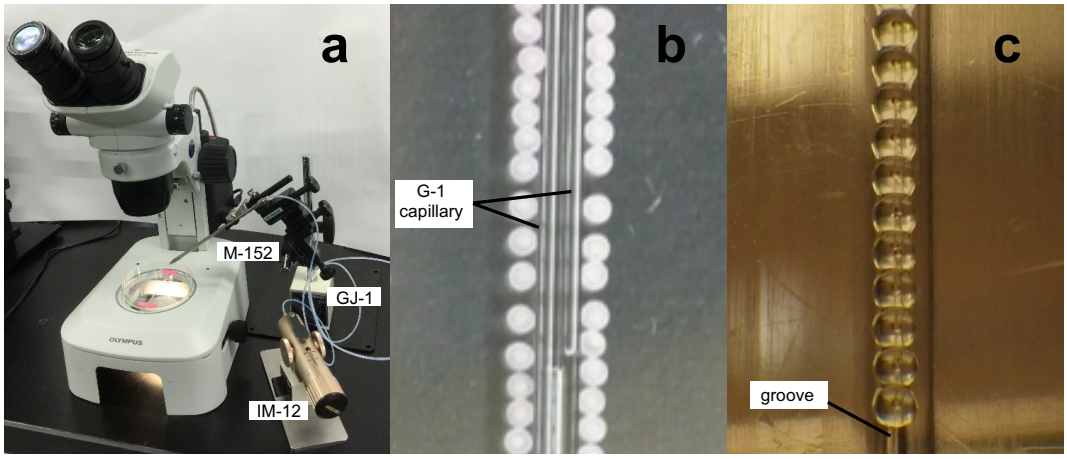

Fig. 1.1 Set-up of instruments for microinjection

(a) For microinjection, pneumatic injector (IM-12), manipulator (M-152), magnetic stand (GJ-1) (Narishige). A plastic dish for fugu microinjection is set up as in the figure. (b) Fugu eggs are arranged with a soaking solution in a line along both sides of glass capillaries (G-1, Narishige) on a plastic dish (90 mm in diameter) using the trait of egg adhesion to glass. (c) Red sea bream eggs are arranged with a soaking solution in a groove on an acryl plate. By arranging tightly, eggs are prevented from moving.

1.3.4 Evaluation of the effects of each factor on survival rate of injected eggs

The effects of the following three factors in microinjection on the survival rates after microinjection were investigated: the soaking solution for fertilized eggs during microinjection treatment in experiment 1; the elapsed time from *in vitro* fertilization to microinjection in experiment 2; and the elapsed time from stripping to microinjection in experiment 3. It took 5-10 minutes to perform microinjection into all eggs in each lot (fugu: lots of 57-115 eggs, red sea bream: lots of 49-142 eggs).

In the experiments with fugu eggs, the effects of the three factors were evaluated by the survival rate on 6 or 7 days post fertilization (dpf) because it is unclear whether fugu eggs are alive or not due to being opaque at the early stages. As a control group, the fertilized eggs were arranged in sea water along the glass capillary on a plastic dish without microinjection.

In the experiments with red sea bream eggs, the effects of the three factors were estimated by the survival rate on 2 dpf (38-40 hours post fertilization). As a control group, the fertilized eggs were arranged in sea water along the groove on the acryl plate without microinjection. Each experiment was performed in triplicate, described as trial-I, trial-II, and trial-III. Since microinjection requires a high level of dexterity that varies from person

to person, the experiments were confirmed by several people performing the trials.

1.3.5 Experiments on fugu eggs

1.3.5.1 Experiment T1: evaluation of various soaking solutions during microinjection

The soaking solutions investigated were Leibovitz's L-15 medium (L-15; Invitrogen, Carlsbad, CA, USA), Iwamatsu balanced salt solution, which is developed for medaka (Iwamatsu solution: 0.65% NaCl, 0.04% KCl, 0.02% $MgSO_4 \cdot 2H_2O$, 0.02% $CaCl_2 \cdot H_2O$, pH 7.4) [**12**], phosphate buffered saline (PBS: 137 mM NaCl, 2.7 mM KCl, 10 mM Na_2HPO_4, 1.8 mM KH_2PO_4, pH 7.4), sea water, diluted sea water (1/2, 1/3, 1/6, and 1/12), and distilled water (DW) (**Table 1.1**). In all experiments, sea water was sterilized using ultraviolet light and filtration (pore size 0.22 μm), and all diluted sea water solutions were diluted using DW. All experiments were performed within 1 hour after carrying out the stripping method.

1.3.5.2 Experiment T2: evaluation of the elapsed time from *in vitro* fertilization to microinjection

In vitro fertilization was performed at 25-30 minutes after stripping. After fertilized eggs were aligned in a plastic dish with sea water for microinjection, the sea water in the dish was replaced with Iwamatsu solution as soaking solution. Microinjection was started at 10, 30, and 50 minutes after *in vitro* fertilization (**Table 1.2**).

1.3.5.3 Experiment T3: evaluation of the elapsed time from stripping to microinjection

In vitro fertilization and subsequent microinjection was conducted at 30 (1st), 60 (2nd), 90 (3rd), 120 (4th), and 150 (5th) minutes after stripping in trial-I and trial-II, while in trial-III it was conducted at 25 (1st), 85 (2nd), 145 (3rd), and 205 (4th) minutes after stripping. The timelines of experiments are detailed in **Table 1.3**. After fertilized eggs were aligned in a plastic dish with sea water for microinjection, the sea water in the dish was replaced with Iwamatsu solution as soaking solution, the same as in experiment T2. As control groups, the fertilized eggs were arranged along a glass capillary with Iwamatsu solution on a plastic dish without microinjection for each time (1st-5th).

1.3.6 Experiments on red sea bream eggs

1.3.6.1 Experiment R1: evaluation of various soaking solutions during microinjection

After *in vitro* fertilization was carried out, fertilized eggs were arranged in a groove on an acryl plate with the following soaking solutions, and then microinjection was performed. The investigated soaking solutions were L-15, Iwamatsu solution, sea water, 1/3 sea water, and PBS (**Table 1.4**). In all experiments, like the fugu experiment, sea water was sterilized.

1.3.6.2 Experiment R2: evaluation of the elapsed time from *in vitro* fertilization to microinjection

In vitro fertilization was performed at 20 minutes in trial-I, 30 minutes in trial-II, and 60 minutes in trial-III after stripping. The fertilized eggs were arranged in a groove on an acryl plate with L-15 as the soaking solution. Microinjection was started at 1, 5, 10, and 15 minutes after the *in vitro* fertilization (**Table 1.5**).

1.3.6.3 Experiment R3: evaluation of the elapsed time from stripping to microinjection

In vitro fertilization and subsequent microinjection were performed at 20 (1st), 50 (2nd), 80 (3rd), 110 (4th), and 140 (5th) minutes after stripping in trial-I. In trial-II, they were performed at 30 (1st), 60 (2nd), 90 (3rd), 120 (4th), 150 (5th), and 180 (6th) minutes after stripping. In trial-III, they were performed at 30 (1st), 60 (2nd), 90 (3rd), 120 (4th), and 180 (5th) minutes after stripping. The timelines of experiments are detailed in **Table 1.6**. The fertilized eggs were arranged in a groove on an acryl plate with L-15 as the soaking solution. As the control groups, fertilized eggs were arranged along the groove on the acryl plate with L-15 without microinjection for each time.

1.3.7 Statistical analysis

Statistical analyses were performed by R version 3.4.0 and fmsb package (https://cran.r-project.org/web/packages/fmsb/). Differences of survival rates among groups were compared by Fisher's exact test with Benjamini-Hochberg correction for multiple

comparisons. Differences were considered significant in the case of $P < 0.05$.

C1.4 Results

1.4.1 Experiments on fugu

1.4.1.1 Experiment T1: evaluation of various soaking solutions during microinjection

The mixture of Cas9 RNA and sgRNA was microinjected into fugu fertilized eggs using various soaking solutions. **Figure 1.2a** shows the survival rates of fugu eggs 7 days after microinjection in various soaking solutions in trial-I. The soaking solution that exhibited the highest survival rate was 1/3 sea water (59.2%). Iwamatsu solution, L-15, 1/2 sea water, 1/6 sea water, and 1/12 sea water also exhibited high survival rates, 51.5%, 48.8%, 58.4%, 55.2%, and 53.6%, respectively. On the other hand, PBS, sea water, and DW exhibited low survival rates, 27.0%, 32.4%, and 36.0%, respectively. In the control groups, the survival rate was 91.5% (at the start of the experiment) and 81.6% (at the end of the experiment). In trial-IIa, the survival rate in the control group was low (31.6%) because the egg quality was not good. Iwamatsu solution showed the highest survival rate (33.8%) and sea water the lowest (4.2%); L-15 and PBS showed intermediate rates (22.2% and 17.5%, respectively) (**Fig. 1.2b**). In trial-IIb, diluted sea water (1/2, 1/3, and 1/6) and Iwamatsu solution showed high survival rates (more than 50%), while sea water showed a low rate (18.0%) (**Fig. 1.2c**). In trial-III, the survival rate in each soaking solution was almost the same (40.5-58.3%) (**Fig. 1.2d**). The soaking solution which showed the highest survival rate was Iwamatsu solution (58.3%). These results indicate that Iwamatsu solution and diluted sea water show high survival rates through all the experimental trials. Details of the number of injected eggs and the number and rate of survival of eggs in all trials are described in **Table 1.1**.

Table 1.1 Summary of experiment T1 on fugu eggs

Trial	Soaking solutions[*1]	Number of injected eggs	Number of surviving eggs[*2]
I	non-injected 1(control)	94	86 (91.5%)
I	Iwamatsu solution	103	53 (51.5%)
I	L-15	84	41 (48.8%)
I	PBS	115	31 (27.0%)
I	Sea water	111	36 (32.4%)
I	1/2 Sea water	113	66 (58.4%)
I	1/3 Sea water	103	61 (59.2%)
I	1/6 Sea water	96	53 (55.2%)
I	1/12 Sea water	84	45 (53.6%)
I	DW	114	41 (36.0%)
I	non-injected 2 (control)	87	71 (81.6%)
II-a	non-injected (control)	79	25 (31.6%)
II-a	Iwamatsu solution	77	26 (33.8%)
II-a	L-15	90	20 (22.2%)
II-a	Sea water	57	10 (17.5%)
II-a	PBS	71	3 (4.2%)
II-b	non-injected (control)	99	85 (85.9%)
II-b	Sea water	89	16 (18.0%)
II-b	1/2 Sea water	102	68 (66.7%)
II-b	1/3 Sea water	107	61 (57.0%)
II-b	1/6 Sea water	103	69 (67.0%)
II-b	Iwamatsu solution	99	52 (52.5%)
III	non-injected 1 (control)	103	86 (83.5%)
III	Iwamatsu solution	96	56 (58.3%)
III	L-15	84	34 (40.5%)
III	1/3 Sea water	100	47 (47.0%)
III	PBS	108	50 (46.3%)
III	Sea water	98	42 (42.9%)
III	DW	97	48 (49.5%)
III	non-injected 2 (control)	102	78 (76.5%)

[*1]: non-injected 1 & 2 indicate the control lots at the start and the end of the experiment, respectively.
[*2]: % indicates the rate of the surviving eggs to the injected eggs. Number of surviving eggs was counted at 6 dpf in trial-II and at 7 dpf in trial-I & trial-III.

1.4.1.2 Experiment T2: evaluation of the elapsed time from *in vitro* fertilization to microinjection

The mixture of Cas9 RNA and sgRNA was microinjected into fugu fertilized eggs at 10, 30, and 50 minutes after the *in vitro* fertilization. In trial-I, the survival rate of the control group was 82.7% (**Fig. 1.2e**). The survival rates of experimental groups were consistent: 62.4% for 10 minutes, 56.3% for 30 minutes, and 70.1% for 50 minutes. In trial-II and trial-III, the experimental groups also showed consistent survival rates: 30-48% in trial-II (**Fig. 1.2f**) and 43-55% in trial-III (**Fig. 1.2g**). Throughout the experiment, I did not find a clear relationship between the elapsed time and the survival rate of injected eggs. Details of the number of injected eggs and the number and rate of survival of eggs in all trials are described in **Table 1.2**. The longer the elapsed time after fertilization, the more opaque and stiffer the chorions of fugu eggs became. Therefore, it was difficult to perform the microinjection at 30 and 50 minutes after fertilization. On the other hand, until about 15 minutes after fertilization, it was comparatively easy to observe that the solution being injected was flowing into the egg because of its transparency. And it was easy to penetrate the chorion with the glass needle because of its softness. These results indicate that microinjection sooner after fertilization (i.e., up to 15 minutes after fertilization) contributes to ease of handling.

Table 1.2 Summary of experiment T2 on fugu eggs

Trial	Time after fertilization	Number of injected eggs	Number of surviving eggs*
I	non-injected (control)	98	81 (82.7%)
I	10 min	101	63 (62.4%)
I	30 min	96	54 (56.3%)
I	50 min	97	68 (70.1%)
II	non-injected (control)	103	86 (83.5%)
II	10 min	110	46 (41.8%)
II	30 min	73	22 (30.1%)
II	50 min	116	56 (48.3%)
III	non-injected (control)	101	64 (63.4%)
III	10 min	104	57 (54.8%)
III	30 min	96	47 (49.0%)
III	50 min	82	35 (42.7%)

*: % indicates the rate of the surviving eggs to the injected eggs. Number of surviving eggs was counted at 6 dpf in trial-I and at 7 dpf in trial-II & trial-III.

1.4.1.3 Experiment T3: evaluation of the elapsed time from stripping to microinjection

The mixture of Cas9 RNA and sgRNA was microinjected into fugu fertilized eggs at several intervals after the stripping. **Figure 1.2h** shows the results of trial-I. In the control groups in which microinjection was not performed, the survival rates gradually decreased (control groups designated as “non-injected”; 30 min, 83.5%; 60 min, 80.2%; 90 min, 76.5%; 120 min, 68.2%; 150 min, 75.5%). In contrast, when microinjection was performed, the survival rates decreased rapidly depending on the time until 90 min after stripping (designated as “injected”; 30 min, 50.5%; 60 min, 36.8%; 90 min, 19.6%). The rates at 120 minutes after stripping increased more than that at 90 minutes after stripping. At 150 minutes after stripping, the survival rate of injected eggs slightly decreased (39.8%). The tendency was similar among all three trials (**Fig. 1.2i, j** and **Table 1.3**). The tendency that the survival rates of injected eggs increased once was consistent with that of trial-II (120 min, 19.1%; 150 min, 43.4%), and trial-III (slight increase: 145 min, 28.2%; 205 min; 43.8%). Details of the number of injected eggs and the number and rate of the survival of eggs in all trials are described in **Table 1.3**. These results indicate that microinjection at an earlier time period from stripping contributes to a higher survival rate (i.e., until 2.5 hours after stripping).

Table 1.3 Summary of experiment T3 on fugu eggs

Trial	Times after stripping	non-injected (control) or injected	Number of injected eggs	Number of surviving eggs[*2]
I	1st: 30 min	non-injected	103	86 (83.5%)
		injected	101	51 (50.5%)
I	2nd: 60 min	non-injected	96	77 (80.2%)
		injected	87	32 (36.8%)
I	3rd: 90 min	non-injected	102	78 (76.5%)
		injected	97	19 (19.6%)
I	4th: 120 min	non-injected	110	75 (68.2%)
		injected	95	49 (51.6%)
I	5th: 150 min	non-injected	102	77 (75.5%)
		injected	93	37 (39.8%)
II	1st: 30 min	non-injected	101	64 (63.4%)
		injected	96	29 (30.2%)
II	2nd: 60 min	non-injected	80	70 (87.5%)
		injected	79	18 (22.8%)
II	3rd: 90 min	non-injected	78	65 (83.3%)
		injected	102	22 (21.6%)
II	4th: 120 min	non-injected	82	56 (68.3%)
		injected	89	17 (19.1%)
II	5th: 150 min	non-injected	80	48 (60.0%)
		injected	106	46 (43.4%)
III	1st: 25 min	non-injected	98	81 (82.7%)
		injected	101	63 (62.4%)
III	2nd: 85 min	non-injected	100	89 (89.0%)
		injected	112	84 (75.0%)
III	3rd: 145 min	non-injected	69	54 (78.3%)
		injected	85	24 (28.2%)
III	4th: 205 min	non-injected	113	96 (85.0%)
		injected	80	35 (43.8%)

[*]: % indicates the rate of the surviving eggs to the injected eggs. Number of surviving eggs was counted at 6 dpf in trial-III and at 7 dpf in trial-I & trial-II.

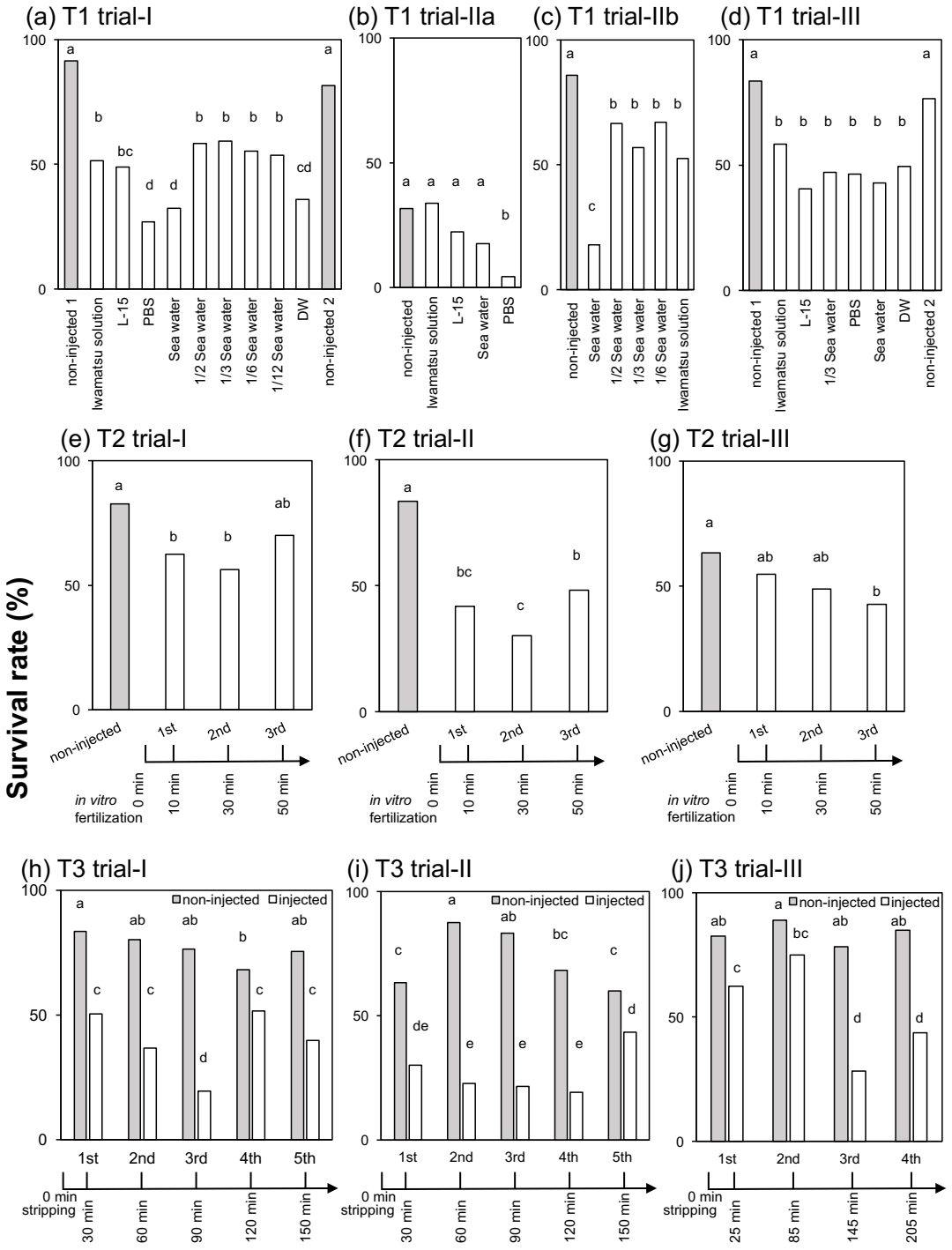

Fig. 1.2 Effect of the three parameters on the survival of microinjected fugu eggs

The results of the experiment T1 in trial-I (a), trial-IIa (b), trial-IIb (c), and trial-III (d): evaluation of the effect of different soaking solutions on the survival of fertilized eggs during microinjection. The results of the experiment T2 in trial-I (e), trial-II (f), and trial-III (g): evaluation of the elapsed time from *in vitro* fertilization to microinjection. The results of the experiment T3 in trial-I (h), trial-II (i), and trial-III (j): evaluation of the elapsed time from stripping to microinjection. The survival rates indicate the number of surviving eggs at 6 or 7 dpf / the number of injected eggs. Gray columns indicate the control groups for which microinjection was not performed. Different letters above each column indicate significant differences by Fisher's exact test with Benjamini-Hochberg correction for multiple comparisons, $P < 0.05$

1.4.2 Experiments on red sea bream eggs

1.4.2.1 Experiment R1: evaluation of various soaking solutions during microinjection

The mixture of Cas9 RNA and sgRNA was microinjected into red sea bream fertilized eggs using various soaking solutions. **Figure 1.3a** shows the survival rates of red sea bream eggs 2 days after microinjection in various soaking solutions in trial-I. The soaking solutions that exhibited the highest survival rates were L-15 (49.0%) and Iwamatsu solution (49.0%). On the other hand, PBS, sea water, and 1/3 sea water showed low survival rates, 23.9%, 4.6%, and 1.7%, respectively. In the control groups, the survival rates were 94.2% (at the start of the experiment) and 100% (at the end of the experiment). Similarly, in trial-II, L-15 and Iwamatsu solution showed high rates, 70.8% and 67.5%, respectively (**Fig. 1.3b**). While 1/3 sea water showed a low rate in trial-I, it showed a high survival rate in trial-II (85.2%). Sea water showed a low rate in trial-I (22.9%). PBS showed an intermediate rate (54.5%). In the control groups, the survival rates were 88.5% (at the start of the experiment) and 71.3% (at the end of the experiment). In trial-III, the survival rates, sorted in decreasing order were: 79.4% (Iwamatsu solution), 61.4% (L-15), 53.8% (PBS), 46.3% (1/3 sea water), and 41.8% (sea water) (**Fig. 1.3c**). In the control groups, the survival rates were 90.9% (at the start of the experiment) and 86.5% (at the end of the experiment). These results indicate that L-15 and Iwamatsu solution show high survival rates through all the experiments. Details of the number of injected eggs and the number and rate of the survival of eggs in all trials are described in **Table 1.4.**

1.4.2.2 Experiment R2: evaluation of the elapsed time from *in vitro* fertilization to microinjection

The mixture of Cas9 RNA and sgRNA was microinjected into red sea bream fertilized eggs at 1, 5, 10, and 15 minutes after the *in vitro* fertilization. **Figure 1.3d** shows the results of trial-I. The survival rates of the experimental groups were 42-77% at 2 dpf (1 min, 77.0%; 5 min, 44.9%; 10 min, 49.3%; 15 min, 42.3%). The survival rate of the control group was 87.8%. In trial-II, the survival rates of experimental groups were 14-56% (1 min, 38.3%; 5 min, 55.8%; 10 min, 43.7%; 15 min, 14.3%) (**Fig. 1.3e**). In trial-III, the survival rates of the experimental groups were 15-40% (1 min, 36.8%; 5 min, 40.4%; 10 min, 15.4%; 15 min, 26.3%) (**Fig. 1.3f**). As in fugu, the chorion of the eggs

became stiffer, the longer the time period after fertilization. Microinjection could not be effectively performed at 20 minutes after *in vitro* fertilization because of the hardened chorion. Therefore, it was difficult to perform microinjection 15 or more minutes after fertilization. On the other hand, it was easy to inject into the chorion until 10 minutes after fertilization because the chorion of fertilized eggs at the early stage was soft, and the survival rate of injected eggs was comparatively high. Details of the number of injected eggs and the number and rate of the surviving eggs in all trials are described in **Table 1.5**. These results indicate that microinjection at an earlier time period after fertilization contributes to easier handling (i.e., until 10 minutes after fertilization).

Table 1.4 Summary of experiment R1 on red sea bream eggs

Trial	Soaking solution*1	Number of injected eggs	Number of surviving eggs at 1 dpf*2	Number of surviving eggs at 2 dpf*2
I	non-injected 1 (control)	86	84 (97.7%)	81 (94.2%)
I	L-15	100	61 (61.0%)	49 (49.0%)
I	Iwamatsu solution	98	74 (75.5%)	48 (49.0%)
I	Sea water	65	10 (15.4%)	3 (4.6%)
I	1/3 Sea water	60	6 (10.0%)	1 (1.7%)
I	PBS	67	25 (37.3%)	16 (23.9%)
I	non-injected 2 (control)	68	68 (100%)	68 (100%)
II	non-injected 1 (control)	78	71 (91.0%)	69 (88.5%)
II	L-15	96	73 (76.0%)	68 (70.8%)
II	Iwamatsu solution	83	60 (72.3%)	56 (67.5%)
II	Sea water	70	18 (25.7%)	16 (22.9%)
II	1/3 Sea water	88	79 (89.8%)	75 (85.2%)
II	PBS	88	49 (55.7%)	48 (54.5%)
II	non-injected 2 (control)	80	66 (82.5%)	57 (71.3%)
III	non-injected 1 (control)	77	70 (90.9%)	70 (90.9%)
III	L-15	70	45 (64.3%)	43 (61.4%)
III	Iwamatsu solution	97	81 (83.5%)	77 (79.4%)
III	Sea water	67	32 (47.8%)	28 (41.8%)
III	1/3 Sea water	82	39 (47.6%)	38 (46.3%)
III	PBS	93	52 (55.9%)	50 (53.8%)
III	non-injected 2 (control)	74	72 (97.3%)	64 (86.5%)

*1: non-injected 1 & 2 indicate the control lots at the start and the end of the experiment, respectively.
*2: % indicates the rate of the surviving eggs to the injected eggs.

Table 1.5 Summary of experiment R2 on red sea bream eggs

Trial	Time after fertilization	Number of injected eggs	Number of surviving eggs at 1 dpf*	Number of surviving eggs at 2 dpf*
I	non-injected	74	68 (91.9%)	65 (87.8%)
I	1 min	61	55 (90.2%)	47 (77.0%)
I	5 min	78	60 (76.9%)	35 (44.9%)
I	10 min	73	63 (86.3%)	36 (49.3%)
I	15 min	52	36 (69.2%)	22 (42.3%)
II	non-injected	71	63 (88.7%)	57 (80.3%)
II	1 min	60	35 (58.3%)	23 (38.3%)
II	5 min	52	40 (76.9%)	29 (55.8%)
II	10 min	71	47 (66.2%)	31 (43.7%)
II	15 min	49	27 (55.1%)	7 (14.3%)
III	non-injected	102	98 (96.1%)	97 (95.1%)
III	1 min	68	39 (57.4%)	25 (36.8%)
III	5 min	57	38 (66.7%)	23 (40.4%)
III	10 min	91	40 (44.0%)	14 (15.4%)
III	15 min	57	36 (63.2%)	15 (26.3%)

*: % indicates the rate of the surviving eggs to the injected eggs.

1.4.2.3 Experiment R3: evaluation of the elapsed time from stripping to microinjection

The mixture of Cas9 RNA and sgRNA was microinjected into red sea bream fertilized eggs at several intervals after the stripping. **Figure 1.3g** shows the results of trial-I. The survival rates gradually decreased when microinjection was not performed (control groups designated as “noninjected”: 20 min, 87.8%; 50 min, 96.1%; 80 min, 79.5%; 110 min, 85.7%; 140 min, 67.4%), on the other hand, the survival rates of injected eggs decreased rapidly when microinjection was performed until 110 minutes after stripping (designated as “injected”: 20 min, 77.0%; 50 min, 69.0%; 80 min, 48.4%; 110 min, 24.3%). Similar to the fugu experiment, the survival rate of the injected group at 140 minutes after stripping increased compared to at 110 minutes after stripping. Furthermore, at 140 minutes after stripping, the survival rate of injected eggs was nearly as high as in noninjected eggs (non-injected, 67.4%; injected, 52.7%). In trial-II, the survival rates rapidly decreased in non-injected groups because of poor egg quality (30 min, 80.3%; 60 min, 64.5%; 90 min, 12.7%; 120 min, 6.9%; 150 min, 5.6%) (**Fig. 1.3h**). The survival

rates of injected groups also rapidly decreased until 90 minutes after stripping (30 min, 38.3%; 60 min, 26.5%; 90 min, 1.4%; 120 min, 3.3%; 150 min, 1.4%). Similar to trial-I, the rate of survival at 180 minutes after stripping increased in the injected group (12.3%). In trial-III, the survival rates were consistent through the trial when microinjection was not performed, and the survival rates for those injected decreased gradually (**Fig. 1.3i**). Details of the number of injected eggs and the number and rate of the survival of eggs in all trials are described in **Table 1.6**. These results indicate that microinjection at an earlier time period after stripping contributes to a higher survival rate (i.e., until 2.5 hours after stripping).

Table 1.6 Summary of experiment R3 on red sea bream eggs

Trial	Times after stripping	non-injected (control) or injected	Number of injected eggs	Number of survival eggs at 1 dpf*	Number of survival eggs at 2 dpf*
I	1st: 20 min	non-injected	74	68 (91.9%)	65 (87.8%)
		injected	61	55 (90.2%)	47 (77.0%)
I	2nd: 50 min	non-injected	77	75 (97.2%)	74 (96.1%)
		injected	58	55 (94.8%)	40 (69.0%)
I	3rd: 80 min	non-injected	88	72 (81.8%)	70 (79.5%)
		injected	93	64 (68.8%)	45 (48.4%)
I	4th: 110 min	non-injected	91	83 (91.2%)	78 (85.7%)
		injected	74	45 (60.8%)	18 (24.3%)
I	5th: 140 min	non-injected	86	74 (86.0%)	58 (67.4%)
		injected	91	67 (73.6%)	48 (52.7%)
II	1st: 30 min	non-injected	71	63 (88.7%)	57 (80.3%)
		injected	60	35 (58.3%)	23 (38.3%)
II	2nd: 60 min	non-injected	76	71 (93.4%)	49 (64.5%)
		injected	68	46 (67.6%)	18 (26.5%)
II	3rd: 90 min	non-injected	79	29 (36.7%)	10 (12.7%)
		injected	73	51 (69.9%)	1 (1.4%)
II	4th: 120 min	non-injected	72	43 (59.7%)	5 (6.9%)
		injected	61	39 (63.9%)	2 (3.3%)
II	5th: 150 min	non-injected	72	29 (40.3%)	4 (5.6%)
		injected	72	39 (54.2%)	1 (1.4%)
II	6th: 180 min	non-injected	85	49 (57.6%)	11 (12.9%)
		injected	73	45 (61.6%)	9 (12.3%)
III	1st: 30 min	non-injected	102	98 (96.1%)	97 (95.1%)
		injected	125	77 (61.6%)	48 (38.4%)
III	2nd: 60 min	non-injected	86	84 (97.7%)	81 (94.2%)
		injected	100	61 (61.0%)	49 (49.0%)
III	3rd: 90 min	non-injected	68	68 (100%)	68 (100%)
		injected	67	24 (35.8%)	10 (14.9%)
III	4th: 120 min	non-injected	75	73 (97.3%)	71 (94.7%)
		injected	101	44 (43.6%)	27 (26.7%)
III	5th: 180 min	non-injected	109	107 (98.2%)	93 (85.3%)
		injected	99	52 (52.5%)	16 (16.2%)

*: % indicates the rate of the surviving eggs to the injected eggs.

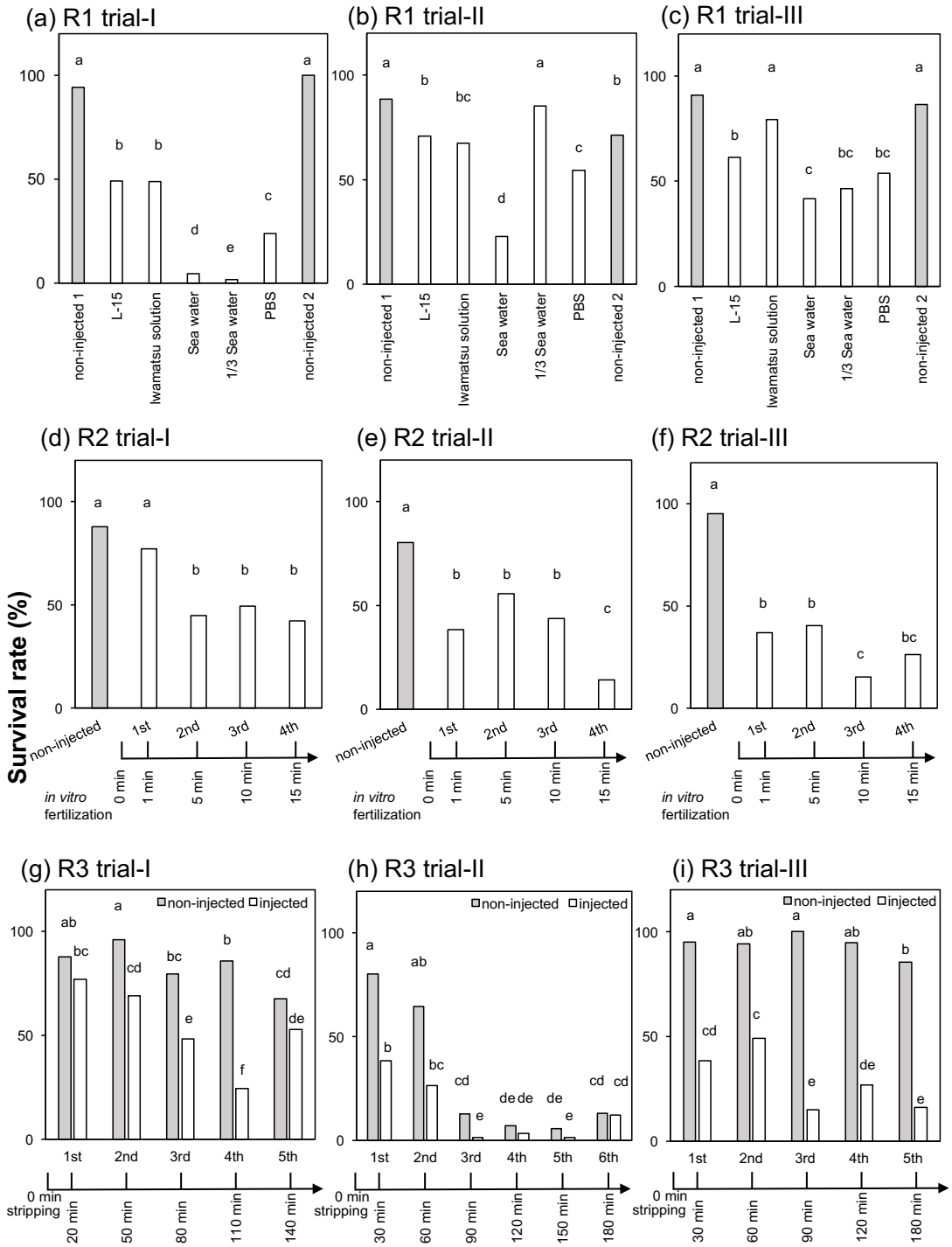

Fig. 1.3 Effect of the three parameters on the survival of microinjected red sea bream eggs

The results of the experiment R1 in trial-I (a), trial-II (b), and trial-III (c): evaluation of the effect of different soaking solutions on the survival of fertilized eggs during microinjection. The results of the experiment R2 in trial-I (d), trial-II (e), and trial-III (f): evaluation of the elapsed time from *in vitro* fertilization to microinjection. The results of the experiment R3 in trial-I (g), trial-II (h), and trial-III (i): evaluation of the elapsed time from stripping to microinjection. The survival rates indicate the number of surviving eggs at 2 dpf/the number of injected eggs. Gray columns indicate the control groups for which microinjection was not performed. Different letters above each column indicate significant differences by Fisher's exact test with Benjamini-Hochberg correction for multiple comparisons, $P < 0.05$

C1.5. Discussion

Optimization of microinjection parameters for each fish species has been important for successful genome editing because the characteristics of fish eggs vary depending on the species. In the present study, I investigated the optimal conditions for the microinjection method for fertilized eggs of fugu and red sea bream. I investigated the effects of the following three factors on the survival rates: (1) the soaking solution of fertilized eggs during microinjection, (2) the elapsed time from *in vitro* fertilization to microinjection, and (3) the elapsed time from stripping to microinjection. To the best of my knowledge, there have been no previous reports on microinjection performed in fugu for production of transgenic or genome edited fish. It was reported that microinjection was performed for the production of transgenic red sea bream by previous report [**8**]; however, they did not investigate the optimal conditions for microinjection.

In experiment 1 on the soaking solutions of fertilized eggs during microinjection, it was observed that the survival rates were low with sea water both in fugu and in red sea bream. On the other hand, the rates were high with Iwamatsu balanced salt solution and diluted sea water in fugu, and with Leibovitz's L-15 medium and Iwamatsu balanced salt solution in red sea bream (**Fig. 1.2a-d**, **Fig. 1.3a-c**, **Table 1.1**, and **Table 1.4**). These results suggested that solutions with a lower osmotic pressure than sea water are advantageous for eggs to survive during the microinjection process. It seems that the fluids in the cytoplasm and/or yolk sac may flow out through the pore generated by the glass microinjection needle if the eggs are surrounded by a solution with a higher osmotic pressure than the physiological osmotic pressure. However, the survival rates with 1/3 sea water were not consistent through the three experimental trials in red sea bream experiment R1, shown in **Table 1.4** (1.7% in trial-I, 85.2% in trial-II, and 46.3% in trial-III). This suggests that 1/3 sea water was not suitable as a soaking solution for red sea bream eggs during microinjection. At present, the reason for these results is unclear and further validation is required. A low osmotic pressure solution has another advantage: the lower buoyant force of low osmotic fluid helps pelagic eggs such as red sea bream eggs to sink and settle in the soaking solution. Sinking and settling eggs can be handled more easily than floating eggs. Indeed, use of L-15 as a soaking solution contributed to the successful production of transgenic red sea bream in a previous report [**8**]. Taking these things into consideration, I recommend Iwamatsu solution or diluted sea water (1/2-

1/12) as a soaking solution for fugu eggs and L-15 or Iwamatsu solutions as a soaking solution for red sea bream eggs, respectively.

In experiment 2 on the elapsed time from *in vitro* fertilization to microinjection, in both fugu and red sea bream, there was no direct relationship between the survival rate and the elapsed time (**Fig. 1.2e-g**, **Fig. 1.3d-f**, **Table 1.2**, and **Table 1.5**). However, the longer the time period elapsed after fertilization, the more difficult it is for the glass needle to penetrate the egg chorion. Thus, increasingly, handling mistakes can prevent efficient microinjection of a lot of eggs and cause dead eggs due to physical damage. For fish in which *in vitro* fertilization is easy to perform, such as fugu and red sea bream, it is easy to prepare newly fertilized eggs with soft chorions over periods of several hours. Therefore, microinjection can be continued for several hours by repeating *in vitro* fertilization. On the other hand, for relatively large fish that are difficult to manipulate under laboratory conditions, such as Pacific bluefin tuna (*Thunnus orientalis*), it is difficult to prepare newly fertilized eggs because of the difficulty of obtaining unfertilized eggs and sperm without sacrificing the parent fish. Other effective methods need to be developed.

In experiment 3, I investigated elapsed time from stripping to microinjection. In both fugu and red sea bream, the survival rate of injected eggs decreases more rapidly than non-injected eggs. The present results revealed a higher survival rate at an earlier time period after stripping: i.e., until 2.5 hours, both in fugu and red sea bream (**Fig. 1.2h-j**, **Fig. 1.3g-i**, **Table 1.3**, and **Table 1.6**). Therefore, it is concluded that microinjection needs to be carried out before 2.5 hours after stripping.

In experiment 3, the survival rate for the first injection of each trial varied: 50.5% in trial-I, 30.2% in trial-II, and 62.4% in trial-III with fugu eggs; 77.0% in trial-I, 38.3% in trial-II, and 38.4% in trial-III with red sea bream eggs (**Fig. 1.2h-j**, **Fig. 1.3g-i**, **Table 1.3**, and **Table 1.6**). One of the possible reasons for these differences is variation in egg quality. Egg quality is affected by maternal condition, for example, nutritional reserves, genetic variation [**13**], and degree of ripening [**14-16**]. To perform microinjection with a high survival rate of injected eggs, it may be important to select genetically superior parent fish which produce high quality eggs, and to determine the degree of ripening of the parent fish.

I also found an unexpected phenomenon that the survival rate of injected eggs

increased after several hours from stripping, for example, from 19.6% survival rate for the 3rd injection (90 min) to 51.6% for the 4th injection (120 min) in experiment T3 trial-I (**Fig. 1.2h** and **Table 1.3**). The reason for this remains unclear, but the increase of the survival rate may be related to the development of the egg in which the blastodisc is being constructed and the cell cycle is progressing dramatically. Further investigation is required to reveal the cause of this phenomenon.

Taking the present results from this study into consideration, I suggest a microinjection timeline with fugu as in **Fig. 1.4a**. Iwamatsu balanced salt solution or diluted sea water (from 1/2 to 1/12) as the soaking solution is recommended for obtaining a high survival rate after the microinjection treatment. After the first *in vitro* fertilization, microinjection can be continued until the egg chorion becomes too hard to penetrate with a glass needle and it becomes difficult to observe the inner part of the egg (ca. 15 minutes after *in vitro* fertilization). The subsequent *in vitro* fertilization needs to be performed before the cycle of microinjection has finished. This *in vitro* fertilization and microinjection cycle can be continued for 2.5 hours after stripping of eggs and sperm with a high survival rate of the injected eggs.

Figure 1.4b shows this established timeline for red sea bream microinjection. Leibovitz's L-15 medium, which is a cell culture medium, or Iwamatsu balanced salt solution are effective as soaking solutions. Microinjection needs to be performed until 10 minutes after *in vitro* fertilization, and the subsequent *in vitro* fertilization needs to be performed until the chorion becomes hard (ca. 10 minutes after fertilization). This *in vitro* fertilization and microinjection cycle can be continued for 2.5 hours after stripping with a high survival rate of the injected eggs.

Using this optimized microinjection methods, I have successfully established genome edited breeds with fugu and red sea bream. With fugu, 3760 eggs were microinjected in a day and 164 founder fish with mutations caused by genome editing were obtained [**chapter 3**]. With red sea bream, 1399 eggs were microinjected in a day and 104 founder fish with mutations caused by genome editing were obtained [**1, chapter 2**]. Therefore, this established method can be effectively used to generate genome edited fish. In the present study, I optimized the microinjection method into fertilized eggs for gene disruption mediated genome editing in marine aquaculture fish: fugu and red sea bream. Fish eggs are morphologically different among species, depending, for example,

on whether they are pelagic or demersal [**6-7**], on yolk distribution [**6**], and egg chorion thickness [**7**]. In the present study, I investigated three factors (soaking solution, elapsed time from *in vitro* fertilization, and elapsed time from stripping) to perform microinjection with as many eggs as possible in a day. This strategy will potentially be helpful for establishing microinjection methods for other marine fish species and contribute to basic and applied science using genome editing technology for various fish species.

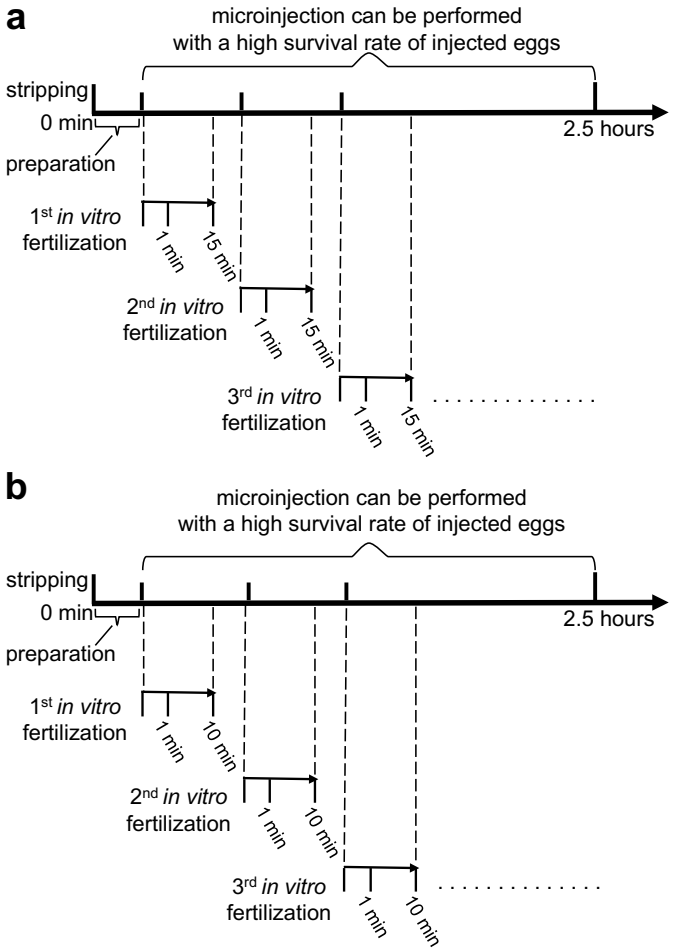

Fig. 1.4 Recommended timelines for the microinjection method

Timelines for the microinjection method which are recommended from the present results in fugu (a), and in red sea bream (b). (a) *In vitro* fertilization and microinjection can be carried out repeatedly on batches of eggs at intervals of 15 minutes for up to 2.5 hours after stripping using Iwamatsu solution or diluted seawater as the soaking solution in fugu experiment. (b) *In vitro* fertilization and microinjection can be carried out repeatedly on batches of eggs at intervals of 10 minutes for up to 2.5 hours after stripping using L-15 or Iwamatsu solution as the soaking solution in red sea bream experiment.

C1.6 References

1. Kishimoto, Kenta, et al. "Production of a breed of red sea bream Pagrus major with an increase of skeletal muscle muss and reduced body length by genome editing with CRISPR/Cas9." Aquaculture (2018).
2. Ansai, Satoshi, et al. "Efficient targeted mutagenesis in medaka using custom-designed transcription activator-like effector nucleases (TALENs)." Genetics (2013): genetics-112.
3. Ansai, Satoshi, and Masato Kinoshita. "Targeted mutagenesis using CRISPR/Cas system in medaka." Biology open 3.5 (2014): 362-371.
4. Edvardsen, Rolf B., et al. "Targeted mutagenesis in Atlantic salmon (Salmo salar L.) using the CRISPR/Cas9 system induces complete knockout individuals in the F0 generation." PloS one 9.9 (2014): e108622.
5. Dong, Zhangji, et al. "Heritable targeted inactivation of myostatin gene in yellow catfish (Pelteobagrus fulvidraco) using engineered zinc finger nucleases." PloS one 6.12 (2011): e28897.
6. Lønning, Sunniva, Elin Køjrsvik, and Inger-briti Falk-petersen. "A comparative study of pelagic and demersal eggs from common marine fishes in northern Norway." Sarsia 73.1 (1988): 49-60.
7. Sano, Kaori, et al. "Comparison of egg envelope thickness in teleosts and its relationship to the sites of ZP protein synthesis." Journal of Experimental Zoology Part B: Molecular and Developmental Evolution 328.3 (2017): 240-258.
8. Kato, Keitaro, et al. "Construction of an expression vector containing a β-actin promoter region for gene transfer by microinjection in red sea bream Pagrus major." Fisheries Science 73.2 (2007): 440-445.
9. Chisada, Shin-ichi, et al. "Myostatin-deficient medaka exhibit a double-muscling phenotype with hyperplasia and hypertrophy, which occur sequentially during post-hatch development." Developmental biology 359.1 (2011): 82-94.
10. Chiang, Yi-An, et al. "TALENs-mediated gene disruption of myostatin produces a larger phenotype of medaka with an apparently compromised immune system." Fish & shellfish immunology 48 (2016): 212-220.
11. Imai, Tadashi, et al. "Prevention of Adhesion of Tiger Puffer Takifugu rubripes Eggs to Experimental Tools by Use of Plastic Wrap and Polyethylene Pipette." Aquaculture Science 60.4 (2012): 511-513.
12. Kinoshita, Masato, et al. Medaka: biology, management, and experimental protocols. John Wiley & Sons, 2009.
13. Gjedrem, Trygve, Nick Robinson, and Morten Rye. "The importance of selective breeding in aquaculture to meet future demands for animal protein: a review." Aquaculture 350 (2012): 117-129.
14. Chuda, Hisashi, et al. "Development of the maturation-and ovulation-induction method in cultured tiger puffer Takifugu rubripes by hormonal treatments." Nippon Suisan Gakkaishi 63.5 (1997): 728-733.
15. Chuda, Hisashi, et al. "Relationship between post-ovulation time and fertilization rate of eggs in artificial insemination of tiger puffer, Takifugu rubripes." Nippon Suisan Gakkaishi (Japanese Edition) 64.6 (1998): 993-998.
16. Brooks, Suzanne, Charles R. Tyler, and John P. Sumpter. "Egg quality in fish: what makes a good egg?." Reviews in Fish Biology and fisheries 7.4 (1997): 387-416.

Chapter 2
Production of a breed of red sea bream *Pagrus major* with an increase of skeletal muscle mass and reduced body length by genome editing with CRISPR/Cas9

C2.1 Abstract

Genome editing is a powerful tool as a new breeding technology including for aquaculture because of the high efficiency of gene targeting without the requirement for exogenous gene integration. CRISPR/Cas9 system, a genome editing tool, has been widely used in various species due to its efficiency and flexibility. I demonstrated the establishment of a new breed of myostatin (*Pm-mstn*) complete knockout red sea bream (*Pagrus major*) using CRISPR/Cas9. This is the first report of the establishment of a new breed in aquaculture marine fish using genome editing. The mutations were formed by deletions in the first exon of the *Pm-mstn*, which cause disruption of the C-terminal active domain of MSTN. The breed exhibited a 16% increase of skeletal muscle, that is, an increase of edible parts. The breed showed the phenotype of short body length and small centrum, which is not observed in mice and other teleost fish. I established the homozygous gene disrupted breed in 2 years, which is far shorter than the conventional breeding method. The present study indicates that genome editing can accelerate the speed of aquaculture fish breeding.

C2.2 Introduction

In aquaculture fish breeding, it is a goal to generate fish with a valuable phenotype such as productivity, enhanced growth, and good taste. To lead to a desirable phenotype for breed improvement, I focused on a growth related factor, myostatin (MSTN), which is a member of the transforming growth factor beta superfamily and functions as a negative regulator of skeletal muscle mass [**1**]. The MSTN was identified as a responsible gene of double muscle phenotype in Piedmontese or Belgian Blue cattle breeds [**2**]. Mutations in the *mstn* gene have been frequently reported not only in double muscling mammals and but also in fish, cattle [**2-3**], mice [**1**], dog [**4**], human [**5**], medaka [**6-8**], and zebrafish [**9**]. Among them, the breeds of beef cattle, designated as Piedmontese and Belgian Blue [**1**], are naturally occurring mutants of the *mstn* and are popular food stuffs with increased meat. Therefore, fish breeds with *mstn* disruption are expected to show an increase of edible parts.

In the present study, I demonstrated the establishment of a fish breed with enhanced muscle production using one of genome editing tools, CRISPR/Cas9 [**10**] in marine aquaculture fish. The genome editing in *mstn* (*Pm-mstn*) was performed in red sea bream, which is a major aquaculture fish in Japan [**11**]. The production of aquaculture of red sea bream in Japan was 67,200 ton in 2016. I established the red sea bream breed with increased skeletal muscle mass in only two years, which is the shortest maturation period of this species.

C2.3 Materials and methods

2.3.1 Ethics statement

This study was conducted in accordance with the Regulations for Animal Experiments of Kyoto University. The fish handling and sampling methods were approved by Kyoto University (No.28-45). All efforts were made to minimize suffering.

2.3.2 Identifying red sea bream myostatin gene

Red sea bream myostatin genes (*mstn*) were searched from the whole genome sequence [unpublished data] of red sea bream broodstock in Kindai University by BLASTP search using red sea bream *mstn* (DDBJ, accession number; AY965686). Then, the phylogenetic

tree of *mstn* was constructed using the protein sequence by the Neighbor-Joining method with MEGA7 (http://www.megasoftware.net). The bootstrap consensus tree inferred from 1000 replicates was taken to represent the evolutionary history of these analyzed genes. The synteny analysis of *mstn* was performed with Genomicus (ver. 91.01, http://www.genomicus.biologie.ens.fr/).

2.3.3 Experimental fish and microinjection for introducing CRISPR/Cas9 system

Unfertilized eggs and sperm of red sea bream were collected from broodstock in Kindai University by the stripping method. The collected unfertilized eggs and sperm were preserved until *in vitro* fertilization by preventing eggs from drying at 17-20°C and on ice, respectively [**12, 13 (chapter 1)**]. *In vitro* transcriptions of Cas9 RNA and sgRNAs were performed by the method of previous report [**14**]. Two sgRNAs were designed in *Pm-mstn* exon 1 (named as sgRNA1 and sgRNA2), and one kind of sgRNA was designed in *Pm-mstnb* exon 1. The mixture of RNAs, 100 ng/μl of Cas9 RNA and 25 ng/μl of each sgRNA targeted *Pm-mstn*, was microinjected into the cytoplasm of the fertilized eggs. The mixture of RNAs, 100 ng/μl of Cas9 RNA and 50 ng/μl of sgRNA targeted *Pm-mstnb* or 100 ng/μl of Cas9 RNA and 50 ng/μl of both sgRNA1 targeted *Pm-mstn* and sgRNA targeted *Pm-mstnb*, was microinjected for the disruption of *Pm-mstnb* or both *Pm-mstn* and *Pm-mstnb*, respectively. Microinjection was performed by the method established in the previous study [**chapter 1**, **13**]. In brief, microinjection was performed using Leibovitz's L-15 medium (Invitrogen) as a soaking solution of fertilized eggs within 1-10 minutes after *in vitro* fertilization until 2 hours after stripping unfertilized eggs and sperm. The injected eggs were incubated in sea water at 17-20°C to hatching.

2.3.4 Detecting mutations using heteroduplex mobility assay (HMA) in first generation (G_0) fish

First, genomic DNA was extracted from whole embryo, caudal fin, or pectoral fin using the alkaline lysis buffer method [**14**]. Second, a 258-bp fragment including the genomic target site of the *Pm-mstn* was amplified with KOD-FX DNA polymerase (TOYOBO, Osaka, Japan) using primers, *Pm-mstn*-hmaFw and *Pm-mstn*-hmaRv (primer list in **Table 2.8**). And, a 203-bp fragment of the *Pm-mstnb* was amplified as above using primers, *Pm-mstnb*-hmaFw and *Pm-mstnb*-hmaRv (**Table 2.8**). Finally, HMA was performed by

analyzing the PCR products using a microchip electrophoresis system (MCE-202 MultiNA) and the DNA-500 reagent kit (Shimadzu, Kyoto, Japan). The G_0 fish were categorized by the degree of multiple band patterns, termed as heteroduplex, using the following criteria; intact wild type band was reduced to under 80% in "high" fish, 80-100% in "low" fish, and was observed at 100% in "none" fish.

2.3.5 Amplicon sequencing of target region in G_0 fish

From muscle, brain, liver, and gonad, the genomic DNA was extracted by a conventional phenol-chloroform method. From pectoral fin, the genomic DNA was extracted as described above. The target regions were amplified with KOD-FX with the following primers, sgRNA1-ampFw or sgRNA2-ampFw with 8-bp random index sequence to 5-prime end for identifying subjects, and sgRNA1-ampRv or sgRNA2-ampRv, respectively (**Table 2.8**). Sequencing analysis of the mixture of the PCR amplicons was performed by paired-read sequencing (100-bp × 2 Gb) with HiSeq 2500 and TruSeq DNA PCR-Free Library Prep Kit (Illumina Inc., San Diego, USA). The sizes of the PCR amplicons were 90-bp and 80-bp including targeted site by sgRNA1 and sgRNA2, respectively. As the control reference, the PCR product from wild type fish was subjected to the sequencing. Induced mutations in each subject were identified by assembling output data using PEAR 0.9.8 [**15**] and classified into each subject and each variant using the 8-bp index. When classifying the assembled data, variants with only one read counts were cut off as errors. The minimum read count per one subject was 2462 (maximum was over 20 k reads). The variations and frequencies of variants were identified after assembling and classifying by alignment and calculation (each variant read counts / total read counts).

2.3.6 Production of F_1 fish

For assessment of the germ line transmission rate, the gametes of G_0 fish were fertilized with that of wild type counterparts, and then genomic DNA was extracted from each embryo. Mutation in each embryo was analyzed by HMA and direct sequencing analysis after PCR amplifying the target region with KOD-FX using primers; *Pm-mstn*-hmaFw and *Pm-mstn*-hmaRv (**Table 2.8**). For producing F_1 fish, the G_0 fish with high mutation frequency in pectoral fin (details are described in results "2.4.3 Selection of highly mutated G_0 individuals") were naturally mated in a 7-ton tank. The resulted F_1 embryos

were reared for further experiments.

2.3.7 Screening of F_1 fish with HMA and sequencing

First, genomic DNA was extracted from pectoral fin or caudal fin in each F_1 fish, which was subjected to PCR amplification of the target region with KOD-FX using primers; *Pm-mstn*-hmaFw and *Pm-mstn*-hmaRv (**Table 2.8**). Second, the PCR products were mixed with an equal amount of the PCR product from wild type. Then, the mixture was denatured at 95°C for 5 min, and re-annealed by cooling to 25°C. Third, the PCR products ("P") and the re-annealed products ("R") were subjected to HMA [**14**]. Wild type shows both "P" and "R" as single bands. Heterozygote shows both "P" and "R" have the same heteroduplex band pattern. Homozygote shows "P" as a single band, but "R" as a heteroduplex band pattern. I also selected compound heterozygote which harbors the different type of frame-shift mutations in each allele. Compound heterozygote shows both "P" and "R" are heteroduplex band patterns, but "R" pattern is different from "P" pattern. To confirm mutation sequences, the PCR products of wild type and homozygote were subjected to direct sequencing, and those of heterozygote and compound heterozygote were subjected to amplicon sequencing (details in Materials and Methods "2.3.5 Amplicon sequencing of target region in G_0 fish"). Finally, to investigate the occurrence of several-hundred-bp large deletions, an 820-bp fragment was amplified from the genomic DNA using primers, large-delFw and large-delRv (**Table 2.8**). The PCR products were subjected to electrophoresis analysis using 1% agarose gel.

2.3.8 Assessment of increase in skeletal muscle

To observe the phenotype in G_0 of disruption of *Pm-mstn*, *Pm-mstnb*, or both *Pm-mstn* and *Pm-mstnb*, fork length (FL) and body weight (BW) were measured on the following days old [*Pm-mstn* G_0 injected with sgRNA1: at 165 days old, *Pm-mstn* G_0 injected with sgRNA2: at 183 days old, *Pm-mstnb* G_0, and both *Pm-mstn* and *Pm-mstnb* G_0: at 163 days old]. To observe the effect of *Pm-mstn* disruption in F_1 fish, FL, BW, and body width of homozygote ($mstn^{-8a/-8a}$), heterozygote ($mstn^{-8a/wt}$), and wild type ($mstn^{wt/wt}$) were measured at 133, 170, 208, 235, 300, 359, 432, and 559 days old. These fish were hatched on the same day and reared in a tank. The phenotype of another genotype of mutants ($mstn^{-14/-14}$ and $mstn^{-14/wt}$), compound heterozygotes ($mstn^{-8a/-14}$ and $mstn^{-8a/-8b}$), and wild

type (*mstn*$^{wt/wt}$) were also evaluated at 217 days old. These fish hatched on the same day and were reared in a tank. *Mstn*$^{-8b}$ has a differently mutated allele from *mstn*$^{-8a}$. Condition factor was calculated as 1000×BW/FL^3 (BW in g, FL in cm).

2.3.9 Computed tomographic (CT) analysis

To investigate the effect of *Pm-mstn* disruption on skeletal muscle increase and bone structure, the compound heterozygotes (*mstn*$^{-8a/+22}$, *mstn*$^{-8b/-8c}$, and *mstn*$^{-14/+2}$: genotypes are described in **Table 2.6**) were subjected to CT analysis because they showed the same phenotypes as *mstn*$^{-8a/-8a}$ and *mstn*$^{-14/-14}$, that is, short FL and high condition factor. Seven compound heterozygotes (FL: 24.14 ± 0.75 cm, BW: 471.88 ± 68.92 g) and seven wild type fish (FL: 26.64 ± 0.69 cm, BW: 447.37 ± 33.27 g) were analyzed at 448 days old. These measured values are consistent with those of the population of fish in **Figs. 2.5** and **2.6a-d** since these mutants showed shorter fork length ($P < 0.001$, by Student's *t*-test) and almost the same body weight ($P = 0.4$, by Welch's *t*-test) in comparison with wild type. The CT 3D data were acquired using Ingenuity Core CT scanner (Philips, Amsterdam, Netherlands). The parameters in Ingenuity Core were configured as follows; [body soft helical mode: thickness; 0.67 mm, increment; -0.33 mm, KV; 120 K, mAs/slice; 200 mA, resolution; standard, collimation; 64×0.625, pitch; 0.203, rotation time; 0.75 s, FOV; 150×150 mm, reconstruction; standard (B), enhancement; 0.0, window; C 20 W 200, center; X 0 Y 0, matrix; 512] and [recon bone mode: thickness; 0.67 mm, increment; -0.33 mm, FOV; 150×150 mm, reconstruction; standard, enhancement; 0.75, window; C 600 W 3000, Center; X 0 Y 0, matrix; 512, filter; Y-Detail (YB)]. The CT cross-sectional and volumetric analyses in skeletal muscle were performed using Avizo 7.0 (FEI Visualization Sciences Group, Oregon, USA). The muscle cross-sectional slices were made in the nearest slice to the first spine of the dorsal and anal fin, respectively (**Fig. 2.6e-1** and **e-2**, white arrow in **Fig. 2.6e-3**). Then, the muscle volume region was manually segmented from otolith to caudal fin (excluding ventral region because of the difficulty of segmentation) (blue region in **Fig. 2.6e-3**), respectively. The length of head, the size of centrum, and the length of neural spine were measured using imageJ (https://imagej.nih.gov/ij/) (details in **Fig. 2.8d-1** and **d-2**).

2.3.10 Off-target analysis

Off-target candidates were searched from whole genome sequence with Cas-OFFinder [**16**] using the following criteria described in previous report [**14**]; harboring 2- or fewer-bp mismatches in the 18-bp targeting sequence followed by a NRG PAM. The regions of off-target candidates were PCR amplified with KOD-FX using primers described in **Table 2.8.** The PCR products were subjected to HMA and direct sequencing analysis.

2.3.11 Statistical analysis

Data were expressed as mean ± standard deviation (SD). Statistical analyses for condition factor, body weight, and fork length in *Pm-mstn* G_0 were carried out by Tukey-Kramer HSD test. Statistical analyses for condition factor, body weight, and fork length in "*Pm-mstnb*", and "*Pm-mstn* and *Pm-mstnb*" G_0 were carried out by Student's *t*-test. Statistical analyses for condition factor, body weight, fork length, body width in *Pm-mstn* F_1 were carried out in each measurement point by Tukey-Kramer HSD test. Statistical analyses for muscle cross-sectional area, muscle volume, A-P length, D-V length, width, neural spine length, and head length in compound heterozygotes were carried out *t*-test. Differences were considered significant in the case of $P < 0.05$.

C2.4 Results

2.4.1 Identifying red sea bream myostatin gene

To increase the edible part (fish meat), I focused on myostatin (MSTN), the deficiency of which leads to a double muscle phenotype. I searched the MSTN gene (*mstn*) of red sea bream from the whole genome sequence using BLASTP (details are in Materials and methods "2.3.2 Identifying red sea bream myostatin gene"). Unlike mammals, many teleost fish have more than one copy of *mstn* in their genome by genome duplication [**17**]. The paralogous gene does not act as a negative regulator of skeletal muscle mass. I also acquired two candidates of *mstn* in the red sea bream genome and then subjected them to constructing a phylogenic tree using the predicted protein sequence. One candidate, designated as *Pm-mstn*, belonged in the same monophyly of fish myostatin genes (for example, medaka BAI53537 and zebrafish AAQ11222) which have been revealed to play a major role in regulating muscle mass [**6-9**] (**Fig. 2.1a**). The *Pm-mstn* presented a conserved synteny with *mstn* of medaka (BAI53537), tiger pufferfish (fugu, ADT89782),

zebrafish (AAQ11222), cattle (BAB79498), mouse (AAI03679), and human (AAB88694) (**Fig. 2.1b**). The other candidate, *Pm-mstnb*, presented a conserved synteny with *mstn* of tiger pufferfish (AAR88254) and zebrafish (AAV11222) (**Fig. 2.1c**). These results indicate that *Pm-mstn* belongs to *mstn* which is a negative regulator of skeletal muscle mass and *Pm-mstnb* belongs to *mstn* paralogous gene generated by genome duplication.

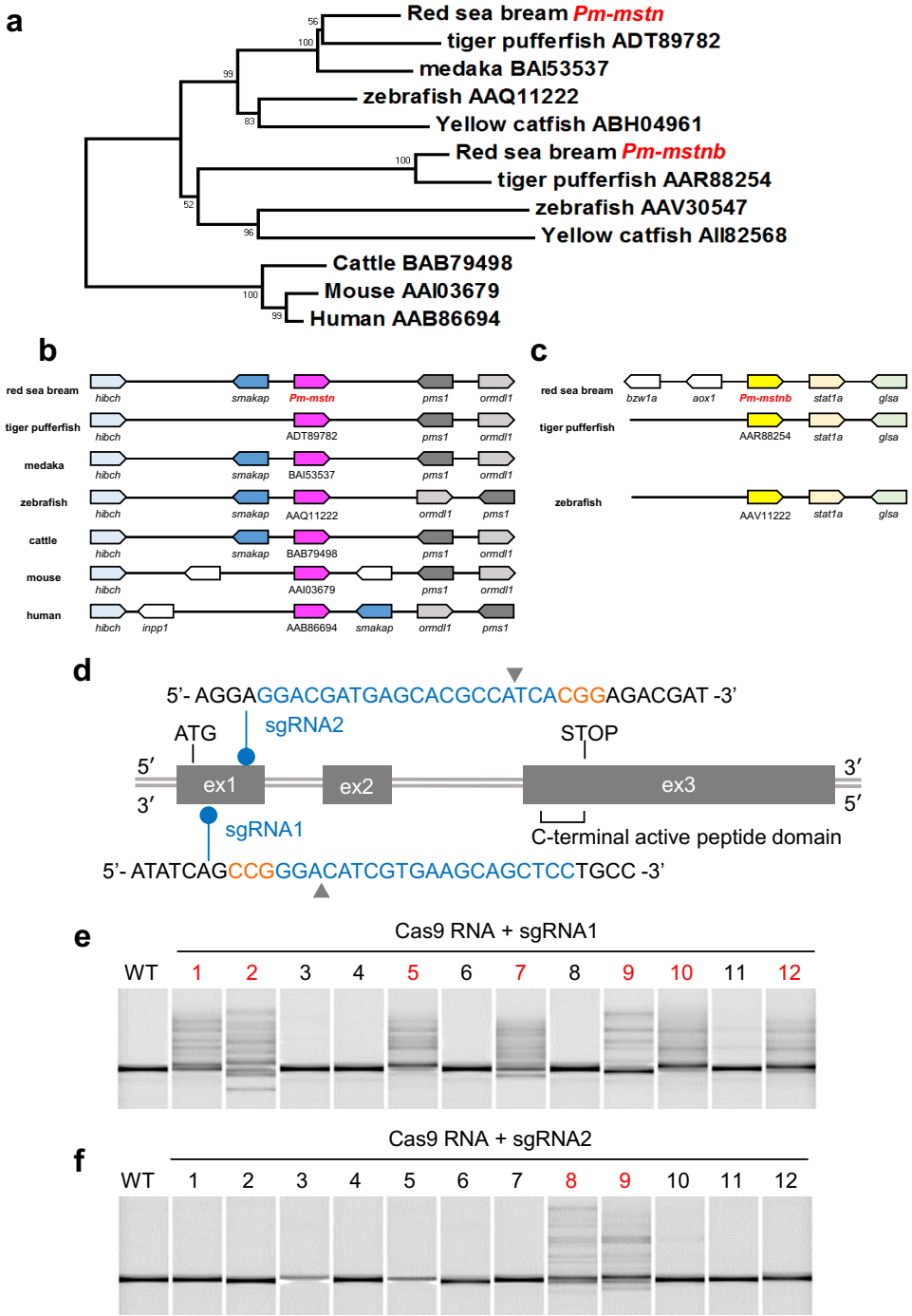

Fig. 2.1 Cloning of *mstn* and somatic mutagenesis analysis in embryos

(a) Phylogenic tree of *mstn*. The percentage of replicate trees in which the associated genes clustered together in the bootstrap test is shown next to the branches. (b, c) Synteny analysis of *mstn*. Genes are depicted by colored polygons and transcriptional orientation is indicated at the angled end. Gene names are indicated under the polygons, and orthologs across species are in the same colors; *Pm-mstn* ortholog in magenta, *Pm-mstnb* ortholog in yellow. The *mstn* sequences of different animals were retrieved from the GenBank database and the accession numbers are shown to the right of the animal names in (a), under the polygons (b, c). (d) Design of the target site for sgRNAs in *Pm-mstn*. The sgRNAs are designed in exon 1. The sgRNA1 was designed in a complementary strand. Gray boxes and bars, exons and introns, respectively. Blue and orange letters, target sequence and NGG protospacer adjacent motif (PAM), respectively. Gray triangles, the cleavage sites recognized by Cas9 nuclease. Exon 3 includes C-terminal active peptide domain of MSTN. The electrophoresis images of HMA in embryos injected with sgRNA1 (e), injected with sgRNA2 (f) [the left edge lanes: wild type, each lane: each embryo injected with Cas9 RNA and sgRNA, lanes with red letter: the embryos with mutations].

2.4.2 Production of Pm-mstn knockout red sea bream

In order to produce mutants in the G_0 generation (G_0), two sgRNAs (sgRNA1 and sgRNA2) were designed in the first exon of *Pm-mstn* so that the C-terminal active peptide domain was completely disrupted (**Fig. 2.1d**). Each sgRNA was microinjected into 966 and 1399 fertilized eggs with Cas9 nuclease RNA, respectively (**Table 2.1**). Using replicates of 12 embryos at 1-2 days post fertilization (dpf), the efficiency of induction of mutation on the target site was investigated using heteroduplex mobility assay (HMA) [**18-19**]. Multiple banding patterns were observed in 7 or 2 out of each replicate of 12 embryos injected with sgRNA1 or sgRNA2, respectively (**Fig. 2.1e** and **f**), revealing that these designed CRISPR/Cas9 systems were effective for disrupting *Pm-mstn*. I incubated the remaining eggs and reared the subsequent hatching larvae continuously (sgRNA1: 569 larvae, and sgRNA2: 628 larvae, **Table 2.1**).

Table 2.1 Summary of *Pm-mstn* mutagenesis mediated genome editing (CRISPR/Cas9) from microinjection to mutant categorization in G_0

Injection	No. of injected eggs	No. of hatched larvae[a]	No. of fish in mutant categorization			
			Surviving fish[b]	Mutation level		
				high	low	none
sgRNA1	966	569 (62.7%)	218 (22.6%)	94	25	99
sgRNA2	1399	628 (44.6%)	212 (15.2%)	88	16	108

The hatching rates in control (without injection) were 96.3% when injection of sgRNA1, and no data when injection of sgRNA2.

[a] Percentages indicate number of hatched larvae / number of injected eggs.

[b] Percentages indicate number of surviving fish at 5.5 or 6 mph / number of injected eggs.

2.4.3 Selection of highly mutated G_0 individuals

Since the induced mutation level varied among the microinjected embryos (**Fig. 2.1e-f**), the mutation level of all injected fish at 5.5 to 6 months post fertilization (mpf) (total length: about 10 cm) was evaluated by HMA with the genomic DNA prepared from caudal fin and classified into three groups: "high" is highly mutated, "low" is slightly mutated, "none" is no mutation (sgRNA1: 94 "high", 25 "low", and 99 "none", sgRNA2: 88 "high", 16 "low", and 108 "none") (**Table 2.1**). In addition, to evaluate the increase of skeletal muscle mass, the condition factor (body weight / fork length^3 × 10^3) of each fish was calculated. The "high" of both sgRNA1 and sgRNA2 injected showed higher value of condition factor than "none" (sgRNA1: 24.8 ± 1.6 in "high" and 23.6 ± 1.4 in "none, sgRNA2: 26.5 ± 1.9 in "high" and 24.8 ± 1.3 in "none") (**Table 2.2**). To save breeding space and cost, only highly mutated individuals were continued to be reared (total 182 fish). The correlation between frame-shift mutation (meaning gene disruption) and condition factor in *Pm-mstn* was investigated using the "high" individuals. The DNA fragment including the target site of each fish was amplified by PCR using genomic DNA prepared from the pectoral fin and was subjected to amplicon sequencing with NGS, and then the "Frame-shift mutation rate" was calculated (number of frame-shift amplicon reads / number of total amplicon reads). The tendency was observed that the skeletal muscle mass (value of condition factor) increased as the frame-shift mutation rate increased (y=4.2x-78.9 in sgRNA1, and y=6.1x-125.7 in sgRNA#2), though the correlation coefficients were not high (r=0.25 and r=0.45, respectively) (**Fig. 2.2**). In some individuals, *Pm-mstn* was disrupted strongly in pectoral fin without increasing of skeletal muscle mass (**Fig. 2.2**).

Table 2.2 Morphological analysis by measurement of G_0 fish

sgRNA	sgRNA1*[1]			sgRNA2*[2]		
Mutation level*[3]	high	low	none	high	low	none
No. of fish	94	25	99	88	16	108
Fork length (cm)	14.6 ± 0.8	14.7 ± 0.5	14.8 ± 0.7	16.0 ± 1.0^a	16.4 ± 1.3^{ab}	16.6 ± 0.8^b
Body weight (g)	78.3 ± 12.6	77.1 ± 10.1	77.2 ± 11.8	109.0 ± 19.8	111.7 ± 22.2	113.9 ± 17.8
Condition factor	24.8 ± 1.6^a	24.0 ± 1.8^{ab}	23.6 ± 1.4^b	26.5 ± 1.9^a	24.9 ± 0.7^b	24.8 ± 1.3^b

^{ab}: Means with different superscripts were significantly different among the three groups in each sgRNA group ("high", "low", and "none") with Tukey-Kramer HSD test, $P < 0.05$. Values ± standard deviation.
*1: measurement was performed at 165 days old.
*2: measurement was performed at 183 days old.
*3: categorized with finclip and HMA.

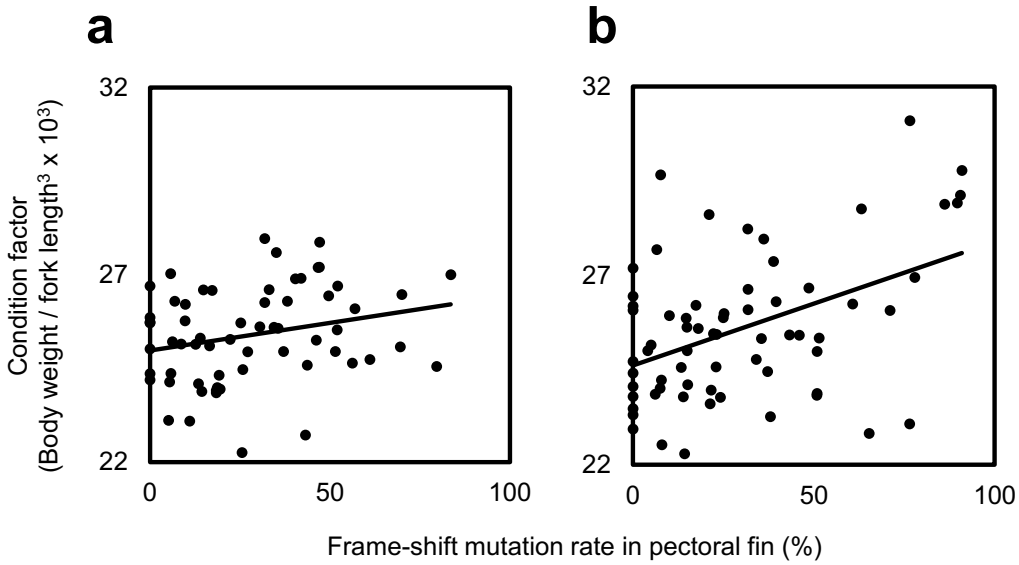

Fig. 2.2 The correlation between increase of skeletal muscle and gene disruption rate in pectoral fin in G_0

(a) Fish injected with sgRNA1. (b) Fish injected with sgRNA2. Condition factor was calculated by body weight / fork length^3 x 10^3. The results of amplicon sequencing in wild type included over 97% from WT. In the frame-shift rate calculation, the sequence variants over 5 % were used as major mutations (frame-shift mutation read number / all sequence read number). The approximate straight lines of a and b were as y=4.2x-78.9 (r=0.25) and y=6.1x-125.7 (r=0.45), respectively. With the increased rate of gene disruption in pectoral fin, a tendency for the condition factor value to increase was observed.

2.4.4 Gene disruption of the paralogue gene Pm-mstnb

To investigate the contribution of the paralogue gene, *Pm-mstnb*, to the double muscle phenotype, disruption of *Pm-mstnb* (Experiment 1) and double disruption of *Pm-mstn* and *Pm-mstnb* (Experiment 2) were conducted. At 163 days post hatch, the mutation level and condition factor of each G_0 individual were investigated. The mutation levels in each fish were evaluated with HMA using genome DNA derived from caudal fin. In Experiment 1, the G_0 fish were classified into two groups of "*Pm-mstnb* high" and "none". In Experiment 2, the G_0 fish were classified into two groups of "*Pm-mstnb* and *Pm-mstn* high" and "none". There was no difference in the value of condition factor between "*Pm-mstn* high" (24.0 ± 2.6) and "none" (24.0 ± 2.1) groups. On the other hand, a significant difference was observed between "*Pm-mstn* and *Pm-mstnb* high" (28.9 ± 4.3) and "none" (25.0 ± 1.5) groups (**Table 2.3**). These findings indicate that *Pm-mstnb* is not responsible for increasing skeletal muscle mass.

Table 2.3 Myostatin paralogous gene disruption

	Experiment 1		Experiment 2	
Mutation level[b]	*Pm-mstnb* high	none	*Pm-mstna* and *Pm-mstnb* high	none
No. of fish	82	47	15	8
Fork length (cm)	14.6 ± 1.3	14.5 ± 1.3	14.3 ± 1.4	15.6 ± 1.5
Body weight (g)	75.2 ± 17.8	74.5 ± 18.7	85.0 ± 19.6	95.6 ± 25.0
Condition factor	24.0 ± 2.6	24.0 ± 2.1	28.9 ± 4.3[a]	25.0 ± 1.5

Measurement was performed at 163 days old.
Values ± standard deviation
[a]; Means with superscript was significantly different between the two groups in each experiment ("high" and "none") with Student's *t*-test, $P < 0.05$.
[b]; categorized with finclip and HMA.

2.4.5 Estimating mutation mosaicism in G_0 fish

Unlike in mammals [**20**], in fish, it is reported that many types of mutation exist in a G_0 individual after genome editing treatment [**14**]. And, it was considered that the ratio of each mutation type varies among tissues in an individual. Indeed, in this study, multiple bands were observed in an embryo in HMA (**Fig. 2.1e-f**) and frame-shift mutation did not have a complete correlation with the value of condition factor (index of increasing muscle mass) (**Fig. 2.2**). These results suggest that a high mosaicism of *Pm-mstn* disruption occurred in this study. To confirm such mosaicism, amplicon sequencing of five tissues (brain, liver, muscle, gonad, and pectoral fin) was performed in each individual belonging to the three different mutation levels in pectoral fin ("Strong", "Intermediate", and "Weak" in **Fig. 2.3**). The frequencies of intact wild type among five tissues are 0-3.4% in "Strong", 5.0-40.0% in "Intermediate", and 34.8-71.7% in "Weak" (black column in **Fig. 2.3**). The frequency of each variant varied among tissues. For example, the frequencies of -8a of mutation in "Strong" were 24.7% in brain, 11.7% in liver, 0% in muscle, 4.6% in gonad, and 0% in pectoral fin (red column in **Fig. 2.3**). The frequencies of intact wild type and each variant were not completely consistent among tissues, but were similar. From these results, it is likely that the frequency of each variant and wild type in fin is reference for that in another tissue (e.g. muscle or germ cell).

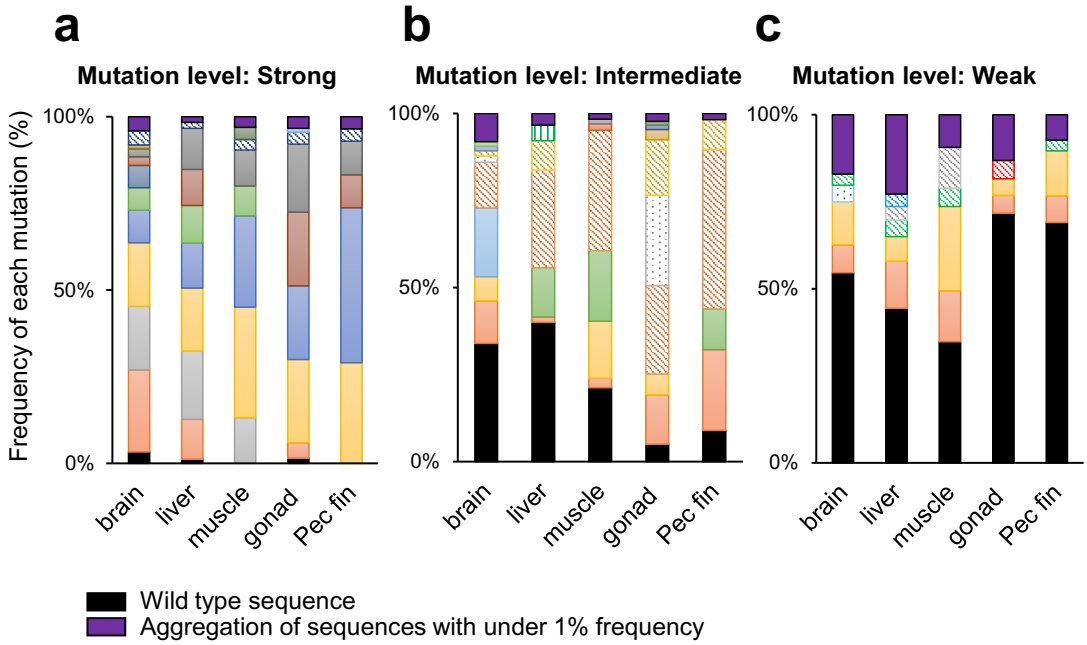

Fig. 2.3 The mosaicism of mutations among different tissues

The rate of each mutation variant in five tissues (brain, liver, muscle, gonad, and pectoral fin) in individuals. The analysis was performed for three individuals which harbor mutations at different levels (a; Strong, b; Intermediate, c; Weak). In the calculation of each mutation rate, the sequence variants over 1% were used as major mutations (each mutated read number / all sequence read numbers). The column which is a specific color and pattern indicates a different mutation variant. Black and purple column, wild type and aggregation of variants with under 1% frequency, respectively.

2.4.6 Inheritance of mutations to F_1 generation

At two years after microinjection, these genome edited red sea bream began to spawn. As a preliminary experiment to produce F_1 generation, gametes from 7 G_0 individuals were artificially inseminated with counterpart gametes from wild type fish, and then the mutation rate in *Pm-mstn* in each F_1 embryo was investigated by HMA and sequencing. In 5 (one female and four males) out of 7 G_0 fish, mutations were observed in F_1 embryos. The germ line transmission rates were from 100% in male #1 to 12.5% in male #4 (**Table 2.4**). Each founder fish harbored 2-6 types of mutation in germ line and several mutation types (e.g. -8a and -14) were the frame-shift mutation causing gene disruption (**Fig. 2.4b, e** and **Table 2.4**). The representative mutation patterns in germ line are showed in **Fig. 2.4**. The variation and frequencies of mutation type differed between pectoral fin and germ line (**Fig. 2.4**). For example, in female #1, 1-base deletion was observed at 12.5%

in germ line, but not observed in pectoral fin (**Fig. 2.4b** and **c**). In male #3, 8-base deletion was observed at 56.3% in germ line, but not observed in pectoral fin (**Fig. 2.4e** and **f**). The individuals which harbored mutations in germ line (100% in male #1, 87.2% in male #2, 81.3% in male #3, 12.5% in male #4, and 66.7% in female #1) showed high mutation rate in pectoral fin (35.1%, 99.4%, 66.8%, 48.7%, and 47.6%, respectively). On the contrary, individuals without germ line transmission showed low mutation rate in pectorain (3.9% in male #5 and 2.5% in male #6).

Table 2.4 Germ line transmission of G_0 fish

Fish	sgRNA	Germ line transmission	Mutations (in/del)	Mutation rate in fin
male #1	2	16/16 (100%)	-3, -6	35.1%
male #2	2	34/39 (87.2%)	-27, -23, -60, -23, -8b	99.4%
male #3	2	13/16 (81.3%)	-8b, -27, -3, -4	66.8%
male #4	2	2/16 (12.5%)	-14, -3	48.7%
male #5	2	0/16 (0%)	none	3.9%
male #6	2	0/16 (0%)	none	2.5%
female #1	1	16/24 (66.7%)	-8a, -1, -8c, -5, -9, -5	47.6%

The alphabet letters with in/del mutations were added for identifying variants (-8a, -8b, and -8c).

a

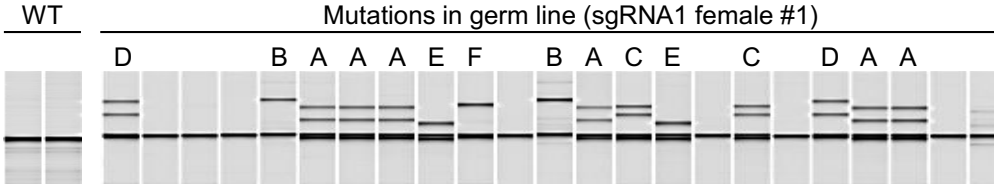

b

Mutations in germ line (sgRNA1 female #1)

ATCAGCCGGGACATCGTGAAGCAGCTCC	WT	8/24	33.3%	
ATCAGCCGGGA-------AGCAGCTCC	-8a	6/24	25%	A
ATCAGCCGGGA-ATCGTGAAGCAGCTCC	-1	3/24	12.5%	B
ATCAGCCG------TGAAGCAGCTCC	-8c	2/24	8.3%	C
ATCAGCCG-----TCGTGAAGCAGCTCC	-5	2/24	8.3%	D
ATCA---------TCGTGAAGCAGCTCC	-9	2/24	8.3%	E
ATCAGCC-----ATCGTGAAGCAGCTCC	-5	1/24	4.2%	F

c

Mutations in pectoral fin (sgRNA1 female #1)

ATCAGCCGGGACATCGTGAAGCAGCTCC	WT	8412/16068	52.6%	
ATCAGCCGGGA-------AGCAGCTCC	-8a	3515/16068	21.9%	*
ATCAGCCG------TGAAGCAGCTCC	-8c	1927/16068	11.9%	*
ATCA---------TCGTGAAGCAGCTCC	-9	656/16068	4.1%	*
ATCAGCCGGG--ATCGTGAAGCAGCTCC	-2	306/16447	1.9%	
ATCAGCCGGGAAGCAGTGAAGCAGCTCC	-4+4	171/16447	1.1%	
ATCAGCCGGGA--CATCGTGAAGCAGCT	WT			
ATCAGCCGGGAAGCATCGTGAAGCAGCT	+2	470/16447	4.5%	

d

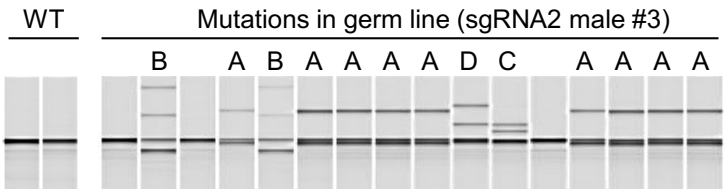

e

Mutations in germ line (sgRNA2 male #3)

GTGGTTATGGAGGAGGACGATGAGCACGCCATCACGGAG	wt	3/16	18.8%	
GTGGTTATGGAGGAGGACGATGAG--------CACGGAG	-8b	9/16	56.3%	A
GTGG--------------------------TCACGGAG	-27	2/16	12.5%	B
GTGGTTATGGAGGAGGACGATGAGCACGCCA---CGGAG	-3	1/16	6.3%	C
GTGGTTATGGAGGAGGACGATGAGCACGC----ACGGAG	-4	1/16	6.3%	D

f

Mutations in pectoral fin (sgRNA2 male #3)

GTGGTTATGGAGGAGGACGATGAGCACGCCATCACGGAG	wt	2541/7755	32.8%	
GTGGTTATGGAGGAGGACGATGAGCACGCCGTCACGGAG	-1+1	2959/7755	38.2%	
GTGGTTATGGAGGAGGACGATGAGCACG------CGGAG	-6	408/7755	5.3%	
GTGGTTATGGAGGAGGACGATGAGCACGCCA---CGGAG	-3	88/7755	1.1%	*
AGCACGCCA----------TCACGGAG	wt			
AGCACGCCAGACGATTTTCACGAGACGATTTTCACGGAG	+22	1078/7755	13.9%	
TTATGGAGGAGGACGATGAGCACGCCATC---ACGGAGA	wt			
TTATGGAGGAGGACGATGAGCACGCCATCGTCACGGAGA	+3	447/7755	5.8%	

Fig. 2.4 Germ line and somatic mutagenesis

Each G_0 fish was mated with a wild type to screen for heritable mutations. Mutation sequences identified in each F_1 embryo by HMA (a, d) and direct sequencing (b, e). Somatic mutation sequences identified in pectoral fin by amplicon sequencing (c, f). a and b are results in embryos from mating wild type and female injected with sgRNA1 (sgRNA1 female #1 in **Table 2.4**). d and e are results in embryos from mating wild type and male injected with sgRNA2 (sgRNA2 male #3 in **Table 2.4**). The alphabet letters above each lane in the electrophoresis images (a, d) indicate the type of mutation in the sequences (b, e). (b, c, e, f). This is shown in order of sequences, the sizes of deletions (−) and insertion (+), numbers (each mutated embryo / all analyzed embryos, or each mutated read count / all read counts), the percentage. Asterisks in c and f indicate the mutations observed also in the germ line. Blue and orange letters, target sequence and PAM, respectively. Red dashes and letters, deletions and insertions. Under bars, microhomologies.

2.4.7 Establishment of a complete gene disrupted breed

At 2-years old, 122 out of 182 G_0 fish classified to "high" group in Results "3.3 Selection of highly mutated G_0 individuals" survived. Because of observation of germ line transmission as mentioned above, mass mating of these G_0 fish was performed to obtain the complete knockout F_1. Fertilized eggs were collected by overflow trapping system for 6 days (2016/04/07, 11, 13, 30, and 05/02, 03). These F_1 fish which contained homozygote, heterozygote, compound heterozygote, and wild type, were reared. At 4.5-6 mpf, a total 1,311 F_1 were genotyped by HMA and DNA sequencing. Finally, 39 homozygote gene disrupted fish (2.9%) were successfully identified. Thus, *Pm-mstn* gene disrupted breeds were established. There were six types of mutation sequence in the homozygous mutants as listed in **Table 2.5**. Out of the six mutation types, four were induced via microhomology mediated joining (MMEJ) [**18**, **26**] (sgRNA1: -8a, sgRNA2: -14, -8b, and -23). I also found compound heterozygote (*Pm-mstn* in one allele was disrupted and *Pm-mstn* in the other allele was disrupted by another type of mutation), heterozygote (*Pm-mstn* in one allele was disrupted, but *Pm-mstn* in the other allele was intact) and wild type in F_1 fish.

Table 2.5 Homozygote successfully obtained in F_1 fish

Mutation	sgRNA	Sequence (5'--3')[*a, b, c]	No. of fish	Double muscle phenotype[*d]
-8a	1	AG**CCGGGACATCGTGAAGCAGCTCC**TGCCCAAAG AGCCGGGA--------AGCAGCTCCTGCCCAAAG	8	yes
-23	1	AG**CCGGGACATCGTGAAGCAGCTCC**TGCCCAAAG AGCCGGGA----------AAG	4	yes
-2	1	AG**CCGGGACATCGTGAAGCAGCTCC**TGCCCAAAG AGCCGG--CATCGTGAAGCAGCTCCTGCCCAAAG	3	no data
-14	2	GA**GGACGATGAGCACGCCATCACGG**AGACGATTA GAGGACGATGAGC----------ACGATTA	18	yes
-8b	2	GA**GGACGATGAGCACGCCATCACGG**AGACGATTA GAGGACGATGAG--------CACGGAGACGATTA	4	yes
-23	2	GA**GGACGATGAGCACGCCATCACGG**AGACGATTA GAG----------GACGATTA	2	no data

-8a and -8b: alphabet letters are used to differentiate each mutation.
[a] An upper and a lower line indicate wild type sequence and mutated sequence, respectively.
[b] The target sites by sgRNA are 3-25 bases to the left, indicating bold lines.
[c] Underlines indicate microhomology.
[d] Double muscle phenotype indicates increase of condition factor. "no data" indicates analysis was not carried out because of the small number, however the appearances were the same as the other homozygote.

2.4.8 Growth evaluation and increase skeletal muscle of Pm-mstn knockout mutant

To investigate the effect of complete *Pm-mstn* disruption on the mass of skeletal muscle, the morphological analysis of homozygous mutants was performed. The representative appearance of the homozygotes harboring an 8-base deletion (*mstn*$^{-8a/-8a}$) at 329 days old is shown in **Fig. 2.5a**. The *mstn*$^{-8a/-8a}$ exhibited a wider body trunk than wild type, implying that *mstn*$^{-8a/-8a}$ had an increased muscle mass. The 8-base deletion causes a frame-shift in the *Pm-mstn* coding sequence and the C-terminal active domain was completely lacking due to the newly emerged stop codon (**Fig. 2.5b).** Growth evaluation was performed from 133 days to 559 days old as described in **Fig. 2.6a-d**. Condition factor of the homozygote (*mstn*$^{-8a/-8a}$: 41.6 ± 6.9) was significantly higher than values of the heterozygote (*mstn*$^{-8a/wt}$: 26.0 ± 1.4) and wild type (*mstn*$^{wt/wt}$: 25.9 ± 1.3) at 559 days old (**Fig. 2.6a**). In addition, the condition factor of *mstn*$^{-8a/-8a}$ showed a significantly higher value than those of other groups throughout the experiment (**Fig. 2.6a**). Body width of the homozygote (6.7 ± 0.5 cm) tended to be slightly wider than those of

heterozygote (6.0 ± 0.4 cm) and wild type (6.2 ± 0.5 cm) at 559 days old though the significant difference was not observed (**Fig. 2.6b**). Significant differences were observed only at 300 and 359 days old (**Fig. 2.6b**). Fork length of the homozygote (26.6 ± 1.6 cm) was significantly shorter than values of the heterozygote (30.9 ± 0.9 cm) and wild type (32.0 ± 1.9 cm) at 559 days old (**Fig. 2.6c**). Significant differences were observed at 170-559 days old except for 133 days old (**Fig. 2.6c**). On the contrary, there was no difference in body weight (homozygote: 770.5 ± 78.5 g, heterozygote: 771.9 ± 90.4 g, wild type: 859.1 ± 163.2 g) at 559 days old and there were no differences for every sampling points (**Fig. 2.6d**). In addition, other *Pm-mstn* knockout mutants such as homozygote harboring other types of mutations (*mstn*$^{-14/-14}$ and *mstn*$^{-8b/-8b}$) and compound heterozygotes (*mstn*$^{-8a/-14}$ and *mstn*$^{-8a/-8b}$) showed the similar tendency as *mstn*$^{-8a/-8a}$ (**Table 2.5** and **Fig. 2.7**). The mutations, *mstn*$^{-8a/-8a}$ and *mstn*$^{-14/-14}$, were induced by sgRNA1 or sgRNA2, respectively, indicating that the different guide RNA sequences generated the same phenotype. To elucidate the effect of *Pm-mstn* gene disruption on skeletal muscle, I evaluated the cross-sectional area and the volume of skeletal muscle using CT scan in compound heterozygotes (described as *mstn*$^{-/-}$) and wild type at 448 days old. The genotypes of *mstn*$^{-/-}$ are listed in **Table 2.6**. **Figure 2.6e-1** and **e-2** show the typical cross-section at first spine of dorsal fin and anal fin, respectively (position exhibited by white arrows in **Fig. 2.6e-3**). The cross-sectional area of *mstn*$^{-/-}$ was remarkably larger than that of wild type, then the area at the anal fin was quantified in each fish (**Fig. 2.6e-2**). The value calculated for quantification in *mstn*$^{-/-}$ significantly increased 34% (40.52 ± 5.06 cm^2) relative to wild type (30.29 ± 1.99 cm^2) (**Fig. 2.6f**). Then, the volumetric analysis was performed to examine the muscle volume of the mutant in blue region shown in **Fig. 2.6e-3**. As a result, *mstn*$^{-/-}$ showed a 16% significant increase in the muscle volume (235.79 ± 35.64 cm^3) compared to wild type (203.03 ± 17.42 cm^3) (**Fig. 2.6g**). It was confirmed that the *mstn*$^{-/-}$ mutants exhibited increased muscle volume in comparison with wild type. These findings confirmed that complete gene disruption of *Pm-mstn* triggered the consistent level of skeletal muscle mass in red sea bream.

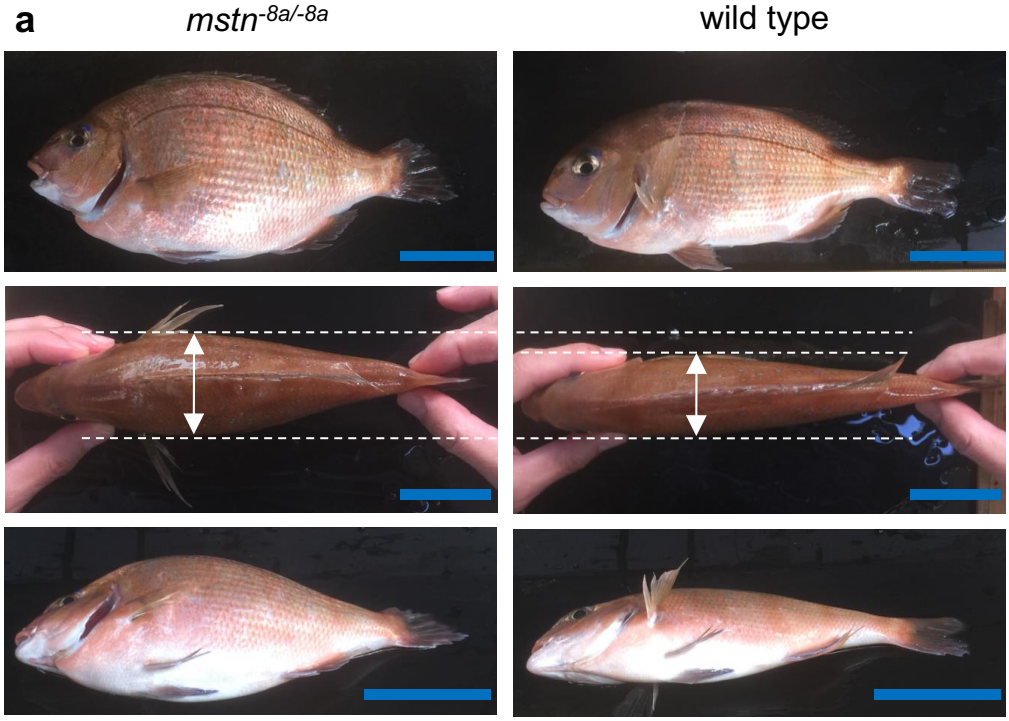

b

```
WT          1   MHPSQIVLYLSLLIVLGPVVLSDQETQQQQQQQQQQQPSATSPEDTEQCATCEVRQQIKT
mstn-8a/-8a 1   MHPSQIVLYLSLLIVLGPVVLSDQETQQQQQQQQQQQPSATSPEDTEQCATCEVRQQIKT

WT          61  MRLNAIKSQILSKLRMKEAPNISRDIVKQLLPKAPPLQQLLDQYDVLGDDNRDVVMEEDD
mstn-8a/-8a 61  MRLNAIKSQILSKLRMKEAPNISREAAPAQSAAAAAASRPVRRAGRRQQGCGYGGGR---

WT          121 EHAITETIMMMATEPESVVQVDGEPRCCFFSFTQKIQANRIVRAQLWVHLRASDEATTVF
mstn-8a/-8a     ------------------------------------------------------------

WT          181 LQISRLMPVTDGNGHIHIRSLKIDVNAGVGSWQSIDVKQVLSVWLRQPETNWGIQINAFD
mstn-8a/-8a     ------------------------------------------------------------

WT          241 SRGNDLAVTSAEPGEDGLQPFMEVKISEGPKRVRRDSGLDCDENSPESRCCRYPLTVDFE
mstn-8a/-8a     ------------------------------------------------------------

WT          301 DFGWDWIIAPKRYKANYCSGECEYMHLQKYPHTHLVNKANPRGSAGPCCTPTKMSPINML
mstn-8a/-8a     ------------------------------------------------------------

WT          361 YFNRKEQIIYGKIPSMVVDRCGCS
mstn-8a/-8a     -------------------------
```

Fig. 2.5 The appearance of red sea bream *Pm-mstn* gene disrupted mutants

(a) The appearances at 329 days old of *mstn*$^{-8a/-8a}$ (left) and wild type (right). Double-headed arrows show body width. The *mstn*$^{-8a/-8a}$ exhibited a wider body trunk than wild type. Blue bars indicate 5 cm. (b) The alignment of predicted amino acids between *mstn*$^{-8a/-8a}$ and wild type. Red boxes and orange letters indicate the homologous sequence and the non-homologous sequence between *mstn*$^{-8a/-8a}$ and wild type. The *mstn*$^{-8a/-8a}$ harbors 117 a.a., on the other hand, wild type harbors 384 a.a. C-terminal active domain in wild type (blue letters) is completely disrupted in *mstn*$^{-8a/-8a}$.

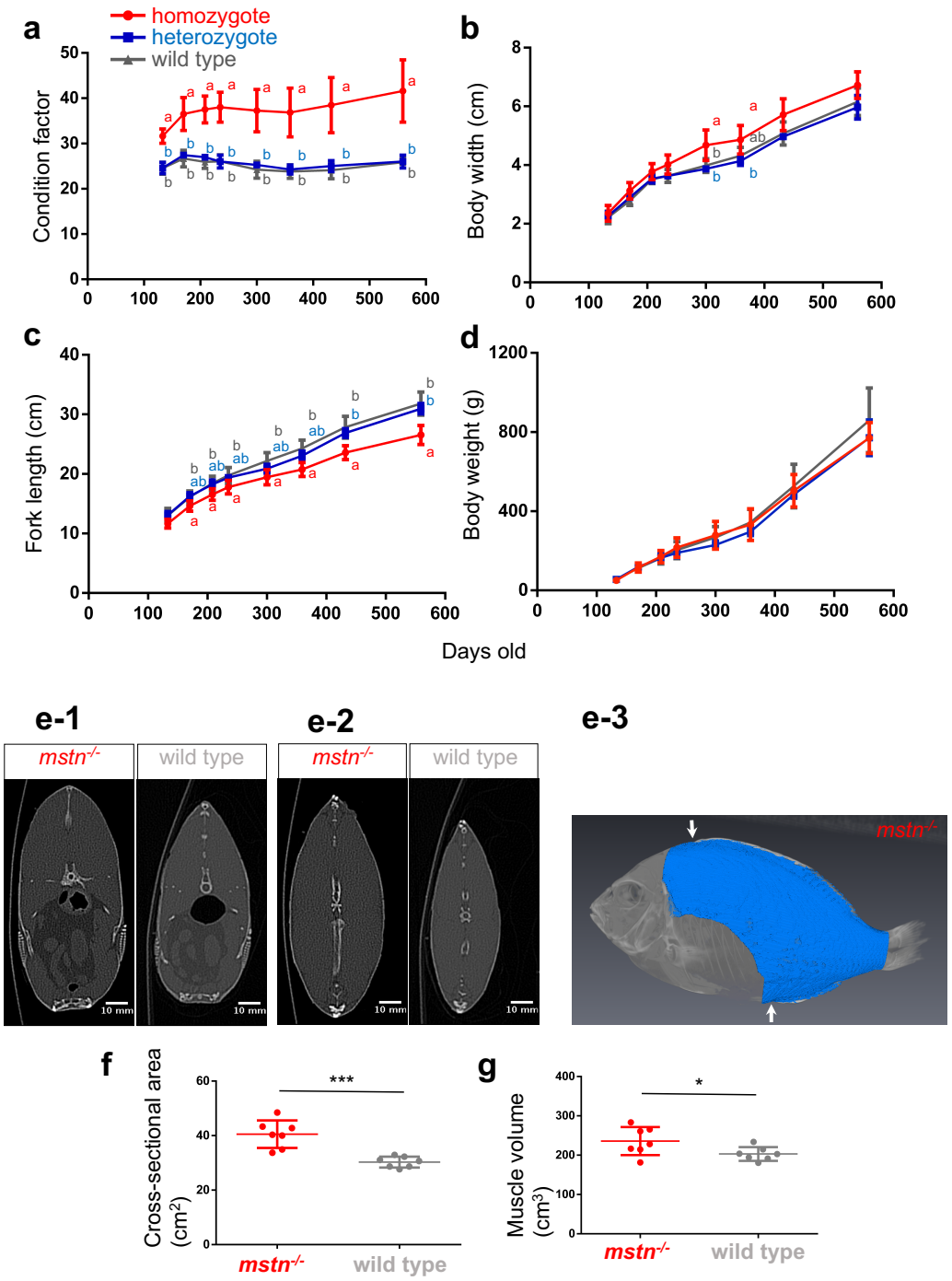

Fig. 2.6 Morphological analysis of red sea bream MSTN gene disrupted mutants

(a-d) Measurement of body weight, fork length, and body width until 133-559 days old of *mstn*$^{-8a/-8a}$, *mstn*$^{-8a/wt}$, and *mstn*$^{wt/wt}$. Comparison of condition factor (a, body weight/fork length^3×10^3), body width (b), fork length (c), and body weight (d). Means ± SD [*mstn*$^{-8a/-8a}$: n=5, *mstn*$^{-8a/wt}$: n=3, *mstn*$^{wt/wt}$: n=6, (*mstn*$^{-8a/-8a}$: n=4 at 559 days old, *mstn*$^{wt/wt}$: n=5 at 432, 559 days old)]. Means with different superscripts in each measurement point were significantly different with Tukey-Kramer HSD test, $P < 0.05$. (e) The cross-sectional area of *mstn*$^{-/-}$ (left) and wild type (right) at the first spine of dorsal fin (e-1) or anal fin (e-2) (position exhibited by white arrows in **Fig. 2.6e-3**). (f) The value of the cross-sectional area at anal fin (e-2). (g) The value of the muscle volume (blue region shown in **Fig. 2.6e-3**). Means ± SD (each group n=7 at 448 days old). The asterisks indicate significant difference with *t*-test, *: $P < 0.05$, ***: $P < 0.001$.

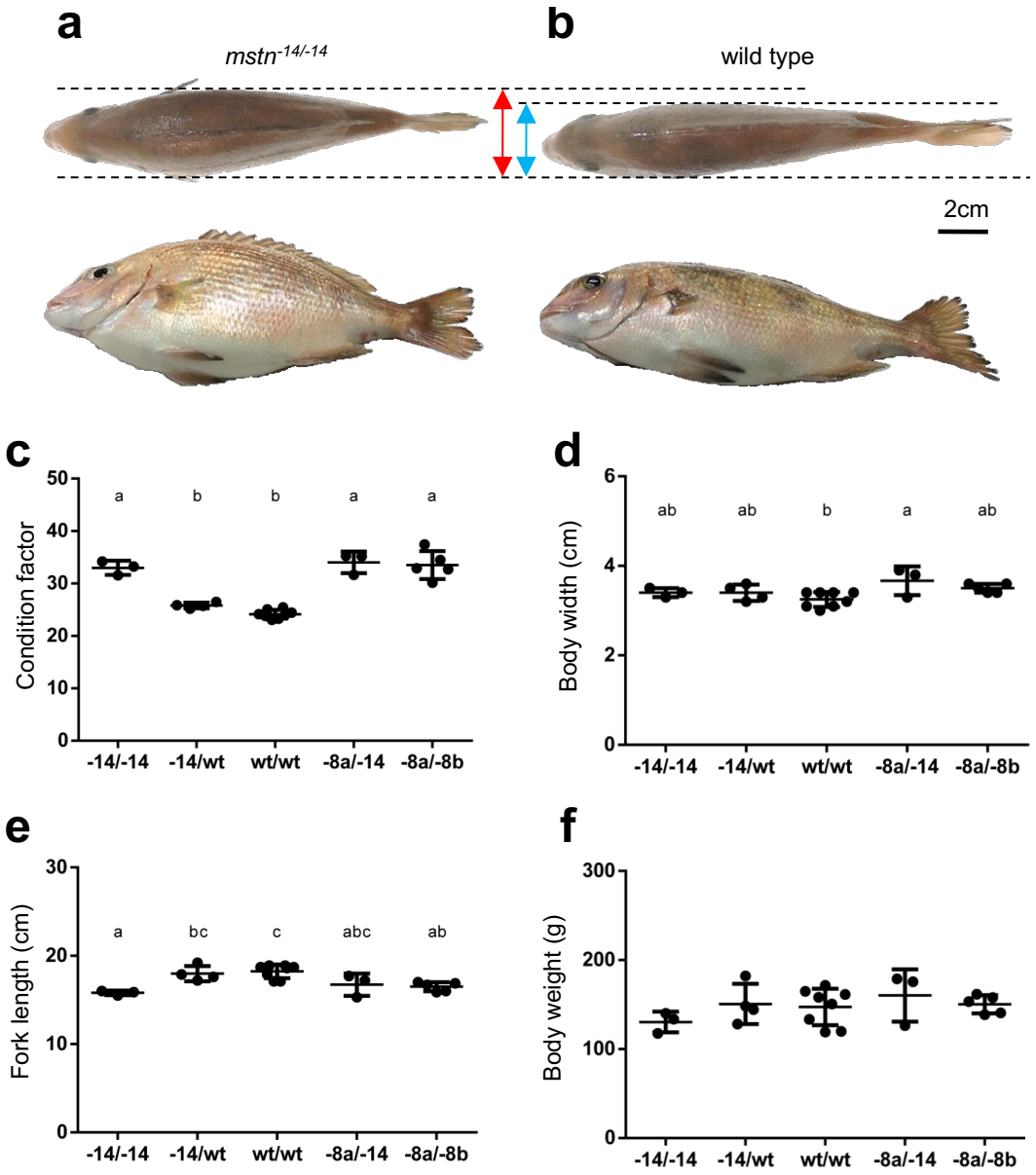

Fig. 2.7 The morphological analysis in *mstn*$^{-14/-14}$ and compound heterozygotes

The appearances of *mstn*$^{-14/-14}$ (left, a) and wild type (right, b). Double-headed arrows show body width. Both fish were sampled on 217 days old. (c-f) Measurement of body weight, fork length, and body width at 217 days old in *mstn*$^{-14/-14}$ and compound heterozygotes (*mstn*$^{-8a/-14}$ and *mstn*$^{-8a/-8b}$). Comparison of condition factor (c, body weight / fork length^3 x 10^3), body width (d), fork length (e), and body weight (f). Means ± SD. *mstn*$^{-8b}$ has a differently mutated allele from *mstn*$^{-8a}$ (each mutation type is described in **Table 2.5**). Means with different superscripts indicate significant difference with Tukey-Kramer HSD test, $P < 0.05$.

Table 2.6 Genotypes of compound heterozygote (*mstn*$^{-/-}$) subjected to CT scan

No.	Mutation type	sequence (5'-3')	
1-5	-8a/+22	AG**CCGGGACATCGTGAAGCAGCTCC**TGCCCAAAG	WT
		AGCCGG--------GAAGCAGCTCCTGCCCAAAG	-8a
		GGACGATGAGCACGCCA----------TCACGG	WT
		GGACGATGAGCACGCCAGACGATTTTCACGAGACGATTTTCACGG	+22
6	-8b/-8c	GA**GGACGATGAGCACGCCATCACGG**AGACGATTA	WT
		GAGGACGATGAG--------CACGGAGACGATTA	-8b
		AG**CCGGGACATCGTGAAGCAGCTCC**TGCCCAAAG	WT
		AGCCG--------TGAAGCAGCTCCTGCCCAAAG	-8c
7	-14/-2+4	GA**GGACGATGAGCACGCCATCACGG**AGACGATTA	WT
		GAGGACGATGAGC----------ACGATTA	-14
		AG**CCGG--GACATCGTGAAGCAGCTCC**TGCCCAAAG	WT
		AGCCGGGAATCATCGTGAAGCAGCTCCTGCCCAAAG	-2+4

The above sequence is WT, and the target sites by sgRNA are indicated in bold lines.
Mutations indicate in red letters.
-8a, -8c, and -2+4 were mutated by sgRNA1, +22, -8b, and -14 were mutated by sgRNA2.

2.4.9 The analysis of bone structure of Pm-mstn mutant

Since the *mstn*$^{-/-}$ mutants exhibited a shorter body length than wild type (**Figs. 2.6c** and **2.7e**), the bone structure at 448 days old was observed with CT scan. **Figure 2.8a-1** and **a-2** represent the typical bone structure of *mstn*$^{-/-}$ and wild type, respectively. It was observed that the size of centrums and skull of *mstn*$^{-/-}$ were smaller in comparison with that of wild type (**Fig. 2.8a-c**). In addition, in several fish of *mstn*$^{-/-}$, osteosarcomas were observed (white arrowhead in **Fig. 2.8a-1**). In the wild type red sea bream, the neural spine usually develops from the backbone at an angle directed toward the caudal fin (**Fig. 2.8a-2**). However, the neural spine in the *mstn*$^{-/-}$ red sea bream develops more perpendicular to the backbone (**Fig. 2.8a-1**). These developmental characteristics result in a higher body height in the *mstn*$^{-/-}$ red sea bream than observed in normal wild red sea bream. Furthermore, to investigate vertebrae in detail, enlarged images of the 7-11th centrums were observed (**Fig. 2.8b-c**). The intervertebral length of *mstn*$^{-/-}$ was shorter than that of wild type (orange arrowheads in **Fig. 2.8c-1** and **c-2**). I measured the size of the 8th centrum (blue triangles in **Fig. 2.8a**) and the neural spine length of the 8th vertebra (**Fig. 2.8d-1** and **d-2**), because it was reported that the defects of centrum are usually observed in posterior abdominal vertebrae, from 7th to 10th centrum (especially in 8th),

in cultured red sea bream [**21**]. In the centrums in MSTN deficient red sea bream (*mstn*$^{-/-}$), obvious deformity, such as lordosis and scoliosis, was not observed. Anterior-posterior length (A-P length), dorsal-ventral length (D-V length), and width of 8th centrum of *mstn*$^{-/-}$ were significantly shorter than those of wild type (**Fig. 2.8e-1**, **e-2**, and **e-3**) (A-P length: *mstn*$^{-/-}$, 6.17 ± 0.25 mm, wild type, 6.77 ± 0.21 mm; D-V length: *mstn*$^{-/-}$, 5.13 ± 0.27 mm, wild type, 5.93 ± 0.24 mm; width: *mstn*$^{-/-}$, 5.18 ± 0.33 mm, wild type, 5.83 ± 0.14 mm). There was no significant difference in neural spine between both groups (**Fig. 2.8f**) (*mstn*$^{-/-}$, 27.56 ± 1.38 mm, wild type, 27.01 ± 0.72 mm, $P = 0.36$). On the other hand, body height of *mstn*$^{-/-}$ was slightly higher than that of wild type though there was not significant difference (*mstn*$^{-/-}$, 11.04 ± 0.71 cm, wild type, 10.48 ± 0.35 mm, $P = 0.09$). As for head length, that of *mstn*$^{-/-}$ was significantly shorter than that of wild type (**Fig. 2.8g**) (*mstn*$^{-/-}$, 88.20 ± 5.15 mm, wild type, 95.37 ± 4.35 mm). These findings indicate that complete *Pm-mstn* disruption contributes to formation of bone structure such as vertebrae and skull. Therefore, the short centrum length, intervertebral length, and head length caused the short body length of *mstn* knockout red sea bream. It was suggested that the body height of *mstn* knockout is higher than that of wild type because neural spine extends in the dorsal-ventral axis.

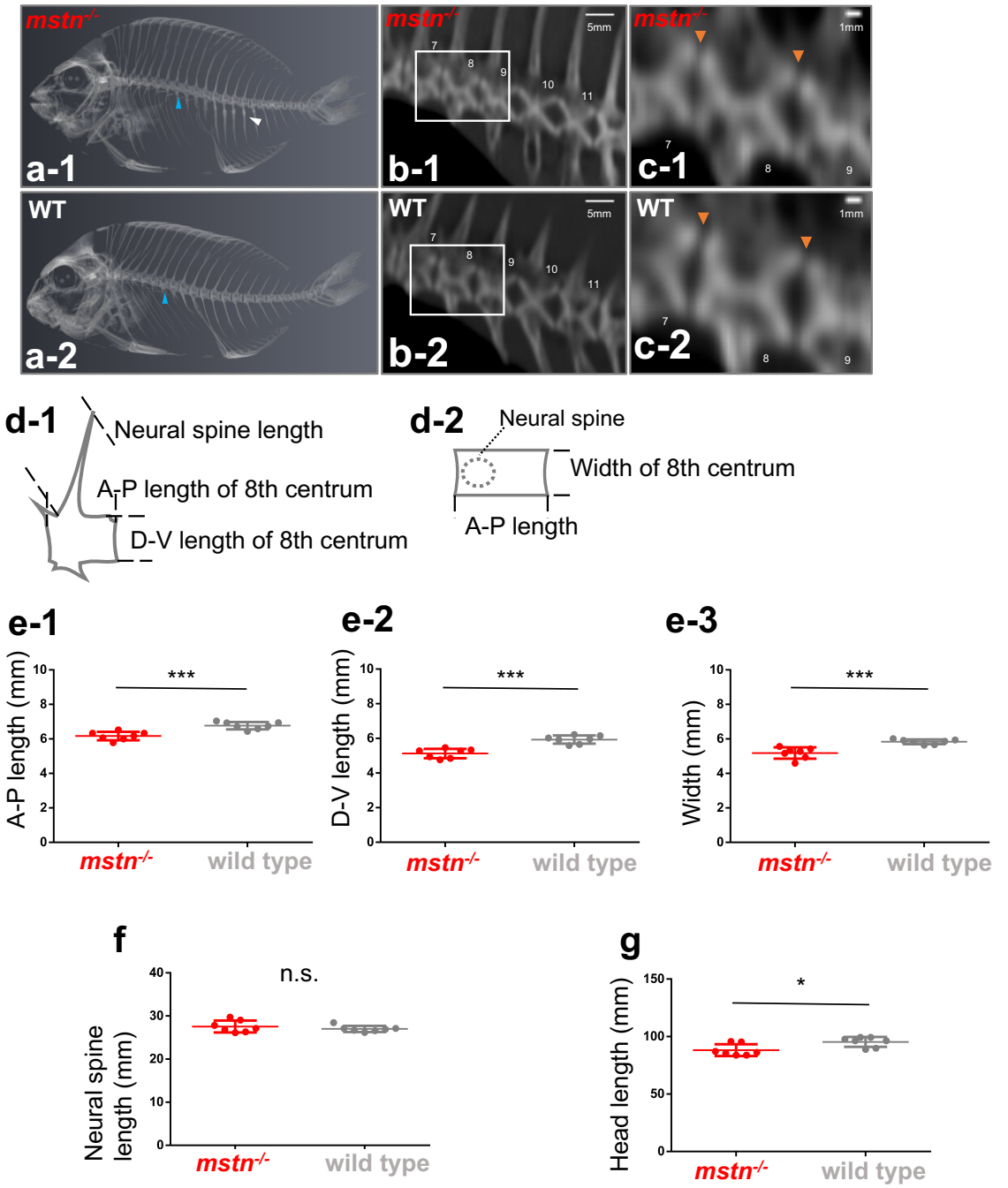

Fig. 2.8 The phenotype analysis of bone structure

Typical bone structure with CT scan of *mstn*$^{-/-}$ (a-1) and wild type (a-2) at 448 days old. White arrowhead indicates osteosarcomas in *mstn*$^{-/-}$. Blue arrowheads indicate 8th centrum. Enlarged area of 7-11th centrum of *mstn*$^{-/-}$ (b-1) and wild type (b-2). Enlarged area of 7-9th centrum of *mstn*$^{-/-}$ (c-1) and wild type (c-2), which is shown in the white squares in b-1 or b-2, respectively. The numbers in b-1, b-2, c-1, and c-2 indicate the order number of centrums. Orange arrowheads indicate intervertebral area. The size of centrum and intervertebral length of *mstn*$^{-/-}$ is smaller than that of wild type. (d-1) (d-2) View of the 8th vertebra of red sea bream. A-P length, anterior-posterior length. D-V length, dorsal-ventral length. The measured data of 8th vertebra: A-P length (e-1), D-V length (e-2), width (e-3), neural spine length (f). (g) Head length. Means ± SD mm (each group n=7). The asterisks indicate significant difference with *t*-test, *: $P < 0.05$, ***: $P < 0.001$.

2.4.10 Off-target analysis

Since it has been reported that there are potential off-target alternations in CRISPR/Cas9 mediated genome editing, off-target candidates were searched with the whole genome sequence (WGS). The criteria of candidates are shown in Materials and Methods. Five and one candidate sequences for sgRNA1 and sgRNA2, respectively, were found in the screening of red sea bream WGS. These candidates harbor two mismatches to sgRNA targeting sites (details are shown in **Table 2.7**). The HMA and DNA sequencing revealed that only on target sequences were altered and that there were no off-target alternations in each candidate both in F_1 and in G_0 (**Table 2.7** and **Fig. 2.9**).

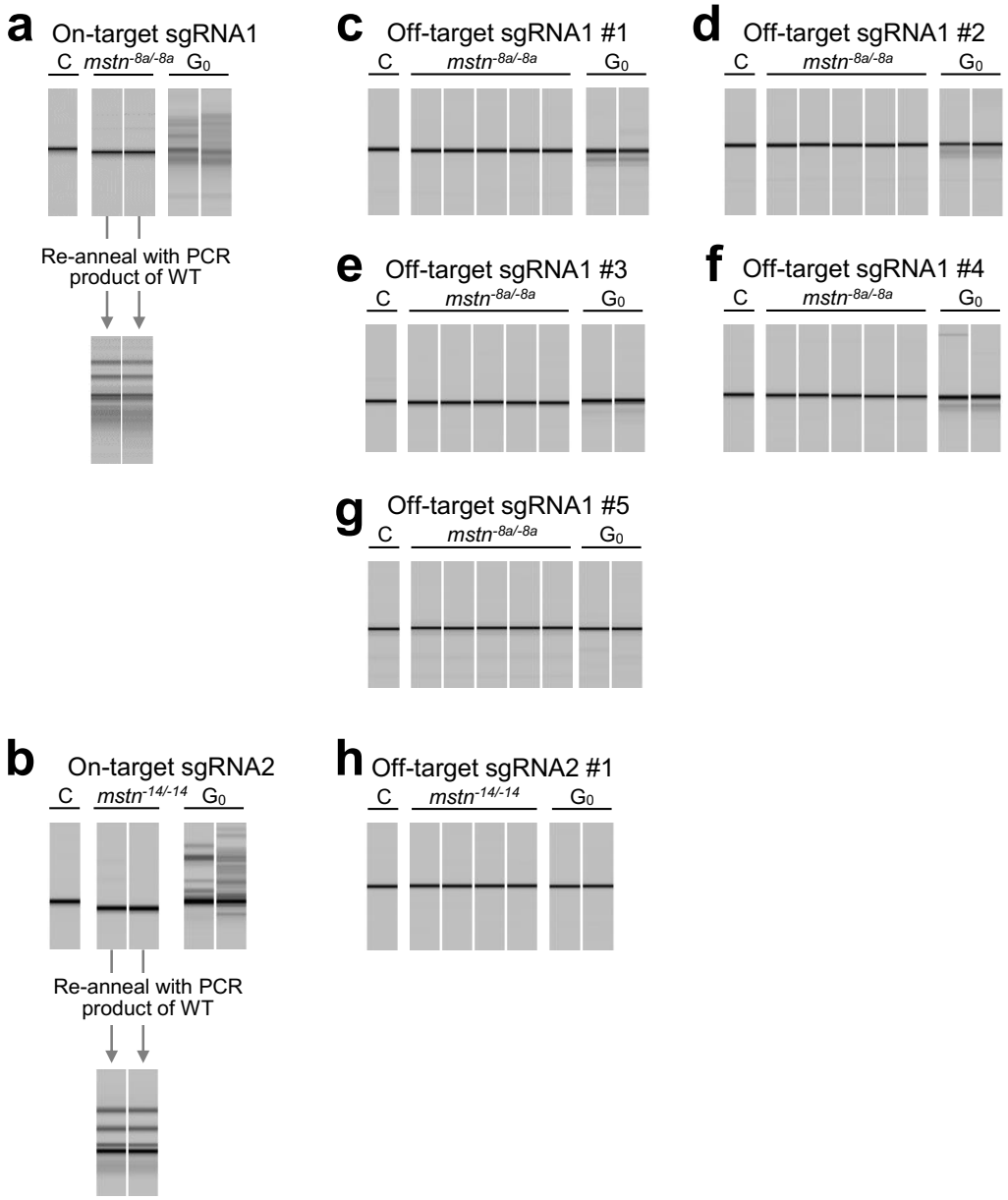

Fig. 2.9 Off-target analysis

Off-target analysis was performed by HMA and direct sequencing after searching from the whole genome database. On-target (*Pm-mstn*) electrophoresis gel images in *mstn*$^{-8a/-8a}$ targeted by sgRNA1 (a), and *mstn*$^{-14/-14}$ targeted by sgRNA2 (b). In a and b, each lower lane indicates the electrophoresis gel image after re-annealed with PCR products of WT, which shows the formation of heteroduplex mobility, that is, homozygous mutation. Off-target electrophoresis gel images in *mstn*$^{-8a/-8a}$ (c-g), and *mstn*$^{-14/-14}$ (h). The left edge lane; wild type as control, each lane in center; F_1 mutants, each lane in the right edge; G_0 embryo. Each PCR product in F_1 off-target analysis was subjected to direct sequencing, resulting in no off-target alternation.

Table 2.7 Summary of off-target analysis

sgRNA	name	Sequence (5'--3') *[1,2]	scaffold, region, F/R*[3]	mis-match	effect*[4]
1	On-target	AGCTGCTTCACGATGTCCCGG	0051, 2109470, R		
1	Off-target #1	AGgTGCTTCACGcTGTCCTGG	0010, 8906854, F	2	none
1	Off-target #2	AGCTGCTTCAgGATGTCaTGG	0011, 246266, R	2	none
1	Off-target #3	AaCTGgTTCACGATGTCCAGG	0050, 3168976, F	2	none
1	Off-target #4	AGCTGCTTCAtGATGaCCTGG	0063, 2312547, F	2	none
1	Off-target #5	AtCTGCcTCACGATGTCCCAG	0103, 1346172, R	2	none
2	On-target	ACGATGAGCACGCCATCACGG	0051, 2109577, F		
2	Off-target #1	ACGAccAGCACGCCATCATGG	0167, 314389, R	2	none

Candidates match with the 18-bp sequence at the 3 prime ends of the targeting sequence adjacent to either NGG or NAG PAM sequence harboring up to 2-bp mismatches.

*1: lower letters indicate the different nucleotides from on-target site.

*2: NGG or NAG in the 3 prime indicate PAM sequence.

*3: F/R indicate forward or reverse on the genomic DNA.

*4: estimated by HMA and sequencing analysis in G_0 and F_1, see in **Fig. 2.9**.

C2.5 Discussion

In this study, a new valuable red sea bream breed was successfully established with genome editing, CRISPR/Cas9 system. This breed exhibits increased skeletal muscle with a slightly increased body width and height and with a reduced length (**Figs. 2.5-2.7**) by disruption of myostatin gene. Therefore, the breed exhibits an increased proportion of edible parts. In the present study, homozygous *mstn* genome editing mutants were established and their phenotype were analyzed at commercial size. In previous reports about genome editing of *mstn* in commercial fish, their phenotype analysis was performed only in G_0 mosaic mutants at early juvenile stage in channel catfish [**22**] and common carp [**23**]. The phenotype analysis was not performed though inheritance of mutation was observed in yellow catfish [**24**]. Interestingly, the present study suggests that *Pm-mstn*

contributes to bone formation in red sea bream, resulting in a shortened body length (**Fig. 2.8**). This phenotype is dissimilar with mutants in mammals and other teleosts. It is confirmed that these phenotypes of *mstn* knockout mutants are not off-target effects because mutants generated by two different sgRNAs show the same phenotypes and there is no off-target alternation at pre-selected candidate sites (**Table 2.7** and **Fig. 2.9**).

The results in the present study indicate that genome editing technology can dramatically shorten the period for generating new aquaculture breeds in comparison to conventional selective breeding. Until now, red sea bream breed (Kindai-Madai) has been produced in Kindai University. To establish the Kindai-Madai, selective breeding was started in 1964 with the goal of producing phenotypes with enhanced growth, productivity, and disease resistance. As for growth enhancement, it took more than 20 years (at the 5th generation) after the start [**11**]. On the contrary, using genome editing, I could establish a new breed (homozygous mutant) providing increase of muscle mass phenotype in only 2 years which is the shortest generation time of red sea bream. The shortened period to generate beneficial aquatic breeds will contribute to the development of aquaculture, for example, cost-saving, improvement in productivity, and ultimately resolution of the global food sustainability.

For reducing the period for establishment of new breeds in this study, the design of the target sequence and sgRNA was one of the critical issues. In general, to establish the homozygote, the following two-step mating process should be done: genome edited founder (G_0) fish are mated with the wild type counterparts to generate heterozygote F_1, then the resultant F_1 fish are mated to each other to generate the homozygote F_2 fish [**25**]. This two-step mating process requires two generation periods. Usually, one generation period of commercially cultured marine fish is several years, for example 2 years for red sea bream. Therefore, to establish the homozygote of commercially cultured marine fish requires a considerable number of years. In this study, I demonstrated to establish the homozygote with one time of mating G_0 fish to each other (hereafter, as “One-step mating”). For the success of the One-step mating, it is considered that microhomology mediated end joining (MMEJ) [**18**, **26**] is the key. I could find the mutation via MMEJ in high frequency, helping me to find homozygous mutant F_1 by the one-step mating (**Fig. 2.4** and **Table 2.5**).

It is confirmed that loss of MSTN function in skeletal muscle in red sea bream is associated with an increase of skeletal muscle mass (**Figs. 2.5-2.7**) similar as in mammals [**1-5**] and in other teleost fish [**6-10**]. Also in genome edited founder (G_0), I have already observed increased skeletal muscle mass (**Table 2.2** and **Fig. 2.2**) the same as in carp and catfish [**22-23**]. In the present study, I found that there was a difference in the gene disruption level among tissues in G_0 fish (**Fig. 2.3**). This is the reason why *Pm-mstn* was disrupted strongly in pectoral fin without increasing of skeletal muscle mass in several G_0 fish (**Fig. 2.2**). Red sea bream has two MSTN genes, *Pm-mstn* and *Pm-mstnb* (**Fig. 2.1a-c**). The results in the present study confirmed that *Pm-mstn* plays a major role in regulating skeletal muscle mass (**Figs. 2.2, 2.5-2.7, and Tables 2.2-2.3**). Since the effect of MSTN is dose dependent in mammal [**27**], I consider that it is not possible to estimate correctly the effect of loss of MSTN function in G_0 mosaic mutants and it is necessary to establish complete MSTN gene disrupted fish. In this study, the completely MSTN gene disrupted fish exhibited outstanding muscle mass than G_0 mosaic mutants or heterozygous mutants (**Figs. 2.5-2.7**), indicating that MSTN functions in a recessive manner, not in a dose dependent manner in red sea bream. In measurement analysis from 133 to 559 days old, the fork length of *Pm-mstn* mutant was shorter than that of wild type fish, on the contrary, body weight of *Pm-mstn* mutant was similar to that of wild type throughout the experiment (**Fig. 2.6c-d**). The body width of *Pm-mstn* mutant tended to be increased, but significant differences were observed only at 300-400 days old (**Fig. 2.6b**). And the body mass index, condition factor of *Pm-mstn* mutant was higher value than that of wild type at each measurement point (**Fig. 2.6a**), but it is not clear by measurement analysis that *Pm-mstn* mutant exhibited enhanced skeletal muscle mass. Thus, I performed the analysis of skeletal muscle mass by CT scan. I found the 34% increase of cross-sectional area and the 16% increase of skeletal muscle volume in *Pm-mstn* mutant. These results confirmed that *Pm-mstn* knockout induces skeletal muscle mass in red sea bream. It is suggested that only 16% increase in muscle volume instead of 34% cross-sectional area increase is due to the shortened fork length in *Pm-mstn* mutants (**Fig. 2.6f-g**). For further study, I plan to investigate how to extend the body length of the mutants because the skeletal muscle mass can be increased if the body length is extended.

It has been recognized that MSTN is a key factor linking muscle mass and bone structure in mice. MSTN knockout mice show that the size of vertebral bodies of *mstn*$^{-/-}$ mice was larger than that of wild type, and the area of temporal bone decreased [**28**]. In teleost fish, MSTN deficient teleost fish (medaka and zebrafish) show larger or same body length compared to wild type [**6-10**]. However, MSTN deficient red sea bream show short body length and short centrum in the present study (**Figs. 2.6c**, **2.7e**, and **2.8**). It is reported that spinal deformity fish (scoliosis) appear at a consistent rate in medaka mutant [**8**], which is different phenotype from MSTN deficient red sea bream. Taking their results and the results in the present study in consideration, it is suggested that MSTN regulates the formation of bone structure also in teleost fish including red sea bream, but the function is different among fish species. In the view of aquaculture, the short body length is disadvantageous because of the decrease of fish meat, so I am planning to investigate the mechanism of MSTN contribution to bone formation in F_2 or later generation.

One of the benefits to generate a new breed by disrupting genes with the genome editing technique is that no foreign gene is added into the host genome, in contrast to transgenesis which introduces foreign genes into the host genome. Gene alteration without foreign gene insertion may occur naturally. Indeed, *mstn* deficient cattle breeds, Piedmontese and Belgian Blue [**2-3**], are naturally occurring mutants. In this meaning, the new breeds generated by genome editing technique cannot be distinguished from naturally selected breeds. For breeds generated by the genome editing technique, significant caution is essential to avoid escape into the wild until ethical and juristic regulations are established in addition to careful assessment of the potential effects on natural stocks. Therefore, at present, the experiments and breeding in the present study are performed in enclosed terrestrial tanks. As shown in the present study, MSTN is a clear example target for genome editing with the aim of improving a commercially valuable trait. Knockout of the appetite regulation gene is the next target to examine growth enhancement in red sea bream.

Table 2.8 Primers used in the present study

primer name	sequence (5'-3')
Pm-mstn-hmaFw	CGATTAAACGCCATAAAGTCTCAG
Pm-mstn-hmaRv	GGAGACGTCTGCGCGCTTCCAC
Pm-mstnb-hmaFw	CAAGCAGATGAGGCTCCACAG
Pm-mstnb-hmaRv	GCTTGGTGGCCATGGTGATG
sgRNA1-ampFw	GAATGAAGGAGGCTCCAAAT
sgRNA1-ampRv	CGTACTGGTCGAGAAGCTG
sgRNA2-ampFw	GAGACGACAACAGGGATGTG
sgRNA2-ampRv	TTCAGTGGCCATCATCATAA
sgRNA1-OTG#1Fw	TCACACATGTCAGAAGTGCT
sgRNA1-OTG#1Rv	GCGTTATTCAAGTGCTTTGGA
sgRNA1-OTG#2Fw	AGTCGTCGTCATCGGAGATT
sgRNA1-OTG#2Rv	AGGTTAACCTTTCAGGGGGA
sgRNA1-OTG#3Fw	CAGCCCCTTAGCCCTACTAT
sgRNA1-OTG#3Rv	CATCCAGAGTGGCATCAGTG
sgRNA1-OTG#4Fw	GATGTCAGTTCGGAGTCCAC
sgRNA1-OTG#4Rv	ACAGCTCACATTTTCCAGCA
sgRNA1-OTG#5Fw	ATGCACTGTCACTGTCATCC
sgRNA1-OTG#5Rv	CCCCTCGGCCTCTTTAAATC
sgRNA2-OTG#1Fw	ATGCACCCAACACATCCGTC
sgRNA2-OTG#1Rv	AGCTCCTGCGACAGAAATGC
large-delFw	ATGCATCCGTCTCAGATTGTG
large-delRv	CGCACGATTCGATTGGCTTGAATC

C2.6 References

1. McPherron, Alexandra C., Ann M. Lawler, and Se-Jin Lee. "Regulation of skeletal muscle mass in mice by a new TGF-p superfamily member." Nature 387.6628 (1997): 83.
2. Kambadur, Ravi, et al. "Mutations in myostatin (GDF8) in double-muscled Belgian Blue and Piedmontese cattle." Genome research 7.9 (1997): 910-915.
3. McPherron, Alexandra C., and Se-Jin Lee. "Double muscling in cattle due to mutations in the myostatin gene." Proceedings of the National Academy of Sciences 94.23 (1997): 12457-12461.
4. Mosher, Dana S., et al. "A mutation in the myostatin gene increases muscle mass and enhances racing performance in heterozygote dogs." PLoS genetics 3.5 (2007): e79.
5. Schuelke, Markus, et al. "Myostatin mutation associated with gross muscle hypertrophy in a child." New England Journal of Medicine 350.26 (2004): 2682-2688.
6. Chisada, Shin-ichi, et al. "Myostatin-deficient medaka exhibit a double-muscling phenotype with hyperplasia and hypertrophy, which occur sequentially during post-hatch development." Developmental biology 359.1 (2011): 82-94.
7. Chiang, Yi-An, et al. "TALENs-mediated gene disruption of myostatin produces a larger phenotype of medaka with an apparently compromised immune system." Fish & shellfish immunology 48 (2016): 212-220.
8. Yeh, Ying-Chun, et al. "Using CRISPR/Cas9-mediated gene editing to further explore growth and

trade-off effects in myostatin-mutated F4 medaka (Oryzias latipes)." Scientific reports 7.1 (2017): 11435.
9. Gao, Yanping, et al. "Depletion of myostatin b promotes somatic growth and lipid metabolism in zebrafish." Frontiers in endocrinology 7 (2016): 88.
10. Jinek, Martin, et al. "A programmable dual-RNA–guided DNA endonuclease in adaptive bacterial immunity." Science (2012): 1225829.
11. Murata, Osamu, et al. "Selective breeding for growth in red sea bream." Fisheries science 62.6 (1996): 845-849.
12. Kato, Keitaro, et al. "Construction of an expression vector containing a β-actin promoter region for gene transfer by microinjection in red sea bream Pagrus major." Fisheries Science 73.2 (2007): 440-445.
13. Kishimoto, Kenta, et al. "An effective microinjection method for genome editing of marine aquaculture fish: tiger pufferfish Takifugu rubripes and red sea bream Pagrus major." Fisheries Science (2018): 1-10.
14. Ansai, Satoshi, and Masato Kinoshita. "Targeted mutagenesis using CRISPR/Cas system in medaka." Biology open 3.5 (2014): 362-371.
15. Zhang, Jiajie, et al. "PEAR: a fast and accurate Illumina Paired-End reAd mergeR." Bioinformatics 30.5 (2013): 614-620.
16. Bae, Sangsu, Jeongbin Park, and Jin-Soo Kim. "Cas-OFFinder: a fast and versatile algorithm that searches for potential off-target sites of Cas9 RNA-guided endonucleases." Bioinformatics 30.10 (2014): 1473-1475.
17. Stinckens, Anneleen, Michel Georges, and Nadine Buys. "Mutations in the myostatin gene leading to hypermuscularity in mammals: indications for a similar mechanism in fish?." Animal genetics 42.3 (2011): 229-234.
18. Ansai, Satoshi, et al. "Design, evaluation, and screening methods for efficient targeted mutagenesis with transcription activator ‐ like effector nucleases in medaka." Development, growth & differentiation 56.1 (2014): 98-107.
19. Ota, Satoshi, et al. "Efficient identification of TALEN ‐ mediated genome modifications using heteroduplex mobility assays." Genes to Cells 18.6 (2013): 450-458.
20. Wang, Haoyi, et al. "One-step generation of mice carrying mutations in multiple genes by CRISPR/Cas-mediated genome engineering." cell 153.4 (2013): 910-918.
21. Hattori, M., et al. "Vertebral deformities in cultured red sea bream, Pagrus major, Temminck and Schlegel." Aquaculture Research 34.13 (2003): 1129-1137.
22. Khalil, Karim, et al. "Generation of myostatin gene-edited channel catfish (Ictalurus punctatus) via zygote injection of CRISPR/Cas9 System." Scientific reports 7.1 (2017): 7301.
23. Zhong, Zhaomin, et al. "Targeted disruption of sp7 and myostatin with CRISPR-Cas9 results in severe bone defects and more muscular cells in common carp." Scientific reports 6 (2016): 22953.
24. Dong, Zhangji, et al. "Heritable targeted inactivation of myostatin gene in yellow catfish (Pelteobagrus fulvidraco) using engineered zinc finger nucleases." PloS one 6.12 (2011): e28897.
25. Barman, Hirak Kumar, et al. "Gene editing tools: state-of-the-art and the road ahead for the model and non-model fishes." Transgenic research 26.5 (2017): 577-589.
26. McVey, Mitch, and Sang Eun Lee. "MMEJ repair of double-strand breaks (director's cut): deleted sequences and alternative endings." Trends in Genetics 24.11 (2008): 529-538.
27. McPherron, Alexandra C., and Se-Jin Lee. "Suppression of body fat accumulation in myostatin-deficient mice." The Journal of clinical investigation 109.5 (2002): 595-601.
28. Elkasrawy, Moataz N., and Mark W. Hamrick. "Myostatin (GDF-8) as a key factor linking muscle mass and skeletal form." Journal of musculoskeletal & neuronal interactions 10.1 (2010): 56.

Chapter 3
The establishment of myostatin knockout tiger pufferfish *Takifugu rubripes* with CRISPR/Cas9 genome editing for a breed improvement in aquaculture and an investigation of the gene function in fugu

C3.1 Abstract

Tiger pufferfish *Takifugu rubripes* (fugu) is an important fish for aquaculture breeding and genetics. Therefore, the method of mutagenesis in fugu is necessary to add valuable traits for aquaculture and to investigate gene function. In the present study, genome editing technology CRISPR/Cas9 was utilized to establish the fugu breed exhibiting high meat production by myostatin gene (*mstn*) knockout. Furthermore, the *mstn* gene function on skeletal muscle and bone structure was investigated in fugu. Two kinds of sgRNAs were designed on *mstn* gene for gene knockout to produce mutants. The mutations were successfully induced in the target *mstn* locus in G_0 fish and these G_0 mutants showed increased skeletal muscle mass. Moreover, I successfully established F_1 homozygous mutants harboring 8 base deletions in *mstn* which cause knockout of the gene. The homozygote exhibited 20-32% increase of skeletal muscle in cross-sectional areas, short body length, and short length of centrums in the direction of anterior-posterior and dorsal-ventral, in comparison with wild type. It was revealed by off-target analysis that the sgRNAs had high specificities for target *mstn* loci. The present results indicated that CRISPR/Cas9 genome editing enables rapid breeding with certainty and reverse genetics analysis in fugu, and that the new fugu breed with skeletal muscle mass is valuable for aquaculture. Furthermore, it is suggested that it is important to investigate a gene function in each fish species of interest because the function and phenotype may be different from the results obtained by model animals.

C3.2 Introduction

Tiger pufferfish, *Takifugu rubripes* (fugu) is an important fish not only for aquaculture in east Asia, Japan, Korea, and China, but also for research of genetics [**1-2**].

In aquaculture, 3.3 thousand tons of fugu are produced in 2016 in Japan. Today, aquaculture of fugu is expanding because of its good taste, its high market price, and conservation of natural resources. The breeding of fugu becomes increasingly important since valuable traits are expected for suppliers and consumers. Therefore, the establishment of new breeding techniques which accelerates the speed of breeding with easy-to-use handling is beneficial for fugu breeding.

In genetics, fugu has been used for a reference to understand the functions of genes, regulatory regions, and the evolution of vertebrate genomes because of its compact genome size (391 Mb reported as FUGU5/fr3, Ensembl release 94, http://asia. ensemble. org/Takifugu_rubripes/). However, the technology of reverse genetic analysis, disruption of gene of interest, has not been established. Thus, the function of gene of interest has been analyzed only by expression analyses, real-time PCR, *in situ* hybridization, transient knockdown by RNAi or morpholino, antibody staining, and *in vivo* expression assay in model fish, zebrafish [**3-4**]. Therefore, the establishment of reverse genetic analysis tool is beneficial for the study of genetics in fugu because the gene function can be analyzed with the phenotype exhibited by the disruption of the gene of interest.

In order to contribute to research of aquaculture and genetics, I attempted to perform target gene disruption with genome editing technology in fugu. I focused on fugu myostatin gene as in **chapter 2**. The increased skeletal muscle mass phenotype resulting from *mstn* gene disruption is expected for a valuable trait for commercial animals [**5-6**] including marine aquaculture fish, red sea bream [**chapter 2**, **7**]. In addition, *mstn* gene disruption is expected to contribute to research of *mstn* gene function in fish bone structure. As described in chapter 2, it has been reported that the phenotypes of body length in *mstn* mutants differ among fish species [**chapter 2**, **7**]. The body length of mutants is longer than that of wild type in small model fish, medaka and zebrafish [**8-11**]. On the other hand, the body length of mutants is shorter than that of wild type in red sea bream [**7**]. In red sea bream, it has been revealed by the phenotype analysis on bone structure with CT scan that the shorten centrums contribute to shorten body length [**7**]. Thus, red sea bream studies suggested that MSTN has a key factor in bone formation in

fish. However, little is known about the difference of the role of MSTN in bone formation among fish species. Therefore, it is necessary to perform the research of *mstn* mutants in several fish in addition to in medaka, zebrafish, and red sea bream, to investigate whether the shorten body length is specific to red sea bream.

In the present study, I demonstrated the establishment of *mstn* gene disrupted line with the CRISPR/Cas9 genome editing in fugu to generate a valuable trait and to investigate the *mstn* gene function. The increase of skeletal muscle and the change of bone structure were analyzed by the morphological analysis using CT scans. The present study indicates that the CRISPR/Cas9 genome editing is effective for aquaculture breeding and research of gene function in fugu.

C3.3 Materials and Methods

3.3.1 Parent fish and gametes for in vitro fertilization

The parents were purchased from a commercial supplier (Watanabe Suisan, Kagawa, Japan). Females were intramuscularly administrated a luteinizing hormone-releasing hormone (LHRH) analogue pellet (des Gly10 [D-Ala6]-LHRH, 400 μg/kg body weight) to promote ovulation. Males were injected intramuscularly with human chorionic gonadotropin (hCG, 500 IU/kg body weight) to promote spermiation. In March of 2015 for generation of first generation mutants (G_0), the unfertilized eggs and sperm were squeezed from each parent by stripping method, then were preserved in lapped plastic cups to prevent eggs and sperm from drying until *in vitro* fertilization at room temperature, 17°C. For the generation of founders (F_1), the promotion of spermiation or ovulation was performed in the 2-years old G_0 male mutants or in the 3-years old G_0 female mutants in the same way as described above. Then, the squeezing of gametes and *in vitro* fertilization were carried out.

3.3.2 Preparation for genome editing of CRISPR/Cas9 tools

Two single guide RNAs (sgRNA#1 and sgRNA#2) were designed in the first exon of *mstn* gene (GenBank, LOC446041) (**Fig. 3.1a**). *In vitro* transcription of RNAs was performed according to the method of previous report [**12**]. In brief, the Cas9 and GFP expression vector, pCS2+hSpCas9 (addgene, #51815) and pCS2+MT+GFP [**13**], was

linearized by NotI digestion. Capped RNA was synthesized using the mMessage mMachine SP6 Kit (Life Technologies, California, USA). The sgRNA expression vectors, DR274 (addgene, #42250), were optimized for recognition of each target site, and then were linearized by DraI. The sgRNAs were synthesized using the AmpliScribe T7-Frash Transcription Kit (Epicentre, Wisconsin, USA). All synthesized RNAs were purified with RNeasy Mini Kit (Qiagen, Hilden, Germany).

3.3.3 Microinjection

The mixture of RNAs, 100 ng/μl of Cas9 RNA and 50 ng/μl of each sgRNA, was microinjected into the embryos at one-cell stage. When the cleavage activation of each sgRNA was estimated, GFP RNA was mixed at 50 ng/μl into the each mixture of Cas9 RNA and sgRNA. I performed microinjection in accordance with the method of previous study [**chapter 1**, **14**]. In brief, for microinjection, *in vitro* fertilization was carried out with a part of the collected eggs and sperm. One minute after *in vitro* fertilization, eggs were arranged in a line along both sides of G-1 glass capillary (Narishige) on a plastic dish (90 mm in diameter). Iwamatsu solution, which is a balanced salt solution (0.65% NaCl, 0.04% KCl, 0.02% $MgSO_4 \cdot 2H_2O$, 0.02% $CaCl_2 \cdot H_2O$, pH 7.4) [**14-15**], is used as the soaking solution of eggs during microinjection. *In vitro* fertilization was performed at intervals of 15 minutes from fertilization until 2.5 hours after stripping, and microinjection of RNA solution into fertilized eggs was performed.

3.3.4 Genomic DNA extraction from fin, larva, embryo, or skeletal muscle

Cut-off fins (pectoral fin or dorsal fin), hatching larva, or embryos were lysed individually in 50 μl of alkaline lysis buffer containing 25 mM NaOH and 0.2 mM EDTA (pH 8.0), and incubated at 95˚C for 10 minutes. In embryos, the chorion was broken in lysis buffer before incubating. Then, samples were neutralized with 50 μl of 40 mM Tris-HCl (pH 8.0) and used as genomic DNA samples. A part of dorsal skeletal muscle was frozen with liquid nitrogen and crushed into a fine powder. Then, the obtained muscle powder was incubated at 55˚C for 10 minutes in lysis buffer containing 10 mM Tris-HCl, 25 mM EDTA, and 200 μg/ml proteinase K (pH 8.0). Then, the genomic DNA was extracted from the lysate by conventional phenol-chloroform and ethanol precipitation method.

3.3.5 Heteroduplex mobility assay

Heteroduplex mobility assay (HMA) was performed to detect mutations [**12, 16-17**]. A 146-bp or a 312-bp fragment containing the entire genomic target sequence of the *mstn* was amplified using primers pair of sgRNA-hmaFw1 and sgRNA-hmaRv or of sgRNA-hmaFw2 and sgRNA-hmaRv (primer sequence lists in **Table 3.4**). The reaction mixture contained 1 μl of genomic DNA as template, 1 × PCR buffer for KOD-FX, 0.4 mM of each dNTP, 0.2 mM of each primer, and 0.05 unit of KOD-FX (Toyobo) in a total volume of 10 μl. The PCR condition was as follows: denature at 94˚C for 2 minutes was followed by 35 cycles of 98˚C for 15 seconds, 58˚C for 15 seconds, and 68˚C for 15 seconds. The resulting amplicons were analyzed using a microchip electrophoresis system (MCE-202 MultiNA; Shimadzu) with the DNA-500 reagent kit (Shimadzu).

3.3.6 Screening of the mutants with HMA

After a small part of the fin was cut off from each of genome edited fugu at 3 to 4 months post hatched (mph) (total length; 4 to 10 cm), a passive integrated transponder (PIT) tag (Biomark, Idaho, USA) was inserted into the dorsal muscle or under the skin of head to identify the individuals. The genomic DNA of the cut off fins was extracted, then subsequent PCR and HMA were performed by the method described above.

In screening of G_0 mutants, I classified each fish into four groups according to the signal intensity of PCR products in HMA. Each group was categorized as follows: “High”, the signal intensity of the fragment derived from wild type sequence was less than 50%; “Middle”, more than 50 to less than 80%; “Low”, more than 80% to less than 100%; “None”, no difference in fragment pattern was observed compared with the pattern of wild type individual.

In screening of F_1 mutants, I selected homozygotes ($mstn^{-8a/-8a}$), heterozygotes siblings ($mstn^{-8a/wt}$), and wild type siblings ($mstn^{wt/wt}$) in F_1 founders mutated with sgRNA#1, and homozygotes ($mstn^{-8b/-8b}$) in F_1 founders mutated with sgRNA#2. I distinguished them by HMA and direct sequencing. The criteria for distinguishing by HMA is that heterozygote shows multiple banding patterns and both wild type fish and homozygote show a single band. To each PCR product showing a single band pattern in HMA (“1st PCR” described in **Fig. 3.10a-b**), I added aliquot of PCR product amplified from a template genomic DNA of wild type. Then, I reannealed the mixture by heating at

95 °C for 5 minutes and gently cooling to room temperature, and performed 2nd HMA ("Re anneal" described in **Fig. 3.10a-b**). The wild type shows only one band again, while homozygote shows a multiple banding pattern similar to heterozygote.

3.3.7 Identification of germ line transmission

The G_0 mutants were mated with wild type fish and genomic DNA was extracted from each F_1 larva. Mutation in each larva was analyzed by HMA using the primer pair (sgRNA-hmaFw1 and sgRNA-hmaRv) (**Table 3.4**). Mutant alleles in each larva were determined by direct sequencing.

3.3.8 Identification of induced mutations in G_0 by amplicon sequencing with NGS

The target regions were amplified by KOD-FX DNA polymerase with the following primers pairs: sgRNA#1-ampseq-Fw and sgRNA#1-ampseq-Rv, or sgRNA#2-ampseq-Fw and sgRNA#2-ampseq-Rv (**Table 3.4**). The forward primers harbor 8-bp random index sequence to 5 prime end for identifying each subject [**9**]. The library production was performed with PCR-Free Library Prep Kit (Illumina Inc.). Then, sequencing analysis was performed by single-end sequencing (100-bp x 2 Gb) with HiSeq2500 (Illumina Inc.) in skeletal muscle sample or in pectoral fin sample, respectively. Paired end reads were merged with PEAR 0.9.8 [**18**]. The obtained reads were classified into each subject using the 8-bp index. The read count and frequency of each read variant were calculated after classification [**7**]. As a reference, the PCR product from wild type fish was subjected to the sequencing. In data processing, the read variants below 1% of frequency were omitted as an error of PCR or sequencing because the error with less than 1% were detected in wild type treated as a control.

3.3.9 Sex determination for fugu with RFLP analysis

The genomic region containing a point mutation site for sex determination in anti-Müllerian hormone receptor type II (*amhr2*) of fugu [**3**] was amplified with KOD-FX polymerase and primer pair of *amhr2*-rflp-Fw and *amhr2*-rflp-Rv (**Table 3.4**). The reaction mixture and condition in PCR were the same as ones described above in Materials and Methods 3.3.5. The PCR product was digested by 0.5 unit of *Sau*3AI restriction enzyme (Takara, Shiga, Japan) at 37°C for 2 hours. The digestion products

were detected with MultiNA. The single fragment of 119-bp was detected in female homozygote (XX). In contrast, the 47-bp and 76-bp of fragments derived from Y-chromosome were detected in male heterozygote (XY) in addition to the 119-bp of fragment derived from X-chromosome.

3.3.10 Measurement of body size of mstn mutants

To investigate the phenotype attributed to *mstn* knockout in G_0, I focused exclusively on the "High" and "None" groups in categorization for fugu mutants using HMA, described above. They were named as $mstn^{sgRNA\#1\text{-}High}$ or $mstn^{sgRNA\#2\text{-}High}$, and $mstn^{None}$. Fish in "None" group were used as control sibling fish. To compare body size in *mstn* G_0 mutants, standard length (SL, the length of a fish measured from the tip of the snout to the posterior end of the last vertebra) and body weight (BW) were measured. In addition, condition factor was calculated as BW/SL^3x10^3 (BW in g, SL in cm). Both *mstn* mutants and control fish were reared in the same tanks throughout the experiments. Measurement of $mstn^{sgRNA\#1\text{-}High}$ and $mstn^{sgRNA\#2\text{-}High}$ were carried out at 5 and 6 mph, respectively.

To clarify the phenotype attributed to *mstn* knockout in F_1, SL and BW of homozygotes ($mstn^{-8a/-8a}$), heterozygote siblings ($mstn^{-8b/-8b}$), and wild type fish siblings ($mstn^{wt/wt}$) were measured and condition factor was calculated as same as in G_0. All fish were reared in the same tanks throughout the experiments. Measurement were carried out at 207 dph.

3.3.11 Magnetic resonance imaging (MRI) scan in G_0 mutants

Eight and seven fish in each of $mstn^{sgRNA\#1\text{-}High}$ and $mstn^{None}$ at 8 mph was randomly chosen and subjected to MRI scan for quantification of skeletal muscle mass. Spin echo (SE) 2D data and gradient echo (GRE) 3D data were acquired using Tim trio (Siemens Medical Solutions, Erlangen, Germany). A 12-channel head coil was used. Each condition of SE and GRE in Tim trio was configured as follows; [SE: repetition time, 2000 ms; echo time, 45 ms, flip angle, 90°; field of view, 104 × 128 mm^2; band width, 130 Hz; slice thickness, 3 mm; spacing, 3 mm; slice number, 30 and fat saturation imaging time, 6 min 55 s] and [GRE: repetition time, 36 ms (millisecond); echo time, 3.43 ms; flip angle, 20°; field of view, 256 × 104 × 104 mm^3; band width, 199 Hz; voxel size, 1

mm^3; imaging time, 3 min 48 s]. The MR volumetric and cross-sectional analyses were performed using Avizo 7.0 (FEI Visualization Sciences Group). Cross-sectional area was calculated in the nearest slice of the SE image to the first spine of the dorsal fin. The muscle region in GRE 3D data was manually segmented from dorsal fin to caudal fin in each fugu. Midline length for skeletal muscle segmentation was measured by counting the number of slices. The regions of bone, skin, dorsal and anal fins were included in the specified region (blue area in **Fig. 3.6d**), but they were so small as to ignore for volume measurements of total skeletal muscle. In this study, the anterior region to dorsal fin was not used for segmentation for the follow reasons; first, the contrast in muscle and intestine of fugu was not clear enough to distinguish from them in the GRE 3D data. Second, PIT tags injected in fugu needed to be removed from muscle in anterior region to dorsal fin because of the distorting effect of the magnetic field in MRI scan analysis.

3.3.12 Computed tomographic (CT) scan in F_1 mutants

To investigate the effect of *mstn* disruption on skeletal muscle increase and bone structure in F_1, five *mstn*$^{-8a/-8a}$ homozygote and wild type siblings were subjected to CT scan at 207 dph (SL: *mstn*$^{-8a/-8a}$, 16.9 ±1.0 cm; WT, 18.2 ± 0.7 cm; $P < 0.05$, BW: *mstn*$^{-8a/-8a}$, 224.6 ± 41.0 g; WT, 219.0 ± 27.9 g; $P = 0.80$, K: *mstn*$^{-8a/-8a}$, 45.8 ±1.8; WT, 35.9 ± 0.6; $P < 0.001$). These measured values analyzed by Student's *t*-test are consistent with those of the population of fish in **Fig. 3.11**. The CT 3D data were acquired using XT H320 (Nikon corporation, Tokyo, Japan). The parameters in Ingenuity Core were configured as follows: tube voltage, 200 kV; tube current; 200 μA, filter, Cu0.1 mm; exposure time, 354 ms; resolution, 100 μm/voxels; geometric magnification, 2.0x; number of imaging, 3141; imaging time, 19 min. The CT cross-sectional analyses in skeletal muscle were performed using imageJ. The lengths of body width, head, and centrum (anterior-posterior: A-P length, dorsal-ventral: D-V length, and width) were measured using imageJ.

3.3.13 Off-target analysis

Off-target candidates were searched from FUGU5/fr3 data base (https://www.ncbi.nlm.nih.gov/assembly/GCF_000180615.1/) with GGGenome (https://gggenome.dbcls.jp/ja/) using the following criteria described in previous report [**12**]; harboring 2- or fewer-bp mismatches including in/del gap [**19**] in the 18-bp targeting sequence followed by a NRG

PAM. The regions of off-target candidate were PCR amplified with KOD-FX using primers described in **Table 3.3**. The samples of DNA template were extracted from the pectoral of G_0 fish in which mutations were highly induced. The PCR products were subjected to HMA and direct sequencing analysis.

3.3.14 Statistical analysis

Statistical analyses in G_0 for condition factor, BW, SL, cross-sectional area, muscle volume, and midline length for segmented volume were carried out by *t*-test between "High" (*mstn*$^{sgRNA\#1\text{-}High}$ or *mstn*$^{sgRNA\#2\text{-}High}$) and "None" (*mstn*^{None}) groups. The analyses in F_1 for condition factor, BW, SL, were carried out by Tukey-Kramer HSD test among homozygote (*mstn*$^{-8a/-8a}$), heterozygotes (*mstn*$^{-8a/wt}$), and wild type (*mstn*$^{wt/wt}$). The analyses in F_1 for cross-sectional area, the body width, head length, and centrum lengths (A-P length, D-V length, and width) were carried out by Student's *t*-test between homozygote (*mstn*$^{-8a/-8a}$) and wild type (*mstn*$^{wt/wt}$).

C3.4 Results

3.4.1 Design and evaluation of induced mutation with CRISPR/Cas9

To generate *mstn* mutants, I targeted first exon of the *mstn* gene (**Fig. 3.1a**). To evaluate correctly whether the designed sgRNAs cleavage the target genomic site and induce mutations, I microinjected the mixture of Cas9 RNA, each sgRNA, and GFP RNA, into the fertilized eggs. Since inner part of fertilized eggs of fugu is almost invisible, there is a possibility of the failure to inject into cytoplasm. Thus, the microinjected eggs into cytoplasm are selected correctly by observing GFP expression derived from GFP RNA injection (**Fig. 3.2**). **Figure 3.2c** shows that the degree of GFP expression correlates with the degree of mutation induction by genome editing. GFP strongly expressing embryos were subjected to the amplification of target region and HMA. Multiple band patterns, i.e. multiple heteroduplexes, were observed in the electrophoresis image of these embryos (**Fig. 3.1b** and **3.1c**). These results indicate that two sgRNAs were successfully induced mutations at the target regions, respectively.

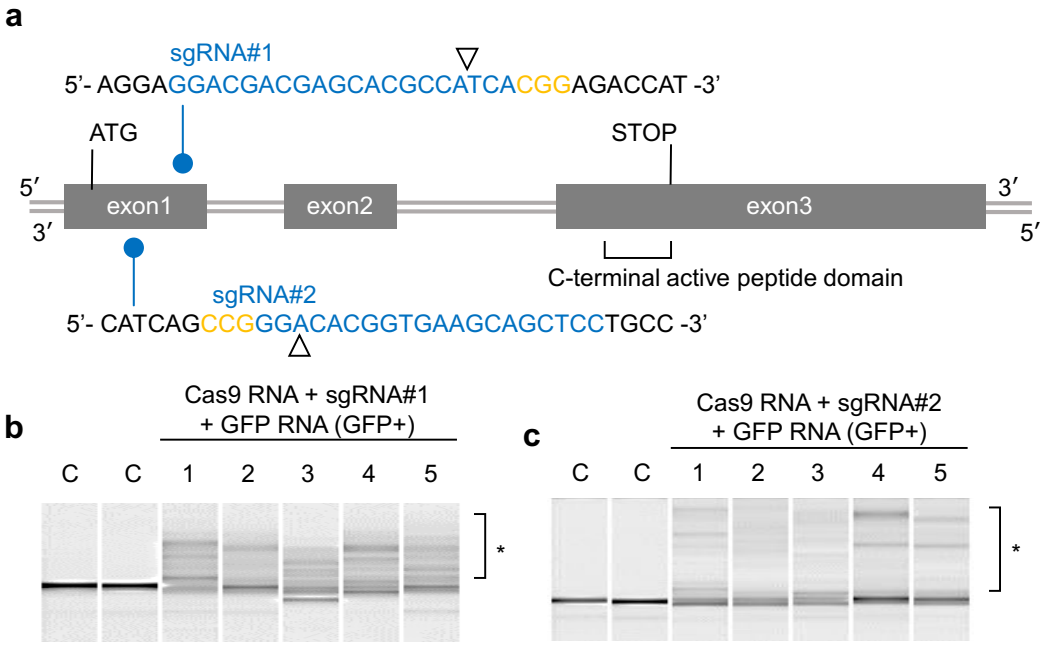

Fig. 3.1 Mutagenesis of *mstn* with CRISPR/Cas9

(a) Design of the target site for sgRNA#1 and sgRNA#2 in *mstn*. The sgRNAs are designed in exon 1. Gray boxes and bars, exons and introns, respectively. Blue and orange letters, target sequence and PAM, respectively. Triangles indicate the cleavage site recognized by Cas9 nuclease. Exon 3 includes C-terminal active peptide domain of MSTN protein. (b, c) The electrophoresis images of HMA in embryos injected with Cas9 RNA, GFP RNA, and each sgRNA. GFP expression positive embryos, "GFP+", indicate correctly injected embryos (**Fig. 3.2**). Multiple heteroduplex bands were observed in PCR amplicons from each the injected embryo (#1-5), whereas a single band was observed from each "C" embryo without injection. The asterisks indicate heteroduplex.

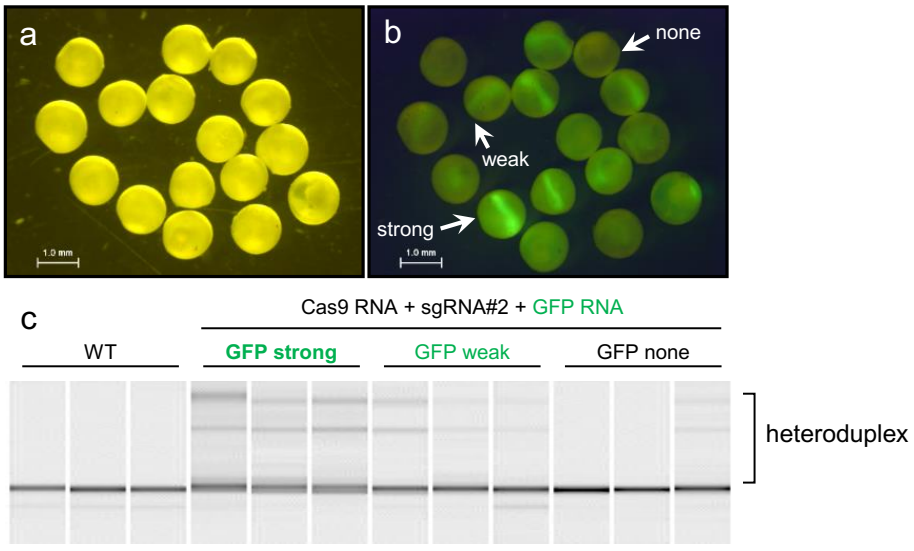

Fig. 3.2 The correlation with GFP expression level and mutagenesis in co-injection with GFP RNA

Embryos at 2 dpf. Embryos were injected with Cas9 RNA (100 ng/μl), sgRNA#2 (50 ng/μl), and GFP RNA (50 ng/μl). Bright field (a), and GFP fluorescent image (b). The injected embryos are categorized by GFP expressing level into the following three groups; "strong", "weak", and "none". (c) Electrophoresis gel images of the three groups (n=3 in each group). Strong heteroduplex mobility shift level was observed in embryos with strong GFP expression level, weak mobility shift level was observed in embryos with weak expression level, and weak or none mobility shift was observed in without GFP expression.

3.4.2 Generation of G_0 mutants with CRISPR/Cas9

The workflow in this study is shown in **Fig. 3.3**. To generate *mstn* G_0 mutants, each sgRNA, sgRNA#1 and sgRNA#2, was injected into the fertilized eggs with Cas9 RNA (#1, 3760; #2, 2160), respectively. At 3-4 mpf, these fish were examined for the degree of induced mutations using HMA, and were categorized into four groups of "High", "Middle", "Low" and "None" according to signal intensity and electrophoresis bands pattern of PCR (**Table 3.1**). In the results of HMA, the G_0 mutants were screened (sgRNA#1: "High", 76 fish; "Middle", 51; "Low", 37; "None", 109, sgRNA#2: "High", 25; "Middle", 32; "Low", 16; "None", 140). The "High" fish harbor a lot of induced mutations and were expected to show loss-of-function of MSTN. Each of G_0 mutants in "High" were named as $mstn^{sgRNA\#1\text{-}High}$ or $mstn^{sgRNA\#2\text{-}High}$, and control sibling fish in "None" group, $mstn^{None}$. The HMA gel images and electropherograms in High and None fish are shown in **Fig. 3.4**. The criterion of categorization is described in Materials and Methods "3.3.5 Screening of the mutants with HMA".

Table 3.1 Summary of mutagenesis mediated CRISPR/Cas9 genome editing in G_0

Injection	No. of injected eggs	No. of hatched larvae *1	No. of fish in G_0 mutant categorization				
			Surviving fish*2	Mutation level			
				High	Middle	Low	None
sgRNA#1	3760	1156 (30.7%)	273 (7.3%)	76	51	37	109
sgRNA#2	2160	414 (19.2%)	213 (9.9%)	25	32	16	140

*1; Percentages indicate number of hatched larvae / numbers of injected eggs

*2; Percentages indicate number of surviving fish at 3 or 4 mph / number of injected eggs.

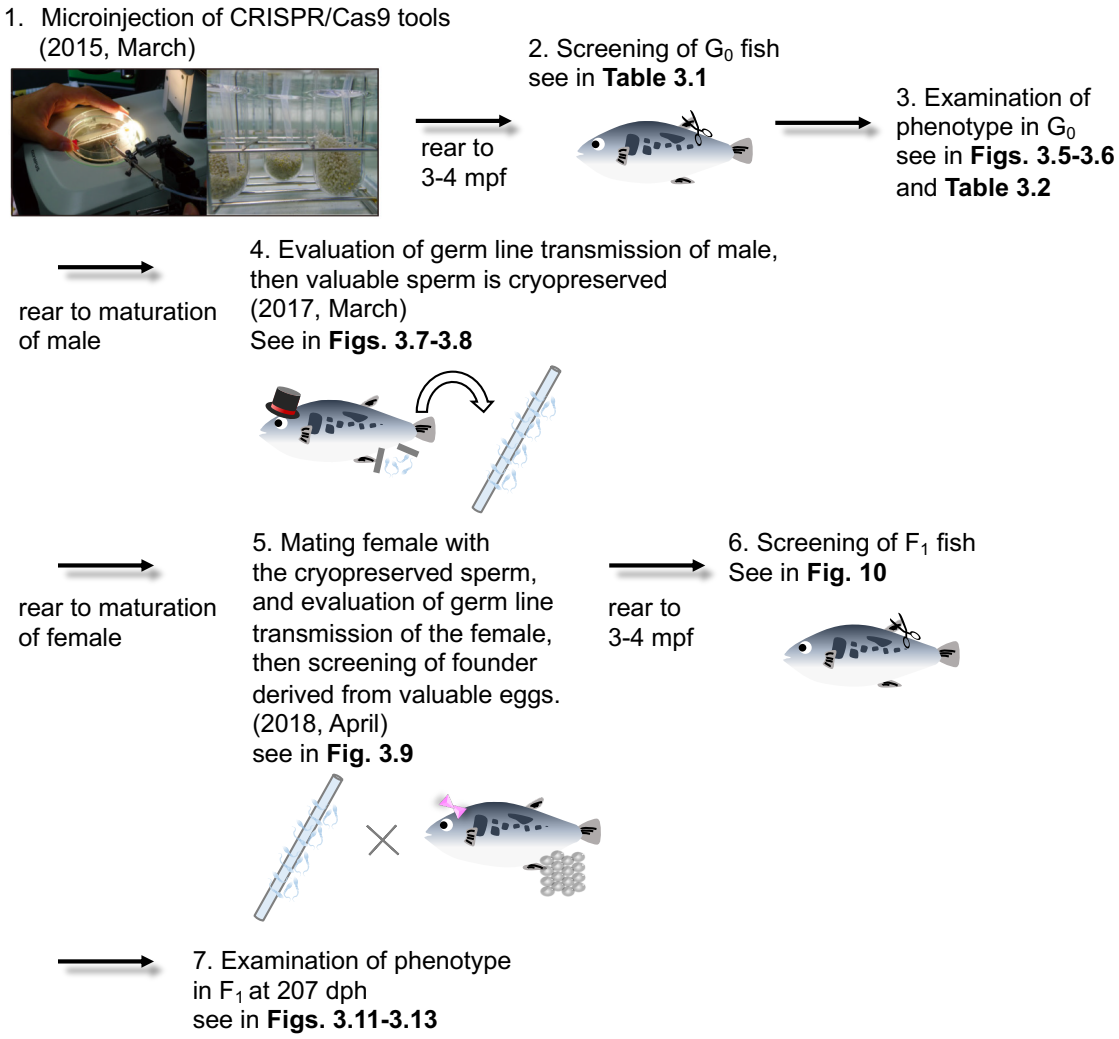

Fig. 3.3 A workflow in this study

Schematic depiction of steps in this study: microinjection, screening and phenotyping in G_0, production of F_1, and phenotyping in F_1.

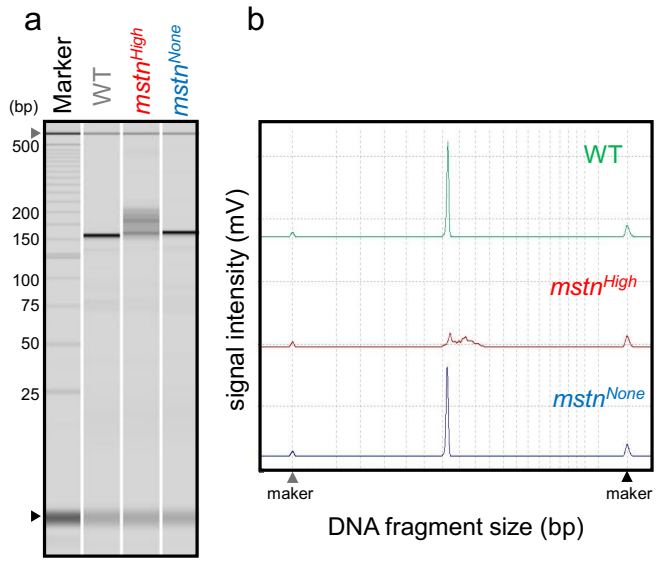

Fig. 3.4 Categorization of *mstn* G_0 mutants evaluated by HMA
An example of electrophoresis gel image in mutants injected with sgRNA#1 (a) and electropherograms (b).

3.4.3 Morphological analysis in G_0 mutants

As in **Fig. 3.5a** and **3.5b**, the mutants ($mstn^{sgRNA\#1\text{-}High}$ and $mstn^{sgRNA\#2\text{-}High}$) exhibited increased skeletal muscle in comparison to control fish classified to the $mstn^{None}$ at 8 mpf. Body width of *mstn* mutants was larger than that of control fish. In addition, condition factor (value of muscle mass), body weight (BW), and standard length (SL) were compared between G_0 mutants and control fish ($mstn^{sgRNA\#1\text{-}High}$ at 5 mph, $mstn^{sgRNA\#2\text{-}High}$ at 6 mph) (**Fig. 3.5c** and **3.5d, Table 3.2**). Condition factor and body weight of the *mstn* mutants were significantly higher than those of control. On the other hand, there were no differences in standard length between High groups and None groups. Note that standard length in $mstn^{sgRNA\#1\text{-}High}$ was slightly longer than that of control ($P = 0.077$, **Table 3.2**). The *mstn* mutants generated by two different sgRNAs exhibited almost the same phenotype as each other, increase of condition factor and body weight, and same standard length as wild type. To elucidate the effect of *mstn* knockout on skeletal muscle in the G_0 mutants, $mstn^{sgRNA\#1\text{-}High}$ were subjected to MRI scan. These G_0 mutants harbored highly induced mutations in pectoral fins judged from multiple band patterns observed in electrophoresis images (**Fig. 3.6a**). The cross-sectional area at the first spine of the dorsal fin was observed and quantified. **Figure 3.6b** shows typical images using the MRI scan. The cross-sectional area of $mstn^{sgRNA\#1\text{-}High}$ was remarkably larger than that of $mstn^{None}$,

and the value calculated for quantification in *mstn*$^{sgRNA\#1\text{-}High}$ significantly increased 27 % (23.93 ± 2.91 cm^2) relative to *mstn*^{None} (18.84 ± 1.69 cm^2) ($P < 0.01$, **Fig. 3.6c**). The MR volumetric analysis was performed to examine the muscle volume of the mutant in blue region shown in **Fig. 3.6d**. As a result, *mstn*$^{sgRNA\#1\text{-}High}$ showed a 26% significant increase in the muscle volume (44.76 ± 5.84 cm^3) compared to *mstn*^{None} (35.57 ± 4.58 cm^3) ($P <$ 0.01, **Fig. 3.6e**). While, there were no significant difference between the two groups in the midline length for the segmented skeletal muscle volume (*mstn*$^{sgRNA\#1\text{-}High}$, 6.13 ± 0.38 cm and *mstn*^{None}, 6.54 ± 0.92 cm) (**Fig. 3.6f**). Therefore, these results indicate that the fugu *mstn* G_0 mutants generated by the CRISPR/Cas9 represented skeletal increased muscle mass phenotype.

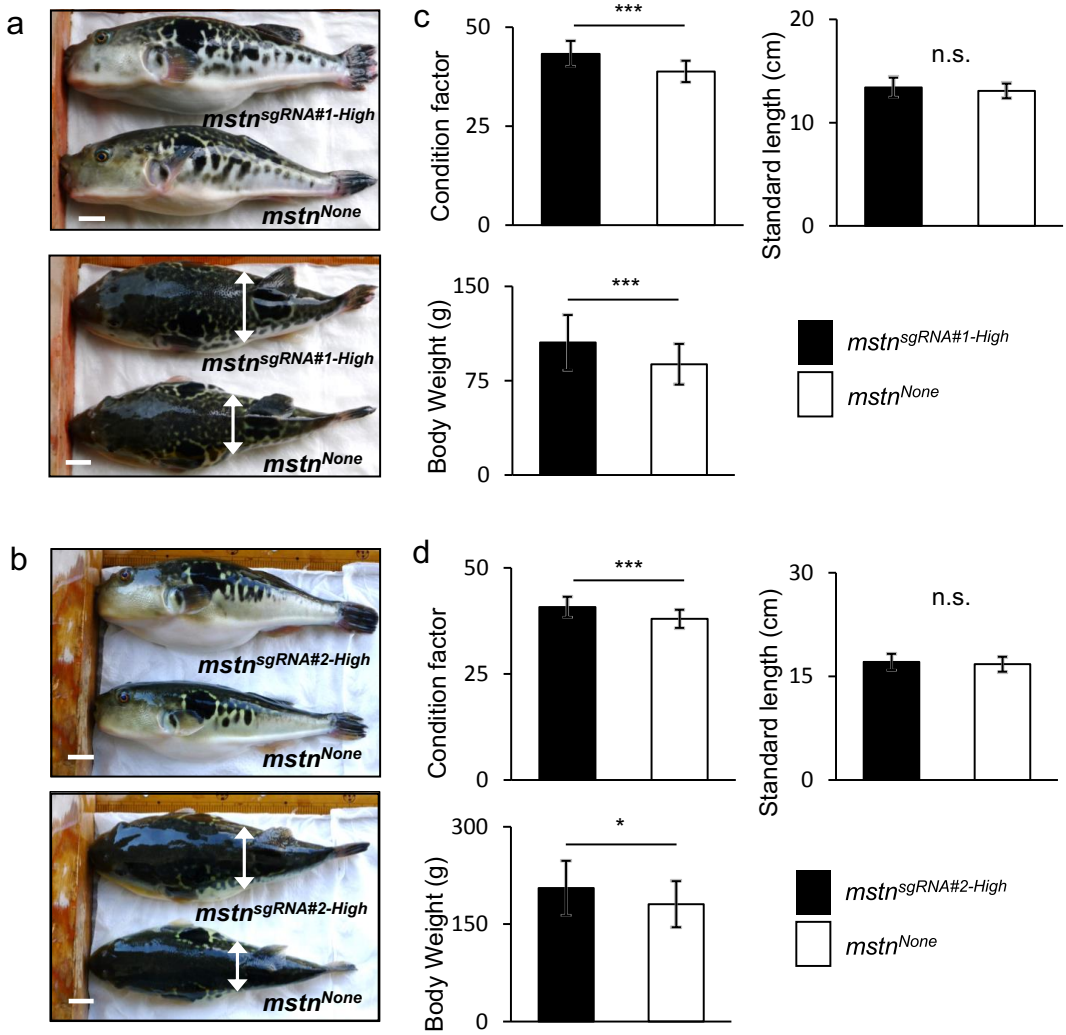

Fig. 3.5 Morphological analysis of *mstn* G_0 mutants

The appearance of G_0 mosaic mutated fish injected with Cas9 RNA and sgRNA#1 (a) and sgRNA#2 (b). Strongly mutated fish ($mstn^{sgRNA\#1\text{-}High}$ or $mstn^{sgRNA\#2\text{-}High}$, upper) and not mutated sibling ($mstn^{None}$, lower) at 8 mph. Two white double-arrows, body width at anterior to dorsal fin. Scale bars, 2 cm. (c, d) Measurement of body weight and standard length at 5 mph (c, sgRNA#1) and 6 mpf (d, sgRNA#2). Comparison of condition factor (body weight / standard length^3 x 10^3), body weight, and standard length between Strongly mutated fish (black columns) and not mutated siblings (white columns). Means ± SD. *: $P < 0.05$, ***: $P < 0.001$ by *t*-test.

Table 3.2 Morphological analysis by measurement of G_0 fish

sgRNA	sgRNA1[*1]			sgRNA2[*2]		
Mutation level[*3]	High	None	*P* value	High	None	*P* value
No. of fish	71	40	-	20	22	-
Standard length (cm)	13.4 ± 1.0	13.1 ± 0.7	0.077	17.1 ± 1.2	16.8 ± 1.1	0.34
Body weight (g)	105.3 ± 21.9	87.9 ± 16.2	< 0.001	205.6 ± 42.1	180.6 ± 35.4	< 0.05
Condition factor	43.3 ± 3.3	38.8 ± 2.7	< 0.001	40.8 ± 2.4	38.0 ± 2.1	< 0.001

Statistical analysis was performed with Student's *t*-test between "High" and "None" group.
Values ± standard deviation
*1; measurement was performed at 5 mpf.
*2; measurement was performed at 6 mpf.
*3; categorized with finclip and HMA.

3.4.4 Identification of induced mutations in skeletal muscle in G_0

To identify the mutations in skeletal muscle by genome editing, genomic DNA was extracted from a part of skeletal muscle in the representative two mutants used for the MRI scan ($mstn^{sgRNA\#1\text{-}High\ \#1}$ and $mstn^{sgRNA\#1\text{-}High\ \#2}$). **Figure 3.6g** and **3.6h** show mutation patterns and their frequencies by amplicon sequencing using the DNA sample from skeletal muscle. Thirteen types of variants were detected in $mstn^{sgRNA\#1\text{-}High\ \#1}$ as follows: deletions, 8; insertions, 2; deletions and insertions, 3 (**Fig. 3.6g**). The rate of frame-shift mutations was 51.57 %, while intact wild type sequence was detected in the ratio of 2.81 % (**Fig. 3.6i**). Seven types of variants were detected in $mstn^{sgRNA\#1\text{-}High\ \#2}$ as follows: deletions, 4; deletions and insertions, 3 (**Fig. 3.6h**). The rate of frame-shift mutations was 59.03 %, while intact wild type sequence was not detected (**Fig. 3.6j**). These results indicate that the *mstn* gene disruption caused by the CRISPR/Cas9 genome editing contributed to the phenotype, increased skeletal muscle mass of G_0.

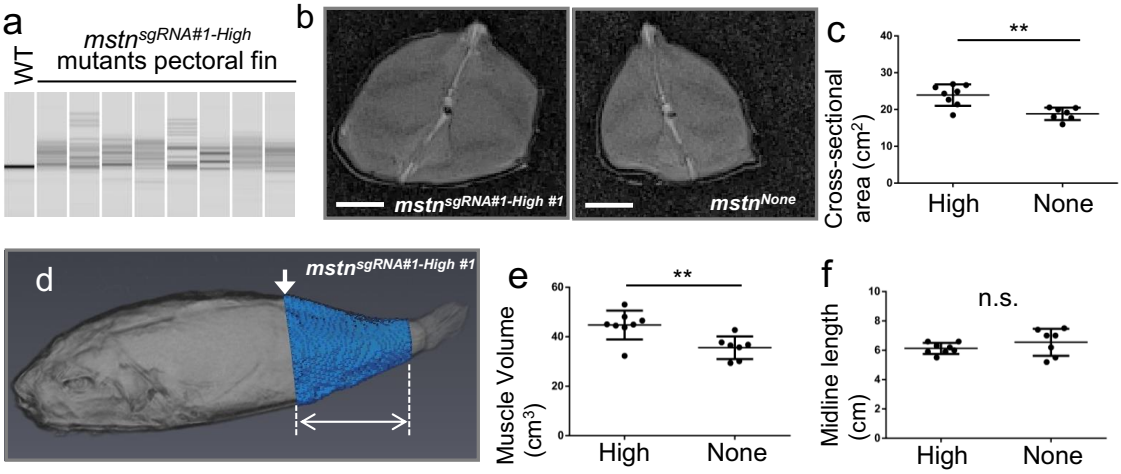

g

mstn sgRNA#1-High #1 skeletal muscle

sequence	genotype	number	frequency
AGGAGGACGACGAGCACGCCATCACGGAGACCATCA	WT	102 / 14293	2.8 %
AGGAGGACGACGAG-----CACGGAGACCATCA	-8a	2793 / 14293	19.5%
AGGAGGACGACGAGCACGC---CACGGAGACCATCA	-3	1480 / 14293	10.4%
AGGAGGACGACGAGCACGC-------GAGACCATCA	-7	995 / 14293	7.0 %
AGGAGGACGACGAGCACGC--TCACGGAGACCATCA	-2	814 / 14293	5.7 %
AGGAGGACGACGAGCACG----------CCATCA	-12	714 / 14293	5.0 %
AGGAGGACGACGAGCACGC-----CGGAGACCATCA	-5	598 / 14293	4.2 %
AGGAGGACGACGAGCACG------CGGAGACCATCA	-6	552 / 14293	3.9 %
AGGAGGACGAC---------GAGACCATCA	-15	229 / 14293	1.6 %
CCA----------TCACGGAGACCATCA	WT		
CCACGGAGACCATCGAGCACGTCACGGAGACCATCA	+18	3774 / 14293	26.4%
AGGAGGACGACGAGCACGCCATCACGGAGACCATCA	WT		
AGGAGGACGACGC--------TCACGGAGACCATCA	-9+1	606 / 14293	4.2 %
CACGC----------CATCACGGAGACCATCA	WT		
CACGCGGCGAGGAGACCATCATGACGGAGACCATCA	-4+18	497 / 14293	3.5 %
GAGGACGACGAGCACGCCA--TCACGGAGACCATCA	WT		
GAGGACGACGAGCACGCCACGTCACGGAGACCATCA	+2	459 / 14293	3.2 %
GACGACGAGCACGC-----CATCACGGAGACCATCA	WT		
GACGACGAGCACGCGACGAGCTCACGGAGACCATCA	-2+7	380 / 14293	2.7 %

i

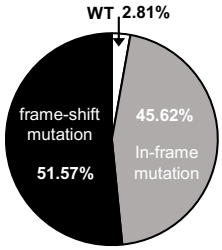

h

mstn sgRNA#1-High #2 skeletal muscle

sequence	genotype	number	frequency
AGGAGGACGACGAGCACGCCATCACGGAGACCATCA	WT	0 / 13533	0 %
AGGAGGACGACGAGC------TCACGGAGACCATCA	-6	4579 / 13533	33.8%
AGGAGGACGACGAG----CACGGAGACCATCA	-8a	3069 / 13533	22.7%
AGGAGGACGACGAGCA------CACGGAGACCATCA	-6	387 / 13533	2.9 %
AGGAGGACGACGAGCACGC--CACGGAGACCATCA	-3	304 / 13533	2.3 %
GGAGGACGACGAGCACG-CCATCACGGAGACCATCA	WT		
GGAGGACGACGAGCACGACGAGCACGGAGACCATCA	-4+5	2928 / 13533	21.6%
GGAGGACGACGAGCACGC-CATCACGGAGACCATCA	WT		
GGAGGACGACGAGCACGCTCCTCACGGAGACCATCA	-2+3	1992 / 13533	14.7%
AGGACGACGAGCACGCC---ATCACGGAGACCATCA	WT		
AGGACGACGAGCACGCCGGGACCACGGAGACCATCA	-2+5	274 / 13533	2.0 %

j

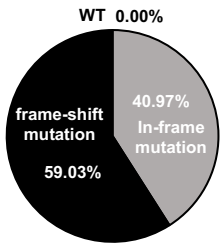

Fig. 3.6 Phenotype analysis in skeletal muscle in G_0 mutants

(a) Electrophoresis gel image in PCR amplicon from pectoral fin of *mstn*$^{sgRNA\#1\text{-}High}$ mutants used in MRI scan analysis. (b) Cross-sectional area images at the first spine of the dorsal fin (position at a white arrow in d) in *mstn*$^{sgRNA\#1\text{-}High\ \#1}$ and *mstn*^{None}. Scale bars, 1 cm. (c) Quantification of cross-sectional area using MRI scan. (d) Surface rendered 3D (whole body) image of *mstn*$^{sgRNA\#1\text{-}High\ \#1}$. Blue region in d is skeletal muscle volume quantified (e), and white double-head arrow in d is midline length for the segmented muscle volume (f). (c, e, f) Means ± SD ["High", n=8; "None", n=7]. **, $P < 0.01$ by *t*-test. (g, h) Identification of induced mutations in skeletal muscle of *mstn*$^{sgRNA\#1\text{-}High}$ using amplicon sequencing. This is shown in order of sequences, the genotypes of deletions (-) and insertions (+), the count numbers of read by single-end sequencing (each read number / total read number) and the frequencies of each genotype (%). Red dashes and letters, deletions and insertions. (i, j) The ratio of gene disruption in *mstn*$^{sgRNA\#1\text{-}High}$.

3.4.5 Inheritance from G_0 to F_1 founder in male and cryopreservation of sperms

In March 2017, I attempted to cryopreserve valuable sperms which harbor the frame-shift mutation via microhomology mediated end joining (MMEJ) for establishing *mstn* homozygote knockout line. MMEJ pathway uses microhomology sequences to align the broken ends before joining, thereby causing deletions flanking the original break [**20**]. It is reported that the mutation via MMEJ was widely observed among multiple individuals treated with same sgRNA and multiple tissues in the same fish [**7**, **12**]. Semen was squeezed from each G_0 male parent which harbors mutations in pectoral fin (**Table 3.1**). Then, germ line transmission ratio in each male was estimated by HMA and direct sequencing (**Figs. 3.7** and **3.8**). As in **Fig. 3.7a-c**, in sgRNA#1, germ line transmission rates were 32.5% in no.1, 55.3% in no.2, and 0% in no.3. Mutagenesis via MMEJ, 8 base deletion (designated as "-8a"), was observed at 15.0% in no.1, 0% in no.2, and 0% in no.3. As in **Fig. 3.8a-c**, in sgRNA#2, germ line transmission rates were 100% in no.1, 60.0% in no.2, and 2.5% in no.3. Mutagenesis via MMEJ, 8 base deletion (designated as "-8b"), was observed at 77.5% in no.1, 35.0% in no.2, and 0% in no.3. Therefore, I cryopreserved sperms of sgRNA#1 male no.1 (**Fig. 3.7a**) and those of sgRNA#2 male no.1 (**Fig. 3.8a**) in order to produce homozygous mutants in 2018 with initial maturation of mutated G_0 females.

In order to evaluate whether germ line mutagenesis can be predicted form mutation in somatic line such as pectoral fin which can be sampled from fish alive, spectrum of mutagenesis in germ line (**Figs. 3.7a-c** and **3.8a-c**, designated as "GL" in **Figs. 3.7d-f** and **3.8d-f**) was compared with spectrum of mutagenesis in somatic line (**Figs. 3.7d-f** and **3.8d-f** designated as "SL" in **Figs. 3.7d-f** and **3.8d-f**) by amplicon sequencing with NGS. In two parents (sgRNA#1 no.2 and no.3), the patterns of mutation variants were completely different between GL and SL (**Fig. 3.7h** and **3.7i**). In sgRNA#1 no.1, the targeted mutation, "-8a", was observed at 15.0% in GL and at 23.8% in SL (**Fig. 3.7g**). In sgRNA#2 no.1, the targeted mutation, "-8b", was observed at 77.5% in GL and at 52.6% in SL (**Fig. 3.8g**). In sgRNA#1 no.2, the targeted mutation, "-8b", was observed at 35.0% in GL and at 17.3% in SL (**Fig. 3.7h**). These results indicate that the occurrence of targeted mutation via MMEJ in GL is similar to some extent with that in SL. Other mutation except MMEJ mutation is not similar too much.

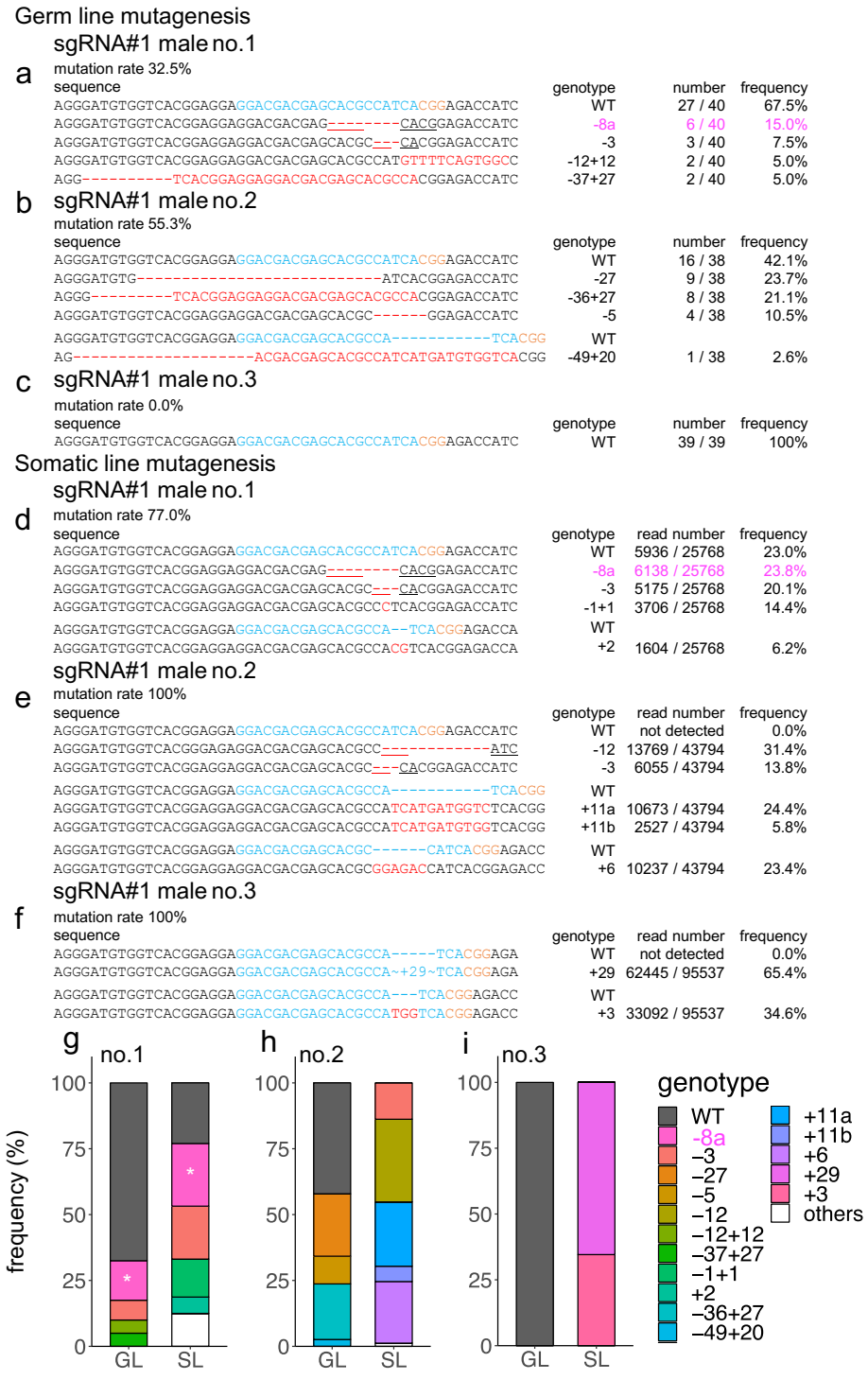

Fig. 3.7 Germ line and somatic mutagenesis in G_0 injected with sgRNA#1

(a-c) Germ line mutations in three males. (d-f) Somatic line mutations from pectoral fin in the three males, analyzed with amplicon sequencing. These are shown in order of sequences, the sizes of deletions (-) and insertion (+), numbers in germ line (each mutated embryo / all analyzed embryos) or read number in somatic line (each read number / all read number), and the frequencies. Blue and orange letters, target sequence and PAM, respectively. Red dashes and letters, deletions and insertions. Under bars, microhomologies. The mutations in magenta letter indicate the targeted mutation via MMEJ (designated as "-8a") for production of homozygote F_1 founders. (g-i) The comparison with germ line ("GL") and somatic line ("SL") mutagenesis. The column which is a specific color indicates a different mutation variant. The asterisks indicated the "-8a" mutation.

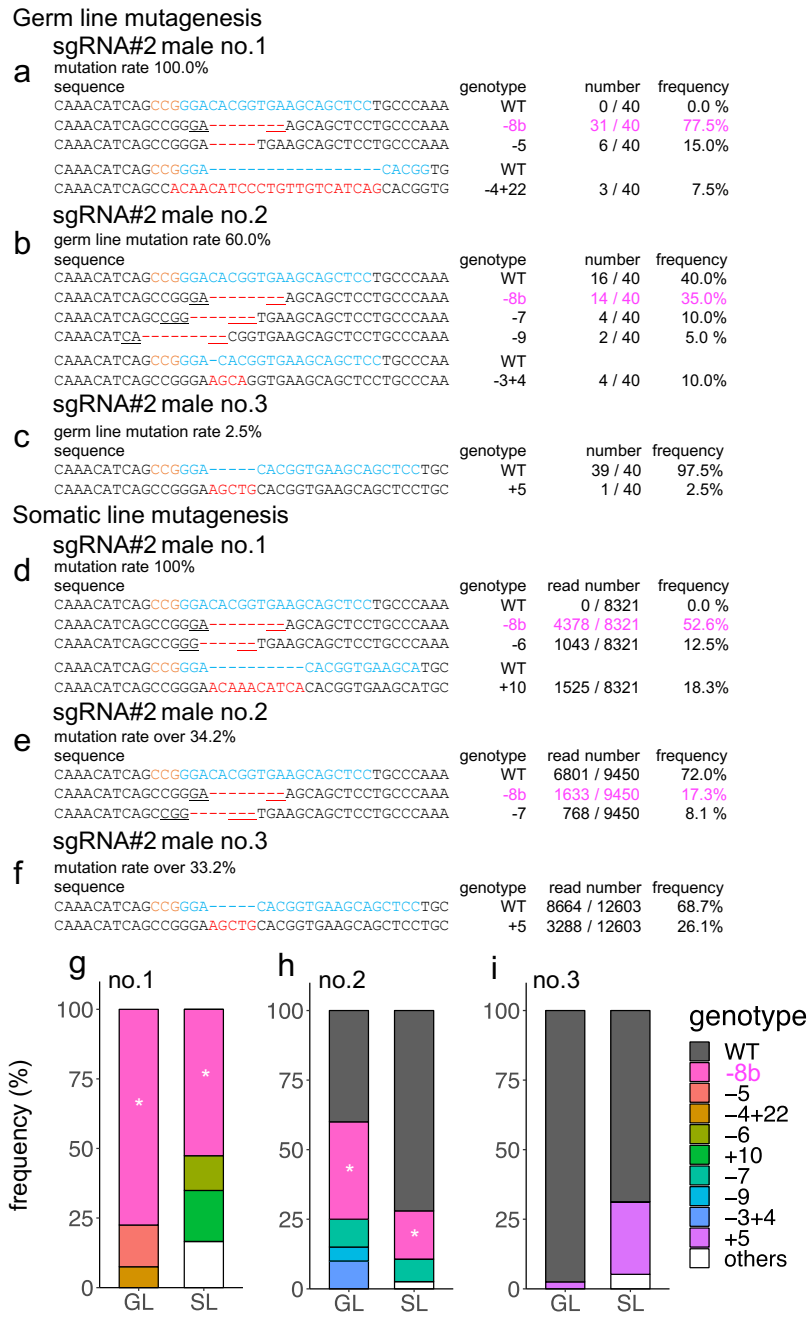

Fig. 3.8 Germ line and somatic mutagenesis in G_0 injected with sgRNA#2

(a-c) Germ line mutations in three males. (d-f) Somatic line mutations from pectoral fin in the three males, analyzed with amplicon sequencing. These are shown in order of sequences, the sizes of deletions (-) and insertion (+), numbers in germ line (each mutated embryo / all analyzed embryos) or read number in somatic line (each read number / total read number), and the frequencies. Blue and orange letters, target sequence and PAM, respectively. Red dashes and letters, deletions and insertions. Under bars, microhomologies. The mutations in magenta letter indicate the targeted mutation via MMEJ (designated as "-8b") for production of homozygote F_1 founders. (g-i) The comparison with germ line ("GL") and somatic line ("SL") mutagenesis. The column which is a specific color indicates a different mutation variant. The asterisks indicated the "-8b" mutation.

3.4.6 Production of mstn knockout homozygotes with artificial insemination

In April 2018, unfertilized eggs were collected from two 3-years old female injected with sgRNA#1 and sgRNA#2, respectively. These females were judged by HMA to be mutated in pectoral fin and were enough large for maturation. A part of unfertilized eggs was fertilized *in vitro* with wild type counterpart gametes in order to investigate germ line mutagenesis. In addition, 100 g of unfertilized eggs was fertilized *in vitro* with cryopreserved G_0 sperm in order to produce homozygotes. The female parents' germ line mutations were shown in **Fig. 3.9**. Total germ line transmission rates were 45.0% in sgRNA#1 no.1 and 94.7% in sgRNA#1 no.2 (**Fig. 3.9a** and **b**). The -8a mutation was inherited at 20.0% only in female no.1 (**Fig. 3.9a**). Total germ line transmission rates were intermediate: 47.5% in sgRNA#1 no.1 and 40.0% in sgRNA#1 no.2 (**Fig. 3.9c** and **d**). The -8b mutation was inherited at 7.5% in female no.1 (**Fig. 3.9c**) and at 7.5% also in female no.2 (**Fig. 3.9d**). Therefore, homozygote F_1 founder, *mstn*$^{-8a/-8a}$, could be obtained by mating female no.1 with cryopreserved sperm of male no.1 (**Fig. 3.9e**). In addition, homozygote F_1 founder, *mstn*$^{-8b/-8b}$, could be obtained by mating either female no.1 or no.2 with cryopreserved sperm of male no.1. I selected the female no.1 (**Fig. 3.9f**) because compound heterozygotes such as *mstn*$^{-8b/-2}$ and *mstn*$^{-8b/-7}$ can be also produced.

3.4.7 Screening of F_1 homozygotes

Total 576 (sgRNA#1) and 480 (sgRNA#2) F_1 fish were screened with HMA and subsequent direct sequencing was performed at 3 to 4 mpf. As a results, I successfully obtained homozygotes: *mstn*$^{-8a/-8a}$, 20 fish (3.47%; male, 12 and female, 8); *mstn*$^{-8b/-8b}$, 13 fish (2.71%; male, 6 and female, 7). Heterozygotes siblings (*mstn*$^{-8a/wt}$) and wild type siblings (*mstn*$^{wt/wt}$) were also set asides as controls for comparison of phenotype. The band shift pattern in HMA of these homozygotes were shown in **Fig. 3.10a** (*mstn*$^{-8a/-8a}$) and **Fig. 3.10b** (*mstn*$^{-8b/-8b}$). The PCR products from homozygotes showed single band patterns with small size and the products re-annealed with wild type PCR products showed heteroduplex band patterns. The genotypes of homozygotes are shown in **Fig. 3.10c**. The predicted protein sequences of homozygotes are shown in **Fig. 3.10d**. The *mstn*$^{-8a/-8a}$ harbors 122 amino acid (a.a.) residues: 114 homologous, 8 non-homologous with wild type. The *mstn*$^{-8b/-8b}$ harbors 98 a.a. residues: 76 homologous, 22 non-homologous with wild type. In contrast, the intact MSTN protein (wild type protein) consisted in 376 a.a.

containing an active domain in its C-terminal. Therefore, the C-terminal active domain was completely disrupted in *mstn*$^{-8a/-8a}$ and *mstn*$^{-8b/-8b}$ (Blue letters and box, **Fig. 3.10d-e**).

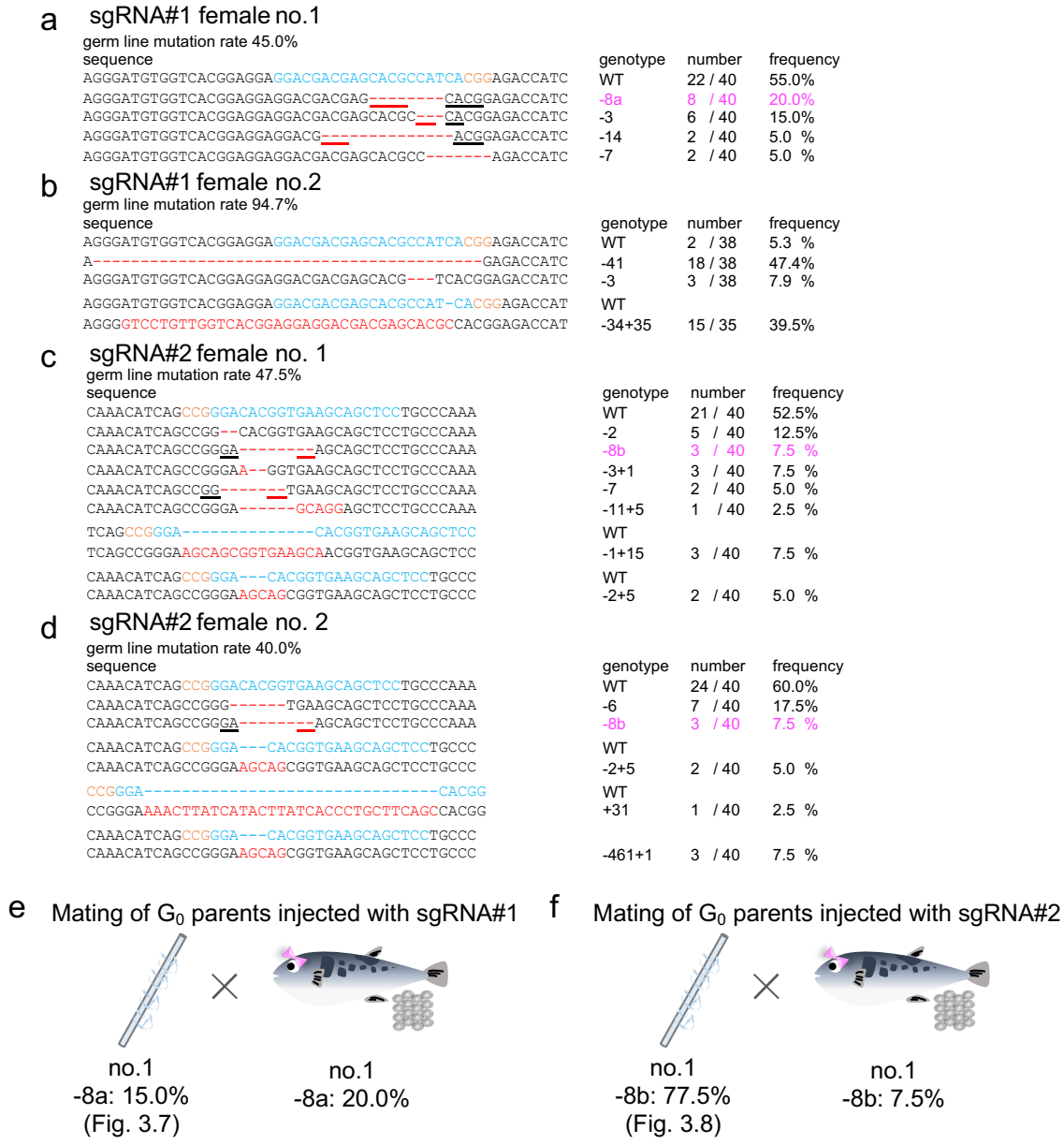

Fig. 3.9 Germ line mutagenesis in G_0 female parents

Two female G_0 parents were screened for heritable mutations. G_0 female parents injected with sgRNA#1 (a, b), with sgRNA#2 (c, d). These are shown in order of sequences, the sizes of deletions (-) and insertion (+), numbers in germ line (each mutated embryo / all analyzed embryos), and the frequencies. Blue and orange letters, target sequence and PAM, respectively. Red dashes and letters, deletions and insertions. Under bars, microhomologies. The mutations in magenta letter indicate the targeted mutation via MMEJ, "-8a" and "-8b", for production of homozygote F_1 founders. (e, f) Mating pairs of G_0 parents for production of homozygotes.

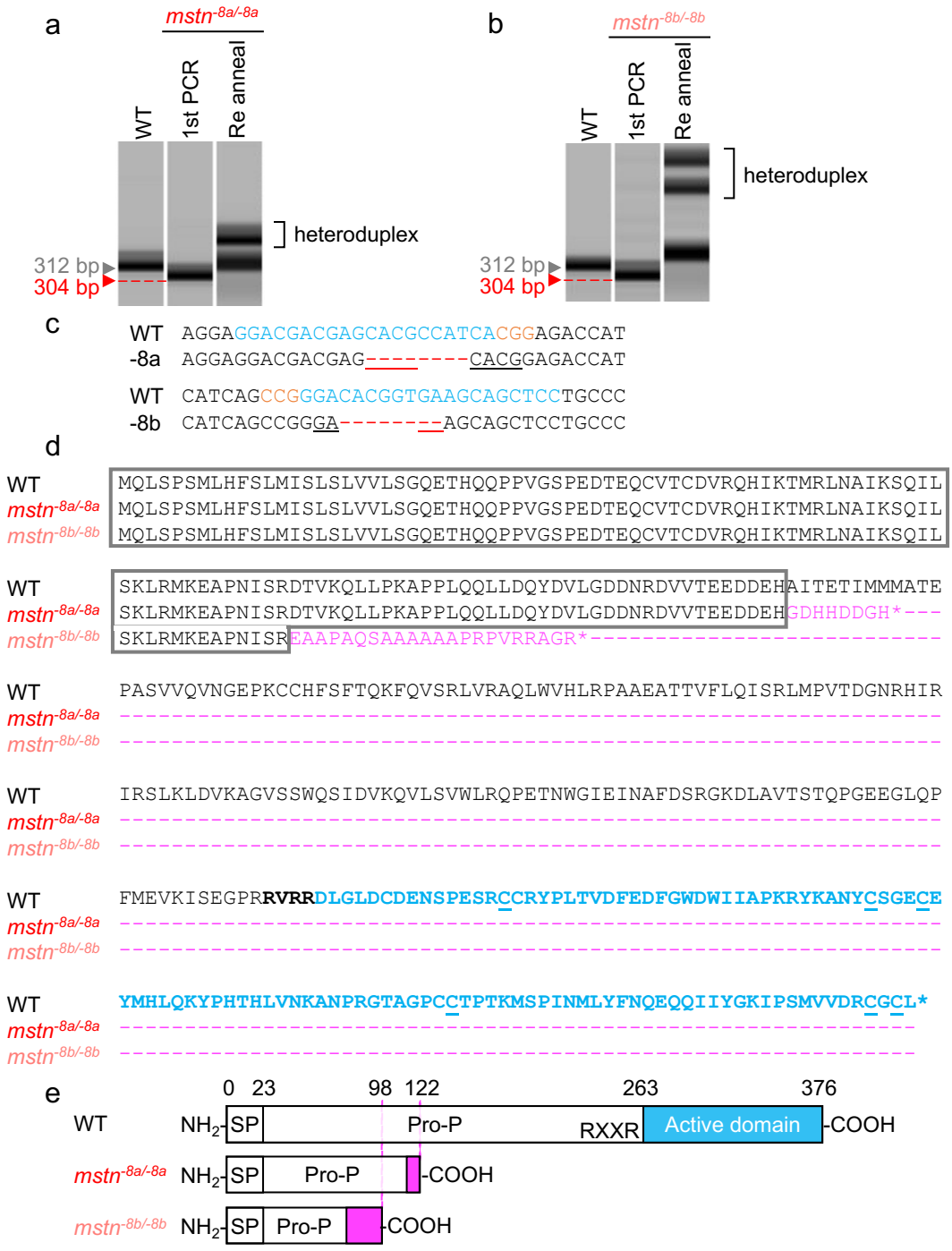

Fig. 3.10 Genotype and protein sequence of homozygote

The HMA band shift images of *mstn*$^{-8a/-8a}$ (a) and *mstn*$^{-8b/-8b}$ (b). (c) The genotype of *mstn*. Blue and orange letters, target sequence and PAM, respectively. Red dashes, deletions. Under bars, microhomologies. (d) The alignment of predicted amino acids. Grey boxes and magenta letters indicate the homologous and non-homologous regions with wild type, respectively. Blue letters, C-terminal active domain; "RXXR", proteolytic cleavage site; underlined blue letters, cysteine residues essential for the activity of MSTN. (e) The MSTN protein form. SP, Signal peptide; Pro-P, pro-peptide; magenta boxes, non-homologous residues with wild type; blue box, C-terminal active domain. The *mstn*$^{-8a/-8a}$ and *mstn*$^{-8b/-8b}$ harbor 122 and 98 a.a., respectively On the other hand, wild type harbors 376 a.a.

3.4.8 Morphological analysis in F_1 mutants

Figure 3.11a-b shows the morphological features of F_1 homozygous mutant at 207 dpf. The homozygote mutant (*mstn*$^{-8a/-8a}$) exhibited increased skeletal muscle mass in comparison to wild type fish as same as in G_0 mutant and shorter body length than wild type. Condition factor of homozygote was significantly higher than those of heterozygote (*mstn*$^{-8a/wt}$) and wild type (*mstn*$^{wt/wt}$) (**Fig. 3.11c**: *mstn*$^{-8a/-8a}$, 45.24 ± 3.86; *mstn*$^{-8a/wt}$, 37.60 ± 1.85; *mstn*$^{wt/wt}$, 35.65 ± 2.31). There are not significant differences in body weight (**Fig. 3.11d**: *mstn*$^{-8a/-8a}$, 242.83 ± 48.78 g; *mstn*$^{-8a/wt}$, 226.62 ± 27.86 g; *mstn*$^{wt/wt}$, 224.34 ± 27.23 g). Standard length of homozygote was significantly shorter than those of heterozygote and wild type (**Fig. 3.11e**: *mstn*$^{-8a/-8a}$, 17.44 ± 0.96 cm; *mstn*$^{-8a/wt}$, 18.18 ± 0.71 cm; *mstn*$^{wt/wt}$, 18.44 ± 0.59 cm). There were no sexual differences in each genotype (data not shown).

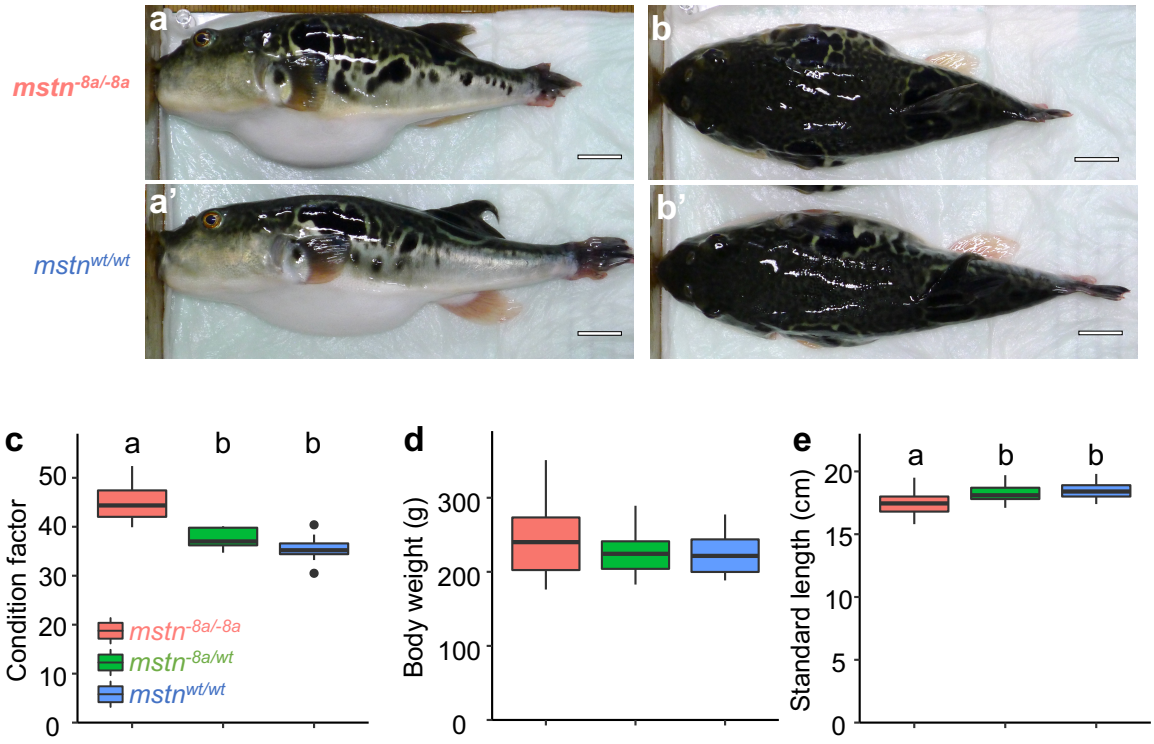

Fig. 3.11 The morphology of *mstn* mutants in F_1

The appearance of F_1 mutants and wild type sibling (side view: a and a', overhead view: b and b'). These photos were at 207 dph. Scale bars, 2 cm. (c-d) The measurement of body weight and standard length at 207 dph. Comparison of and standard length, body weight, and condition factor (body weight / standard length^3 x 10^3) among homozygote (*mstn*$^{-8a/-8a}$, n=16; red boxplots), heterozygote siblings (*mstn*$^{-8a/wt}$, n=17; green boxplots), and wild type siblings (*mstn*$^{wt/wt}$, n=17; blue boxplots). Different superscripts indicate significantly differences with Tukey-Kramer HSD test, $P < 0.05$.

In order to estimate skeletal muscle mass, cross-sectional areas on skeletal muscle were qualified by CT-scan (**Fig. 3.12**). I segmented cross-sectional area (CSA) of skeletal muscle regions in the nearest slice to 5th centrum (CSA-1, **Fig. 3.12a**), 8th centrum (CSA-2, **Fig. 3.12b**), the first spine of dorsal fin (CSA-3, **Fig. 3.12c**), and the 17th centrum (CSA-4, **Fig. 3.12d**), respectively. Each CSA positions were described in **Fig. 3.12e**. In CSA-1 and CSA-2, the dorsal skeletal muscle region of homozygote exhibited remarkable hypertrophy, and internal organ region was compressed as in **Fig. 3.12a-b**. In CSA-3 and CSA-4, entire skeletal muscle region of homozygote exhibited remarkable hypertrophy as in **Fig. 3.12c-d**. Significant increases of skeletal muscle mass of homozygote were observed all of the cross-sectional areas (CSA-1: 1.32 fold change, *mstn*$^{-8a/-8a}$, 992.7 ± 163.7 mm^3, *mstn*$^{wt/wt}$, 754.6 ± 56.3 mm^3; CSA-2: 1.30 fold change, *mstn*$^{-8a/-8a}$, 1280.8 ± 178.56 mm^3, *mstn*$^{wt/wt}$, 981.6 ± 78.4 mm^3; CSA-3: 1.20 fold change, *mstn*$^{-8a/-8a}$, 1304.1 ± 167.72 mm^3, *mstn*$^{wt/wt}$, 1089.8 ± 106.8 mm^3; CSA-4: 1.24 fold change, *mstn*$^{-8a/-8a}$, 679.2 ± 53.4 mm^3, *mstn*$^{wt/wt}$, 548.2 ± 51.3 mm^3) (**Fig. 3.12f**). Body widths of *mstn*$^{-8a/-8a}$ were increased than wild type. I compared the body width value at the position on CSA-3 (BWD-3) and CSA-4 (BWD-4), orange double-head arrows in **Fig. 3.12c** and **3.12d**, respectively. Significant increases of body width of homozygote were observed (BWD-3: *mstn*$^{-8a/-8a}$, 44.3 ± 2.6 mm^3, *mstn*$^{wt/wt}$, 38.1 ± 3.8 mm; BWD-4: *mstn*$^{-8a/-8a}$, 32.8 ± 1.1 mm, *mstn*$^{wt/wt}$, 30.4 ± 2.0 mm) (**Fig. 3.12g**). These results indicate that complete disruption of MSTN induces remarkable skeletal muscle mass.

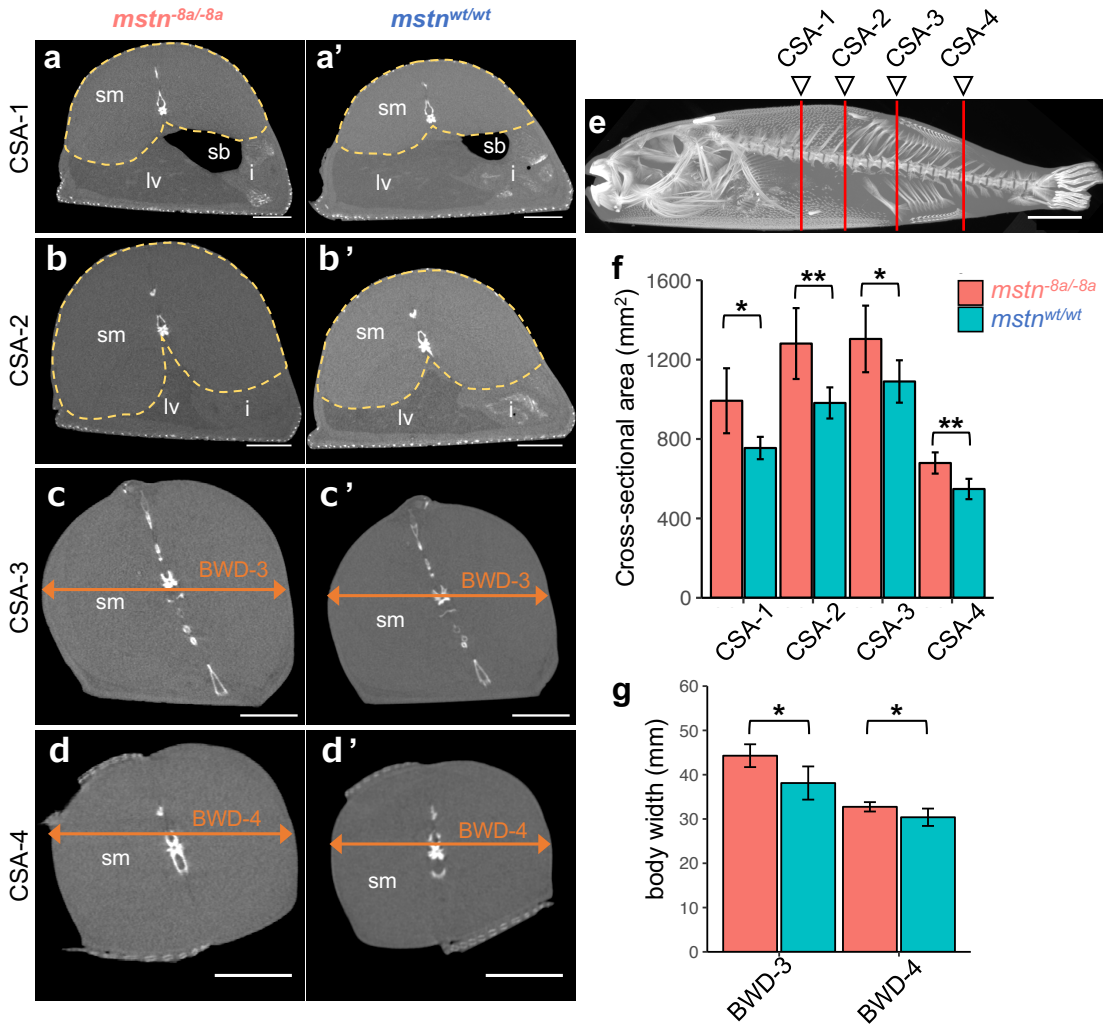

Fig. 3.12 The evaluation of skeletal muscle mass of *mstn* mutants in F_1

The cross-sectional area of *mstn*$^{-8b/-8b}$ (a, b, c, and d) and *mstn*$^{wt/wt}$ (a', b', c', and d') at the position of 5th centrum (CSA-1), 8th cenrum (CSA-2), first spine of dorsal fin (CSA-3), and end spine of dorsal fin (17th centrum, CSA-4). (e) The positions of CSA sections. Comparison of CSA (f) of skeletal muscle and body width (g) between homozygote (*mstn*$^{-8a/-8a}$, n=5; red barplots), and wild type siblings (*mstn*$^{wt/wt}$, n=5; blue berplots). Yellow dotted lined regions indicate segmented skeletal muscle regions (CSA-1 and CSA-2). Orange double-head arrows indicate body width: BWD-3 and BWD-4 in CSA-3 (c) and CSA-4 (d), respectively. (a-d) Skeletal muscle, sm; liver, lv; swim bladder, sb; intestine, i. (f, g) The asterisks indicate significantly differences with student t-test, *: $P < 0.05$, **: $P < 0.01$. Scale bars: 1 cm.

3.4.9 Bone structure analysis in F_1 mutants

I examined the bone structure phenotype in detail by CT-scan (**Fig. 3.13a-b**). Head length from the tip of the snout to 1st centrum, anterior-posterior length (A-P length), dorsal-ventral length (D-V length), and width of centrums identified order numbers from anterior to posterior (1st-21th) were compared between *mstn*$^{-8a/-8a}$ and wild type (see in **Fig. 3.13c-d**). There was no difference in the number of centrum between two groups. Note that one wild type fish had one less preural centrum (six) than another fish (seven), which I concluded the preural centrum of the wild type fish were outlier. There was no difference in the head length between two groups (**Fig. 3.13e**). The mean values of A-P length of all centrums in *mstn*$^{-8a/-8a}$ were shorter than those of wild type. There were significant differences in 3rd-6th and 11th-21th of centrums. (**Fig. 3.13f**). And also, the mean values of D-V length of all centrums in *mstn*$^{-8a/-8a}$ were shorter than those of wild type. There were significant differences in 1st-8th, 10th-11th, 13th-15th, and 17th-21th of centrums (**Fig. 3.13g**). The width in *mstn*$^{-8a/-8a}$ were significantly shorter than wild type (only in 13th and 19th centrums) (**Fig. 3.13h**). These results indicate that homozygous mutants exhibit shorter centrum lengths of the direction from anterior to posterior and the direction from dorsal to ventral than wild type. There are not much differences in widths of centrums between homozygote and wild type. These results indicate that the short body length is caused by the shorten centrum lengths in the direction from anterior to posterior in *mstn*$^{-8a/-8a}$.

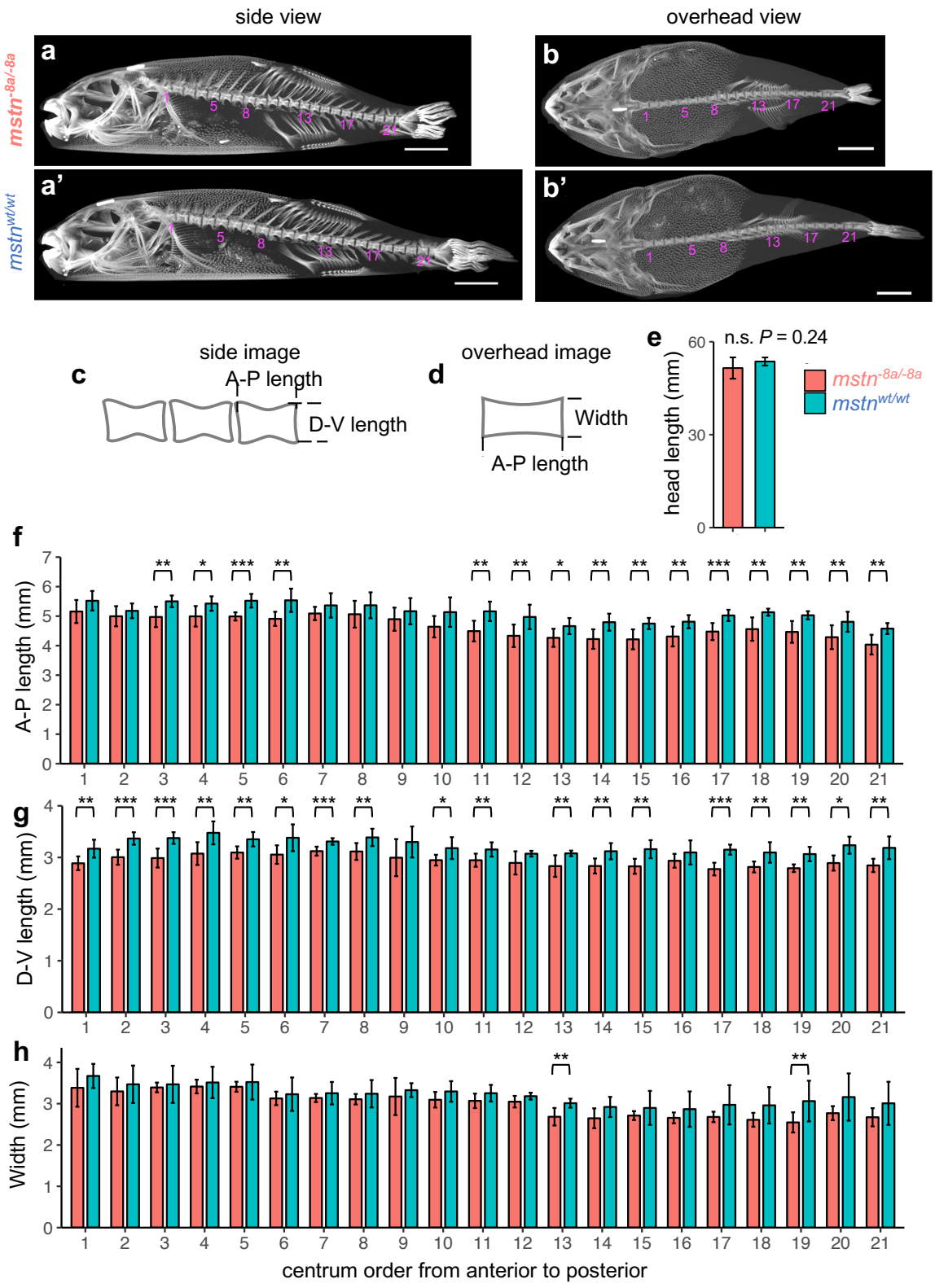
side view
overhead view
mstn-8a/-8a
mstnwt/wt
a
a'
b
b'
1
5
8
13
17
21
c
side image
A-P length
D-V length
d
overhead image
Width
A-P length
e
n.s. P = 0.24
head length (mm)
mstn-8a/-8a
mstnwt/wt
f
A-P length (mm)
g
D-V length (mm)
h
Width (mm)
centrum order from anterior to posterior

Fig. 3.13 The evaluation of size of centrums of *mstn* mutants in F_1

CT scan of skeletons (a and a', b and b'). The CT images were reconstructed by maximum-intensity-projection from tiff-stacks images of side direction (a and a'), and of dorsal-ventral overhead direction (b and b'). The numbers in magenta letter indicate centrum order. These images were at 207 dph. Scale bars, 2 cm. Side (c) and overhead images (d) of fugu centrum. (e) The head length, from the tip of the snout to 1st centrum. The measured values of length: A-P length (f), D-V length (g), and width (h). The horizontal axes indicate centrum order from anterior to posterior. Comparison of centrum lengths between homozygote (*mstn*$^{-8a/-8a}$, n=5; red columns), and wild type siblings (*mstn*$^{wt/wt}$, n=5; blue columns). Each length value of 15th-21th centrum in wild type includes four fish data because one wild type fish had one less preural centrum (six) than another fish (seven), which I concluded the preural centrum length values of the wild type fish were outlier. The asterisks indicate significantly differences with student *t*-test, *: $P < 0.1$, **: $P < 0.05$, ***: $P < 0.01$.

3.4.10 Off target analysis

The numbers of off-target candidates from GGGenome search were 14 and 15 in sgRNA#1 and sgRNA#2, respectively (**Fig. 3.14** and **Table 3.3**). The HMA and DNA sequencing revealed that only on target sequence was altered and that there was no off-target alternation in each candidate (**Figs. 3.14** and **3.15**). In sgRNA#1, single fragments were observed in off-target#1 (OFT#1) and OFT#3-#14 same as wild type. Heteroduplexs bands were observed both in wild type and G_0 sample because endogenous in/del and SNP variations exist in OFT#2 (intron of *pacs1a* gene), (**Fig. 3.14**). In sgRNA#2, single fragments were observed in OFT#1-#7 and OFT#9-#15 same as wild type. Heteroduplexs bands were observed both in wild type and G_0 sample because endogenous in/del variation exists in OFT#8 (no gene locus) (**Fig. 3.15**). These results indicate that the two sgRNAs in this study have high specificity against each target sequence.

sgRNA#1

	18	17	16	15	14	13	12	11	10	9	8	7	6	5	4	3	2	1			
ONT	A	C	G	A	C	G	A	G	C	A	C	G	C	C	A	T	C	A	C	G	G
OFT#1	A	C	G	A	C	C	A	G	C	A	C	G	C	C	A	T	C	A	T	G	G
OFT#2	A	-	G	A	C	G	A	G	C	-	C	G	C	C	A	T	C	A	C	A	G
OFT#3	A	C	G	A	C	G	A	G	G	A	C	G	T	C	A	T	C	A	A	G	G
OFT#4	A	C	G	C	C	G	A	G	-	A	C	G	C	C	A	T	C	A	C	A	G
OFT#5	A	-	G	A	C	T	A	G	C	A	C	G	C	C	A	T	C	A	G	A	G
OFT#6	A	C	T	A	-	G	A	G	C	A	C	G	C	C	A	T	C	A	A	A	G
OFT#7	A	C	G	C	C	G	A	G	-	A	C	G	C	C	A	T	C	A	C	A	G
OFT#8	A	C	G	A	-	G	A	G	C	A	-	G	C	C	A	T	C	A	T	G	G
OFT#9	T	C	G	A	C	G	A	G	C	T	C	G	C	C	A	T	C	A	A	A	G
OFT#10	A	C	G	A	G	G	A	G	C	A	C	G	C	C	A	C	C	A	G	G	G
OFT#11	A	C	G	A	C	G	T	G	C	-	C	G	C	C	A	T	C	A	G	A	G
OFT#12	A	C	G	G	C	G	A	G	C	A	C	A	C	C	A	T	C	A	G	G	G
OFT#13	A	C	G	A	C	G	A	A	G	C	A	C	G	C	C	A	T	C	C	G	G
OFT#14	A	C	G	A	C	G	A	G	C	A	C	G	C	C	A	A	T	C	A	G	C	G	G
																			PAM		
								SEED SEAQUENCE													

sgRNA#2

				1	2	3	4	5	6	7	8	9	10	11	12	13	14	15	16	17	18
ONT	C	C	G	G	G	A	C	A	C	G	G	T	G	A	A	G	C	A	G	C	T
OFT#1	C	T	C	G	G	A	G	A	C	T	G	T	G	A	A	G	C	A	G	C	T
OFT#2	C	C	T	G	G	A	A	A	C	G	G	T	G	A	A	G	C	A	G	C	T
OFT#3	C	C	A	G	G	A	C	G	C	G	G	T	G	A	A	A	G	C	A	G	C	T
OFT#4	C	T	G	G	-	A	C	A	C	G	G	G	G	A	A	G	C	A	G	C	T
OFT#5	C	C	G	G	G	A	C	A	C	G	C	T	G	A	A	G	-	A	G	C	T
OFT#6	C	C	A	G	G	A	C	A	T	T	G	T	G	A	A	G	C	A	G	C	T
OFT#7	C	C	A	G	G	A	C	A	-	G	G	T	G	-	A	G	C	A	G	C	T
OFT#8	C	C	A	G	G	A	C	A	C	A	G	G	T	G	A	A	G	C	A	G	-	T
OFT#9	C	T	T	G	G	A	C	A	T	G	G	T	G	A	A	G	-	A	G	C	T
OFT#10	C	T	C	G	G	A	C	A	C	G	G	T	-	C	A	G	C	A	G	C	T
OFT#11	C	T	G	G	G	A	C	A	C	G	T	G	T	G	A	A	G	C	T	G	C	T
OFT#12	C	T	G	G	-	A	-	A	C	G	G	T	G	A	A	G	C	A	G	C	T
OFT#13	C	T	C	-	A	A	C	A	C	G	G	T	G	A	A	G	C	A	G	C	T
OFT#14	C	T	C	G	G	A	T	A	C	C	G	T	G	A	A	G	C	A	G	C	T
OFT#15	C	T	G	G	G	A	C	A	C	T	G	T	G	-	A	G	C	A	G	C	T
	PAM			SEED SEAQUENCE																	

Fig. 3.14 Potential off-target candidates' sequences in fugu genome

Sequence of the original each sgRNA is in the top row of the grid (described as "ONT"). The candidates were searched by the following criterion: harboring 2 or fewer bp mismatches in the 18-bp targeting sequence followed by a NRG PAM. Positions of mismatch nucleotides are highlighted in yellow for the red letters. Positions of PAM sequences are highlighted in grey. A seed sequence, a 12-bp sequence adjacent to a PAM, is considered as an important sequence for the recognition of sgRNA.

Table 3.3 Potential off-target candidates in fugu genome

sgRNA#1

Name	Scaffold, region	strand	Emsembl gene	feature	Mismatch	Forward PCR Primer (5'- -3')	Reverse PCR rimer (5'- -3')	Effect*
ONT	chr1:22,387,646-22,387,665	F	mstn	exon	-	CCCGTCGGCAGCCCAGAGGACA	TGAGTGTTTACCTCGCTGTG	-
OFT#1	HE591726:160,576-160,595	F	plppr3b	exon	1	CACGCTCCGTTCTTCCTGAC	GGAAGGGAAGCTCTTCCTGT	none
OFT#2	HE591780:191,572-191,590	F	pacs1a	intron	2	CTCTCTGCTCTGTGACTCAT	ACGTGGATGCTGCGACATGC	none
OFT#3	HE591794:119,986-120,006	F	ENSTRUG00000005806	exon	2	TCCCTCCTTTGTGACCATTT	CGCAGCCAGGTGAAGAAGGC	none
OFT#4	HE596171:3,479-3,498	F	none	none	2	TCAAACTTAAAATCTCCTCG	CGAAGCTGTAAGCTTTGCAA	none
OFT#5	chr11:935,929-935,948	F	none	none	2	GGAGGAGTGGTTTAGTAGGC	GTGAGACCAACAGTTGCTCA	none
OFT#6	chr13:7,490,534-7,490,553	F	brsk2	intron	2	GGGCTTAAACACAAGGGCGT	AAATGGACGCTGTCGCTCTG	none
OFT#7	chr19:5,333,925-5,333,944	F	slc25a20	exon	2	TCAAACTTAAAATCTCCTCG	CGAAGCTGTAAGCTTTGCAA	none
OFT#8	chr19:9,847,586-9,847,604	F	ENSTRUG00000007355	intron	2	CTTTGAGTCTGGGTTTGATT	CAACGTGCACTTTAAGAGGA	none
OFT#9	chr21:10,672,921-10,672,941	F	ENSTRUG00000016797	exon	2	CTGGAGAGCGTGATGCACCT	TTATTTACAGATAATCAACC	none
OFT#10	HE591787:111,529-111,549	R	none	none	2	CGCAGTAGAGCTGGGGGACG	GCGTGTGGTCAGGCCTCAGC	none
OFT#11	HE591799:184,089-184,108	R	ENSTRUG00000025262	exon	2	GTTATATTTGTAGTTATTAT	CAGATAATCACCTAGCTACA	none
OFT#12	HE592042:37,022-37,042	R	garem	exon	2	TAGCGGTGACCTTCTCGAAT	CTCATCTGCATGAACCACCG	none
OFT#13	chr17:1,234,353-1,234,375	R	rhbd3	intron	2	CCATGGCAACTAAGGAGAGG	TGTTGTGGGTGACACCAGAG	none
OFT#14	chr18:3,979,830-3,979,852	R	apaf1	exon	2	TCTATATGGACGCTAACAAA	ACGGATGGAAATGCTCTGCG	none

sgRNA#2

Name	Scaffold, region	strand	Emsembl gene	feature	Mismatch	Forward PCR Primer (5'- -3')	Reverse PCR rimer (5'- -3')	Effect*
ONT	chr1:22,387,539-22,387,559	R	mstn	exon	-	CCCGTCGGCAGCCCAGAGGACA	TGAGTGTTTACCTCGCTGTG	-
OFT#1	chr4:1,162,726-1,162,746	F	xpo1b	exon	2	GTAGACATTGAGCATGTCGA	ACTGAAAAGATCTGCTGTGT	none
OFT#2	chr4:11,718,936-11,718,956	F	ENSTRUG00000015507	exon	1	TTTAACAAAGAGGTAACTCG	CTCCTGCTAACAATGAGGCT	none
OFT#3	chr16:8,042,735-8,042,756	F	tmem151ba	exon	2	GGATGCACTTGAAGAATGTA	GCTCCTCAGACGGTGTTACT	none
OFT#4	HE591742:76,430-76,450	R	ENSTRUG00000000061	intron	2	CCTCGGCCTCCACGCTGGTT	GTTGCCCAAGCAGTACCCCT	none
OFT#5	HE591865:9,133-9,152	R	wdr55	exon	2	CATCCACCACCAGCAGACTG	TACTCGTACTCGTGCACCGA	none
OFT#6	HE592092:2,617-2,637	R	none	none	2	TTTATTTTTTGAAACAATTC	ACCGTTGACGTCACATATTT	none
OFT#7	HE592542:6,151-6,169	R	mast2	exon	2	CCGCCTTTGAGAACACGTCC	CGCCTGCTTGGTGATCTTCC	none
OFT#8	HE597876:377-397	R	none	none	2	TCCTAAATCTGATTTACCAA	GAGAGCTGCGAATAAACCTG	none
OFT#9	chr3:4,808,798-4,808,817	R	emp3b	exon	2	GAGATGCTTTCTTTTTTTCA	TCAGGGGATTTCTTTTCTGT	none
OFT#10	chr3:12,429,308-12,429,327	R	kdm5bb	exon	2	TTGGGAGTGCTTTGGAAACG	CCCGCCACCCTGACGCTGGA	none
OFT#11	chr9:13,628,263-13,628,284	R	none	none	2	TCTCCAGTCAATGGGATTAT	CCAGGAGGAAGCGGAGCCAG	none
OFT#12	chr12:2,480,781-2,480,800	R	none	none	2	AGTGTTTGAAGAGTTTGCTT	ATCTGAACCAGTCTGACATA	none
OFT#13	chr14:5,736,765-5,736,784	R	none	none	2	TTCTGGAATTACCAGGAGCT	GGGCCACGGGGCCCAGGCTT	none
OFT#14	chr15:4,653,673-4,653,693	R	zbtb16a	intron	2	GAAGATGGCTCTCTGCCGAA	TCCATGACACCTTCAGGAAG	none
OFT#15	chr17:3,562,708-3,562,727	R	wdr19	exon	2	TCAGCCCAAAAACATTCCAT	GCAGGACAGAGCAGGAAGCC	none

Primer sequences for HMA and the results of analysis (*: in the light edge column) are also shown.

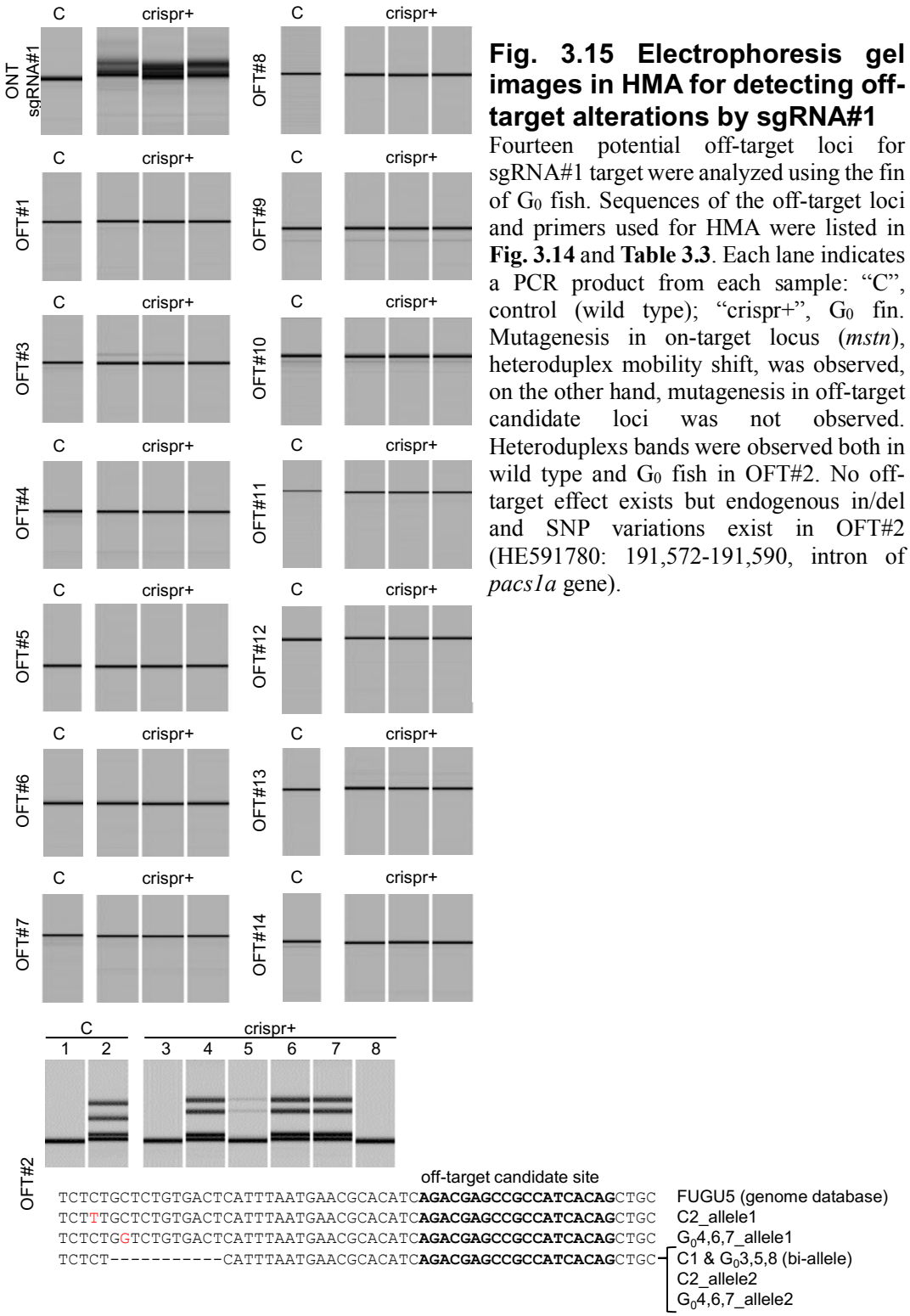

Fig. 3.15 Electrophoresis gel images in HMA for detecting off-target alterations by sgRNA#1

Fourteen potential off-target loci for sgRNA#1 target were analyzed using the fin of G_0 fish. Sequences of the off-target loci and primers used for HMA were listed in **Fig. 3.14** and **Table 3.3**. Each lane indicates a PCR product from each sample: "C", control (wild type); "crispr+", G_0 fin. Mutagenesis in on-target locus (*mstn*), heteroduplex mobility shift, was observed, on the other hand, mutagenesis in off-target candidate loci was not observed. Heteroduplexs bands were observed both in wild type and G_0 fish in OFT#2. No off-target effect exists but endogenous in/del and SNP variations exist in OFT#2 (HE591780: 191,572-191,590, intron of *pacs1a* gene).

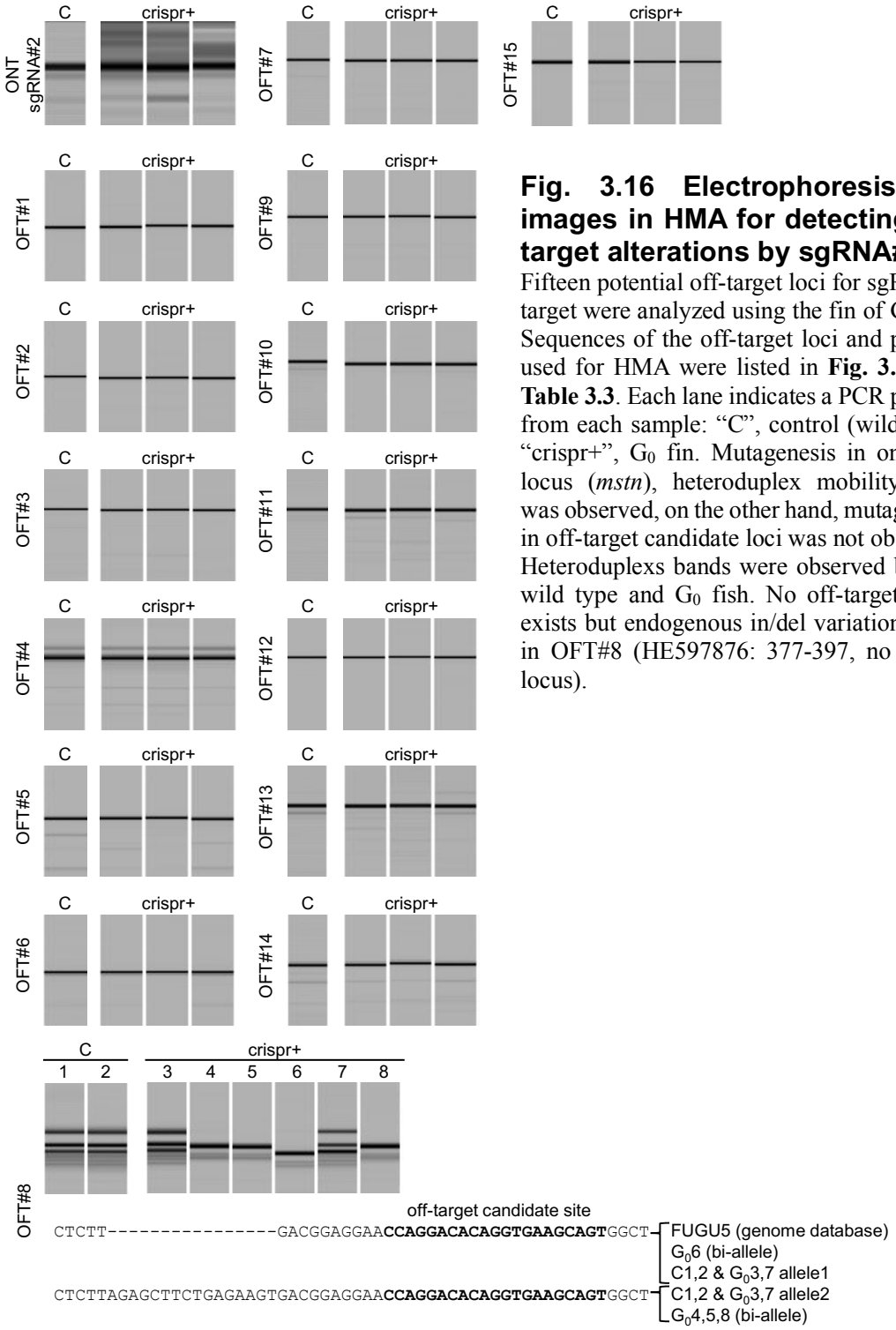

Fig. 3.16 Electrophoresis gel images in HMA for detecting off-target alterations by sgRNA#2

Fifteen potential off-target loci for sgRNA#2 target were analyzed using the fin of G_0 fish. Sequences of the off-target loci and primers used for HMA were listed in **Fig. 3.14** and **Table 3.3**. Each lane indicates a PCR product from each sample: "C", control (wild type); "crispr+", G_0 fin. Mutagenesis in on-target locus (*mstn*), heteroduplex mobility shift, was observed, on the other hand, mutagenesis in off-target candidate loci was not observed. Heteroduplexs bands were observed both in wild type and G_0 fish. No off-target effect exists but endogenous in/del variation exists in OFT#8 (HE597876: 377-397, no gene locus).

C3.5 Discussion

In the present study, I demonstrated that genome editing CRISPR/Cas9 system was effective to produce a new breed of *mstn* knockout fugu exhibiting increased skeletal muscle mass and to investigate the *mstn* gene function in fugu, following the workflow in **Fig. 3.3**. The homozygotes were established in three years which is a shortest sexual maturation period of fugu female, that is, a shortest generation period. The phenotype of skeletal muscle mass caused by MSTN deficiency is consistent with other teleost and mammals [**5-11**, **21-23**]. One of the important findings of the present study is that the phenotypes of shorten body length and shorten centrums are consistent with red sea bream [**chapter 2**, **7**], but inconsistent with small model fish and mice [**8-11**, **24**].

The two sgRNAs were designed in the first exon located in the upstream of C-terminal active peptide coding region, which was expected to disrupt the gene by frame-shift mutation (**Fig. 3.1a**). Microinjection of the mixture of Cas9 RNA and each sgRNA was performed in 2015 in order to produce genome edited G_0 fugu. The target mutagenesis was successfully induced in *mstn* gene judging from the results of HMA in G_0 embryos and pectoral fins (**Figs. 3.1b-c**, **3.4** and **Table 1**). The mutations in G_0 fugu were efficiently induced with high mosaicism in fugu as same as in other fish species [**7, 12, 25-27**]. Moreover, the phenotype of increased skeletal muscle was observed in G_0 fish which showed high mosaicism of *mstn* knockout cells. The G_0 fugu mutants ($mstn^{sgRNA\#1\text{-}High}$ and $mstn^{sgRNA\#2\text{-}High}$) exhibited increase of condition factor and body weight, and 27% increase of cross-sectional area and 26% increase of skeletal muscle volume in comparison with control fish (**Figs. 3.5**, **3.6**, and **Table 3.2**). Recent studies revealed that the phenotype of increased skeletal muscle mass can be also observed in G_0 *mstn* mutants such as mosaic mutated teleost, red sea bream, common carp, and channel catfish [**7**, **25-26**]. Therefore, it is concluded that the *mstn* knockout phenotype of increased skeletal muscle mass can be observed in G_0 generation of genome edited fugu. The present study clarified that $mstn^{sgRNA\#1\text{-}High\ \#1}$ and $mstn^{sgRNA\#1\text{-}High\ \#2}$ harbored 97.2% and 100% of induced mutations and 51.6% and 59.0% of frame-shift mutations in a sampled skeletal muscle region (**Fig. 3.6g-j**). The present results suggested that there were a large number of cells which harbor bi-allelic mutations in G_0 fugu mutants. In addition, it is suggested that there were some cells in which frame-shift mutations occurred in bi-allele because over 50% of frame-shift mutations contributing to complete gene knockout were observed.

In the present study, mating G_0 fish to each other was performed to accomplish production of F_1 homozygote (**Fig. 3.3**). As described in the red sea bream study [**7**], this mating method is necessary in order to reduce the period for establishment of new breeds for aquaculture fish species which have a long sexual maturation period, such as fugu (male, 2 years; female, 3 years). In order to produce F_1 homozygote, it is needed that both male and female parents which harbor a same mutation were selected. In genome editing mediated TALENs in medaka and mediated CRISPR/Cas9 in red sea bream, it was reported that microhomology induces a specific pattern of mutations and mutation via MMEJ is inherited to F_1 founders from G_0 fish with high efficiency [**7, 16**]. In this study, I also observed the frame-shift mutations via MMEJ ("-8a": 8 base deletion in sgRNA#1, and "-8b": 8 base deletion in sgRNA#2) in germ line (**Figs. 3.7-3.9**). In addition, these mutations were observed both in male and female so that F_1 homozygotes (*mstn*$^{-8a/-8a}$ and *mstn*$^{-8b/-8b}$) were successfully produced as same as in the previous report [**7**]. The expected rates from germ line mutagenesis analysis were 3.0% in *mstn*$^{-8a/-8a}$ (15.0% in male and 20.0% in female) and 5.8% in *mstn*$^{-8b/-8b}$ (77.5% in male and 7.5% in female). As results of screening of F_1 fish at 3-4 mpf, the actual observed rates were 3.47% in *mstn*$^{-8a/-8a}$ and 2.71% in *mstn*$^{-8b/-8b}$. In the screening of F_1 *mstn*$^{-8b/-8b}$, the actual observed rate was not consistent with the predicted rate. It is considered that there were competitivity of fish survival between *mstn* knocked out fish or not.

It is reported that the frequency of each variant in a tissue such as fins is reference for that in another tissue in the previous red sea bream study [**7**]. The present study partially supports an opinion in that study [**7**]. The results in the present study suggest that the occurrence of a targeted mutation via MMEJ in germ line is predictable from that in somatic line which can be sampled from fish alive (**Figs. 3.7g-i** and **3.8g-i**). On the other hand, other mutation except MMEJ mutation should not be referred to mutation in different tissues. The results in the present study support the opinion that MMEJ is a key for generation of homozygote in F_1 with the method of mating G_0 fish to each other in the red sea bream study [**7**].

The *mstn* homozygous mutant (*mstn*$^{-8a/-8a}$) in fugu exhibited the same phenotype of skeletal muscle mass (**Figs. 3.11-3.12**) as mammals [**5-6**, **22-24**] and other teleost **[7-11]** because C-terminal active domain is completely defective in *mstn*$^{-8a/-8a}$ and *mstn*$^{-8b/-8b}$ (**Fig. 3.10**). It is reported that activin receptor type IIB is activated by a homodimer of

mature MSTN C-terminal peptides after proteolytic cleavage at "RXXR" site in **Fig. 3.10**, then regulated muscle growth mediated Smad signaling pathway [**28**]. The *mstn*$^{-8b/-8b}$ and compound heterozygote such as *mstn*$^{-8b/-2}$ and *mstn*$^{-8b/-7}$ exhibited the same morphology and high condition factor as *mstn*$^{-8a/-8a}$ (data not shown) as *mstn*$^{-8a/-8a}$. It is suggested that the effect of fugu MSTN on skeletal muscle is a recessive factor because heterozygote did not exhibit increased skeletal muscle mass (**Fig. 3.11**) as same as that of red sea bream MSTN [**7**]. The erosion of skeletal muscle into internal organ region in homozygous mutants is observed (**Fig. 3.12a-b**). In contrast, the erosion is not observed in red sea bream mutants [**7**]. The erosion in fugu mutants may be due to the lack of ribs [**29**] because the red sea bream defines the body cavity by the rigid ribs. Further studies are required to investigate the effect this erosion on internal region. One of important findings is that body length of homozygote is shorter than that of wild type in fugu (**Fig. 3.11e**) as same as in red sea bream [**7**]. On the other hand, the body length of mutants is longer than wild type in small model fish, medaka and zebrafish [**8-11**]. In the present study, it is concluded that the short body length is caused by the shorten centrum lengths in the direction of anterior-posterior in *mstn* homozygote (**Fig. 3.13f**). Note that this phenotype of shorten body length appeared in complete knockout fugu such as *mstn*$^{-8a/-8a}$, but did not appeared in G_0 mosaic mutants (**Fig. 3.5** and **Table 2**). In G_0 mutants, the increase of body weight was observed because there is no difference in body length between G_0 mutants and control fish. In conclusion, the analysis in complete knockout mutants is important for the research of gene function of interest because the phenotype in G_0 may be different from that in complete knockout mutants.

Recently, it is reported that MSTN involves in mechanism in muscle to bone communication in mice [**25**, **30**]. A few studies suggested the effect of MSTN deficiency on bone formation also in teleost, medaka and red sea bream [**7**, **10**]. The present study indicates that MSTN deficiency in fugu causes the anterior-posterior and dorsal-ventral lengths of each centrum to shorten (**Fig. 3.13f-g**). The MSTN deficiency in fugu have a little effect on the width of each centrum (**Fig. 3.13h**). In red sea bream, MSTN deficiency causes short length of centrums in all direction, anterior-posterior, dorsal-ventral, and width [**7**]. In small model fish such as medaka zebrafish, it seems that MSTN mutants have larger centrums than wild type because body length of mutants is longer than that of wild type [**8-11**]. One of important findings is that the phenotype of shorten centrum in

mstn mutant is not specific for red sea bream. It is not clear that this phenotype is specific for marine fish or large fish such as fugu and red sea bream (body weight: > several hundred grams). To clarify the difference among fish species, further detailed studies are required to investigate the effect of MSTN deficiency on centrum formation, bone density, and several markers on osteoblast / osteoclast by analysis on various developmental stages not only in fugu but also in various fish species including red sea bream, medaka, and zebrafish.

One of the problems in genome editing including CRISPR/Cas9, there are potential off-target alternations on non-specific genome site including a few mismatches with designated sgRNA [**12**, **31**]. Off-target causes the following two problems; the incorrect evaluation of the phenotype due to on-target gene disruption, and the unexpected effects as food staff or animal health. In the present study off-target effect is examined by picking up its candidates using off-target search tools and the analysis of HMA and direct sequencing on each candidate in G_0, which revealed that there was no off-target alternation (**Figs. 3.14-3.16** and **Table 3.3**). Note that there are various SNPs and in/del variations between genome database and fish used in this study, and also among fish used in this study (**Figs. 3.15** and **3.16**).

The desirable traits for aquaculture can be obtained rapidly and correctly by genome editing in the shortest maturation period (in fugu: 3 years). In contrast, the generation of a desirable trait depends on uncertainty in the classical selective breeding method and artificial random mutagenesis method. In addition, a long period is required for genetic fixation of a trait, and various individuals is required and reared for finding of targeted trait and mutation. Therefore, the established genome editing breeding method in the present study is beneficial as an alternative technology for conventional fugu breeding method. In addition, this method is beneficial as research of gene function in fugu, which has been used for a reference to understand various questions for vertebrate in genetics.

Table 3.4 Primers used in the present study

primer name	sequence (5'-3')
sgRNA-hmaFw1	AGCGCCGCCGCTGCAGCAGCTC
sgRNA-hmaRv	TGAGTGTTTACCTCGCTGTG
sgRNA-hmaFw2	CCCGTCGGCAGCCCAGAGGACA
sgRNA#1-ampseq-Fw	ATGTGGTCACGGAGGAGG
sgRNA#1-ampseq-Rv	GCCACAGCGAGGTAAACA
sgRNA#2-ampseq-Fw	GCGGATGAAAGAGGCTCC
sgRNA#2-ampseq-Rv	CGTCGTACTGGTCGAGGA
amhr2-rflp-Fw	CACGTTGCGCTACATGTCC
amhr2-rflp-Rv	ACATCCAGATCTCCCACAGC

The primer pairs used in off-target analysis were shown in **Table 3.3**.

C3.6 References

1. Brenner, Sydney, et al. "Characterization of the pufferfish (Fugu) genome as a compact model vertebrate genome." Nature 366.6452 (1993): 265.
2. Kai, Wataru, et al. "Integration of the genetic map and genome assembly of fugu facilitates insights into distinct features of genome evolution in teleosts and mammals." Genome biology and evolution 3 (2011): 424-442.
3. Kamiya, Takashi, et al. "A trans-species missense SNP in Amhr2 is associated with sex determination in the tiger pufferfish, Takifugu rubripes (fugu)." PLoS genetics 8.7 (2012): e1002798.
4. Li, Mingyu, et al. "Structural, gene expression, and functional analysis of the fugu (Takifugu rubripes) insulin-like growth factor binding protein-4 gene." American Journal of Physiology-Regulatory, Integrative and Comparative Physiology 296.3 (2009): R558-R566.
5. Kambadur, Ravi, et al. "Mutations in myostatin (GDF8) in double-muscled Belgian Blue and Piedmontese cattle." Genome research 7.9 (1997): 910-915.
6. McPherron, Alexandra C., and Se-Jin Lee. "Double muscling in cattle due to mutations in the myostatin gene." Proceedings of the National Academy of Sciences 94.23 (1997): 12457-12461.
7. Kishimoto, Kenta, et al. "Production of a breed of red sea bream Pagrus major with an increase of skeletal muscle muss and reduced body length by genome editing with CRISPR/Cas9." Aquaculture (2018).
8. Chisada, Shin-ichi, et al. "Myostatin-deficient medaka exhibit a double-muscling phenotype with hyperplasia and hypertrophy, which occur sequentially during post-hatch development." Developmental biology 359.1 (2011): 82-94.
9. Chiang, Yi-An, et al. "TALENs-mediated gene disruption of myostatin produces a larger phenotype of medaka with an apparently compromised immune system." Fish & shellfish immunology 48 (2016): 212-220.
10. Yeh, Ying-Chun, et al. "Using CRISPR/Cas9-mediated gene editing to further explore growth and trade-off effects in myostatin-mutated F4 medaka (Oryzias latipes)." Scientific reports 7.1 (2017): 11435.
11. Wang, Chao, et al. "Deletion of mstna and mstnb impairs the immune system and affects growth performance in zebrafish." Fish & shellfish immunology 72 (2018): 572-580.
12. Ansai, Satoshi, and Masato Kinoshita. "Targeted mutagenesis using CRISPR/Cas system in medaka." Biology open 3.5 (2014): 362-371.
13. Maegawa, Shingo, et al. "Zebrafish DAZ‐like protein controls translation via the sequence ‘GUUC’." Genes to Cells 7.9 (2002): 971-984.
14. Kishimoto, Kenta, et al. "An effective microinjection method for genome editing of marine

aquaculture fish: tiger pufferfish Takifugu rubripes and red sea bream Pagrus major." Fisheries Science 85 (2019): 217-226.
15. Kinoshita, Masato, et al. Medaka: biology, management, and experimental protocols. John Wiley & Sons, 2009.
16. Ansai, Satoshi, et al. "Design, evaluation, and screening methods for efficient targeted mutagenesis with transcription activator ‐ like effector nucleases in medaka." Development, growth & differentiation 56.1 (2014): 98-107.
17. Ansai, Satoshi, and Masato Kinoshita. "Genome Editing of Medaka." Genome Editing in Animals. Humana Press, New York, NY, 2017. 175-188.
18. Zhang, Jiajie, et al. "PEAR: a fast and accurate Illumina Paired-End reAd mergeR." Bioinformatics 30.5 (2013): 614-620.
19. Lin, Y., Cradick, T. J., Brown, M. T., Deshmukh, H., Ranjan, P., Sarode, N., ... & Bao, G. (2014). CRISPR/Cas9 systems have off-target activity with insertions or deletions between target DNA and guide RNA sequences. Nucleic acids research, 42(11), 7473-7485.
20. McVey, M., Lee, S.E., 2008. MMEJ repair of double-strand breaks (director's cut): deleted sequences and alternative endings. Trends Genet. 24, 529–538.
21. McPherron, A. C., Lawler, A. M. & Lee, S. J. Regulation of skeletal muscle mass in mice by a new TGF-beta superfamily member. Nature 387, 83-90 (1997).
22. Mosher, D. S. et al. A mutation in the myostatin gene increases muscle mass and enhances racing performance in heterozygote dogs. PLoS Genet 3, e79 (2007).
23. Schuelke, M. et al. Myostatin mutation associated with gross muscle hypertrophy in a child. N Engl J Med 350, 2682-2688 (2004).
24. Elkasrawy, M.N., Hamrick, M.W., 2010. Myostatin (GDF-8) as a key factor linking muscle mass and bone structure. J. Musculoskelet. Neuronal Interact. 10, 56–63.
25. Khalil, K., Elayat, M., Khalifa, E., Daghash, S., Elaswad, A., Miller, M., Abdelrahman, H., Ye, Z., Odin, R., Drescher, D., Vo, K., Gosh, K., Bugg, W., Robinson, D., Dunham, R., 2017. Generation of myostatin gene-edited channel catfish (*Ictalurus punctatus*) via zygote injection of CRISPR/Cas9 system. Sci. Rep. 7, 7301.
26. Zhong, Z., Niu, P., Wang, M., Huang, G., Xu, S., Sun, Y., Xu, X., Hou, Y., Sun, X., Yan, Y., Wang, H., 2016. Targeted disruption of sp7 and myostatin with CRISPR-Cas9 results in severe bone defects and more muscular cells in common carp. Sci. Rep. 6, srep22953.
27. Hwang, W. Y., Fu, Y., Reyon, D., Maeder, M. L., Tsai, S. Q., Sander, J. D., ... & Joung, J. K. (2013). Efficient genome editing in zebrafish using a CRISPR-Cas system. Nature biotechnology, 31(3), 227.
28. Lee, Se-Jin, and Alexandra C. McPherron. "Regulation of myostatin activity and muscle growth." Proceedings of the National Academy of Sciences 98.16 (2001): 9306-9311.
29. Amores, Angel, et al. "Developmental roles of pufferfish Hox clusters and genome evolution in ray-fin fish." Genome Research 14.1 (2004): 1-10.
30. Qin, Yiwen, et al. "Myostatin inhibits osteoblastic differentiation by suppressing osteocyte-derived exosomal microRNA-218: A novel mechanism in muscle-bone communication." Journal of Biological Chemistry (2017): jbc-M116.
31. Wang, Haoyi, et al. "One-step generation of mice carrying mutations in multiple genes by CRISPR/Cas-mediated genome engineering." cell 153.4 (2013): 910-918.

General Discussion

In the present study, I established the breeding method with genome editing in marine aquaculture fish, red sea bream and tiger pufferfish (fugu). Firstly, for the purpose of establishing the breeding method, I established the method of microinjection into fertilized eggs of these two species in **chapter 1**. About six thousands of eggs can be injected in a day with this optimized microinjection methods, which make the researchers produce genome editing fish in breeding of two fish species **[chapter 2** and **3**]. Subsequently, I produced the genome editing breed exhibiting increased skeletal muscle mass, that is, increased edible parts, in red sea bream and fugu in **chapter 2** and **3**. It took the shortest maturation period to produce new breeds of homozygotes both in two species (red sea bream, in 2 years; fugu, in 3 years). This period with genome editing is greatly shorter than with classical selective breeding method which takes more than five generation (red sea bream, more than 10 years) to produce new breed, as described in the previous reports [**1**]. In addition, this genome editing breeding is greatly easier-to-use than random mutagenesis breeding method because gene targeting can be performed with high efficiency [**2**]. Therefore, I concluded that genome editing can accelerate a speed of breeding. In the present study, I added one of valuable traits, improvement of productivity, to red sea bream breeding population, “Kindai madai”, and to fugu wild population. The present study exhibited the possibility that the genome editing technology is a powerful breeding technique to generate new traits with valuable traits in aquaculture fish: for example, a growth enhancement, shorten maturation period, infertility, and production of gametes at early developmental stage, by a regulatory factor of food intake, a hormone receptor of sexual determination, and a transcription factor of sexual determination, respectively.

There are several concerns for genome edited breed. Firstly, one of them is to avoid escape into the wild from the standpoint of the potential effects on natural stocks. Now, all of the experimental and breeding procedures in the present study are performed in enclosed terrestrial tanks. In future, it is considered that it is effective, in addition to physical containment, to add an infertility trait with genome editing technology on a certain genome edited breed. Moreover, the infertility trait is effective also for prevention of steal of the breed. Secondly, there is the possibility of off-target alternation. In order

to solve this problem, the genotyping analyses were performed in the potential off-target candidates in red sea bream genome and fugu genome. As results, I concluded that there is no off-target alternation both in the *mstn* knockout red sea bream breed and *mstn* knockout fugu breed. In application to the addition of another traits, the same analysis as in the present study is effective for investigation of off-target effects. In application to another fish species, it is needed for the researchers to perform the project of whole genome sequencing if the genome database cannot be utilized in the species. Finally, the investigation of the safety as food staff is needed, which is still controversial. To solve the problem. it can be effective to perform feeding test with model animals such as rats and mice.

Further studies are needed in order to commercialize genome edited breeds. In particular, the analyses of the efficiency of food conversion and the switching of the metabolic pathway are needed for the investigation of characteristics of the new breed. It seems that there are some differences in metabolic pathway between the new breed and a common breed. Thus, it seems that it is required for the new breed to be established an optimized rearing system, for example, the kinds of feed, the number of times of feeding, and the density of fish in a tank. In the research of livestock chicken breed, broiler, it is suggested that the development of feed is one of the most important tasks for the efficiency of meat production, in addition to the development of a trait in the breed [**3**]. Therefore, aquaculture researchers should perform both the production of new breed with a valuable trait and the development of rearing system optimized for the new breed at the same time. In near future, various breeds with commercially valuable traits will be produced with several breeding method, classical selective breeding, genome based breeding technology using NGS, random mutagenesis, and genome editing technology. Genome edited breed shows more outstanding trait than common breed, as *mstn* knockout breed in the present study. Therefore, it is considered that the investigation of rearing system using genome edited breed will contribute as a model case to research of development of rearing systems which will be important in the future.

Now, it is necessary for the researchers to increase the number of target gene candidates for research of aquaculture breeding with genome editing. A few studies have focused on phenotype by deficiency of a specific gene. Thus, it is needed to perform the studies focused on phenotype by gene knockout using small model fish such as medaka

and zebrafish whose generation periods are greatly shorter than aquaculture fish. It should be noted that the phenotype in model fish is only a prediction of phenotype in aquaculture fish, as the present study revealed that the phenotype of bone structure in *mstn* mutants in red sea bream and fugu are different from that in model fish [**chapter 2 and 3**].

References

1. Murata, Osamu, et al. "Selective breeding for growth in red sea bream." Fisheries science 62.6 (1996): 845-849.
2. Kuroyanagi, Miwa, et al. "New approach for fish breeding by chemical mutagenesis: establishment of TILLING method in fugu (Takifugu rubripes) with ENU mutagenesis." BMC genomics 14.1 (2013): 786.4. Jain, S.M., 2010. Mutagenesis in crop improvement under the climate change. Rom. Biotechnol. Lett. 15, 88–106.
3. Zuidhof, M. J., et al. "Growth, efficiency, and yield of commercial broilers from 1957, 1978, and 2005." Poultry Science 93.12 (2014): 2970-2982.

Acknowledgements

I would like to express the deepest appreciation to Dr. Masato Kinoshita, Division of Applied Biosciences, Graduate School of Agriculture, Kyoto University, for his advice and guidance on a whole research, from the basis of molecular biology experiment and fish breeding to design and conceiving of all experiments. Without his support, I would not work on this project with very few precedent in our laboratory.

I would like to show my great gratitude to Dr. Kenji Sato and Dr. Haruhiko Toyohara, Division of Applied Biosciences, Graduate School of Agriculture, Kyoto University, for their critical reading of this thesis, and for his supervision for my work and giving suggestive comment in the laboratory seminar.

I would like to express my appreciation to the examination committee members Dr. Masatomo Tagawa, Division of Applied Biosciences, Graduate School of Agriculture, Kyoto University, for their critical reading of this thesis.

I would be deeply grateful to Dr. Keitaro Kato and Dr. Youhei Washio, Aquaculture Research Institute, Kindai University, for research in red sea bream, and detailed advice and discussions on my research and my future tasks. I sincerely thank current and former students and staffs in Aquaculture Research Institute, Kindai University for their kind help and wide-ranging discussion, especially, Mr. Matsuura, Ms. Hashi, Mr. Kuno, Mr. Okada, Ms. Shimamura, Mr. Ito, Mr. Matsukawa, Mr. Ohama, Mr. Takahashi, Mr. Miki, Mr. Fujitani, Ms. Suzuki, Mr. Inagaki, and Mr. Kanatsu.

I would be deeply grateful to Dr. Yashutoshi Yoshiura, Dr. Miwa Kuroyanagi, Dr. Takashi Katayama (current address: Miyazu Laboratory, Japan Sea National Fisheries Research Institute, Japan Fisheries Research and Education Agency), Dr. Tadashi Imai, and current and former staffs, Yashima Station, Stock Enhancement and Management Department, Nationals Research Institute of Fisheries and Enhancement of Inland Sea, Japan Fisheries Research and Education Agency, for research in tiger pufferfish, and detailed advices and discussions on my research and my future tasks.

I would be grateful to Dr. Tomohiro Ueno, Human Health Sciences, Graduate School of Medicine, Kyoto University, and Hidenao Fukuyama, Research and Educational Unit of Leaders for Integrated Medical System, for analysis of MRI-scan and CT-scan, and detailed advices and discussions on my research.

I would be grateful to Dr. Atsushi Toyoda and Mr. Yohei Minakuchi, Comparative Genomics Laboratory, Center for Information Biology, National Institute of Genetics, for genome sequencing in red sea bream and bioinformatics analysis.

I thank Dr. Hiroyuki Yoshikawa and Ms. Yasuko Ino, Department of Applied Aquabiology, Japan Fisheries Research and Education Agency, National Fisheries University, Minoru Tanaka, Division of Biological Science, Graduate School of Science, Nagoya University, for another projects about genome editing.

I sincerely thank my current and former colleagues in Laboratory of Marine Biological Function, Division of Applied Biosciences, Graduate School of Agriculture, Kyoto University, for their kind help and wide-ranging discussion. Especially, I would like to offer my special thanks to Dr. Youhei Washio, Dr. Satoshi Ansai, Dr. Akiko Sogo, Mr. Yu Murakami, Dr. Tetsuya Ogino, and all members of the Kinoshita group for technical support and advice.

This work was partially supported by my Grant-in-Aid for JSPS Fellows Grant Number JP 17J10249.

Finally, I appreciate my family, especially my parents, for supporting me.